CHEMICAL APPROACHES TO STUDY MODIFIED NUCLEIC ACIDS

MORGAN CAULEY-LE FEVRE

A THESIS SUBMITTED TO
THE FACULTY OF GRADUATE STUDIES
IN PARTIAL FULFILLMENT OF THE REQUIREMENTS
FOR THE DEGREE OF
MASTER OF SCIENCE

GRADUATE PROGRAM IN CHEMISTRY
YORK UNIVERSITY
TORONTO, ONTARIO

DECEMBER 2024

ABSTRACT

Chemical modifications govern the fate and function of nucleic acids. The methylation of the *N*-6 position of adenosine (m^6A) in RNA is the most studied naturally occurring modification. Methylation of this position is regulated by a complex, dynamic interplay between enzymes known as methyltransferases (writers) and demethylases (erasers). Modifications on functional nucleic acid polymers (aptamers), have also been reported to increase binding affinity and stability *in vivo* towards a particular target. Ligase-catalyzed OligOnucleotide polymERization (LOOPER) is a method to access hetermultivalent aptamers, and the method was successful in the evolution of a modified aptamer towards human α-thrombin. However, LOOPER requires a platform to produce these modified aptamers at scale. Chapter 2 of this thesis focusses on my work to create such a platform, using solid-phase DNA synthesis and orthogonal protecting groups. Two protecting groups were synthesized, and one, allyloxy carbonyl (alloc) was taken forward for this platform due to the ease of the solution-phase deprotection step. Synthesis of the modified phosphoramidite equipped with alloc was undertaken, and the phosphoramidite was eventually incorporated into an oligonucleotide. The protecting group was successfully removed on-instrument, however several coupling protocols to install the chemical modifiers for the aptamer were ultimately unsuccessful. In Chapter 3 of this thesis, I focussed on the optimisation of some hit compounds towards m^6A demethylase ALKBH5, which has been shown to be up- or down-regulation in a variety of cancerous and non-cancerous disease. Selective inhibition of the protein would greatly facilitate knowledge generation around its associated pathologies. From two DNA-encoded library hits towards the protein, hit optimization synthesis of two molecules was performed. A fluorescence polarization (FP) assay to determine IC_{50} data from these compounds was produced and was successfully validated. Unfortunately, with little material of the two compounds generated, only limited FP data was generated, and the results were inconclusive.

ACKNOWLEDGEMENTS

First, I would like to sincerely thank my supervisor Dr. Ryan Hili, for his guidance throughout my graduate career. He has been instrumental in the shaping of myself as a researcher, and his commitment to fostering a supportive academic environment, focussed on rigorous research and intellectual curiosity, as well as prioritizing our well-being, has been aspirational. I would also like to thank my committee members, Professor Arturo Orellana and Professor Philip Johnson. I have appreciated your time, advice, and feedback throughout my time at York University.

Next, I would like to thank the Baumgartner lab. They graciously allowed us into their lab space when the Hili lab first started at York, before we had access to a fume hood of our own. They have provided a variety of support throughout my time here, and I have appreciated sharing our LSB space with Baumgartner colleagues, both past and present.

I want to express my gratitude to all the departmental staff in the chemistry department at York that have contributed to the completion of this work. Specifically, I want to thank Howard Hunter for all the hard work of maintaining the NMR facilities, training me on numerous NMR instruments, and assisting with the set-up of NMR experiments. Additionally, I want to thank the past and present operators of the York Mass Spectrometry facility, Peter Liuni and Maxime Rossato, respectively. MS data has been essential to the characterization of some molecules I have synthesized, and I have sincerely appreciated their expertise and hardworking maintenance of the instruments. I also want to thank Dirk Verdoold, the York glassblower. Some key glassware has broken during my time here, and he has been invaluable in keeping our lab running in that regard with minimal delay.

I want to acknowledge all the members of the Hili lab group I have had the pleasure of working with: Dr. Yasaman Mahdavi-Amiri (my first lab mate!), Dr. Matina Movahedi (my first undergraduate!), Molly Hu, Natalie Khamissi, Dr. Kimberley Chung, Ian Frankel, Emily Anacleto, Luca Di Fabio, and Nicole Frias. Further, I am grateful for having the opportunity to mentor skilled and motivated undergraduates, Matina Movahedi, Prakriti Das, and Karanveer Bhangu. I could not have asked for a better group of lab mates and colleagues to have undertaken the challenges of

grad school with. I also want to acknowledge my peers, past and present, in the Department of Chemistry whom I've had the pleasure of working with and getting to know. Talking with and getting to know you all has been a welcome respite and source of support. There are too many people to name, but know that if we knew each other, you were appreciated.

Finally, I would like to thank my family and friends whose various forms of support were greatly appreciated. I especially want to acknowledge and express my sincere appreciation and love for my wife Noreen Cauley-Le Fevre, without whom this work would not have come to fruition. In the final years of this work, she was faced with the colossal task of raising and taking care of our two young children essentially on her own in Ottawa while I finished my research and writing here at York, while also working on her PhD. Her work in this undertaking was integral, and her support has meant everything to me.

TABLE OF CONTENTS

LIST OF FIGURES

LIST OF SCHEMES

LIST OF TABLES

Chapter 1 – Concerning Nucleic Acids

1.1 Nucleic acids and nucleotides

Nucleic acids, comprising DNA (deoxyribonucleic acid) and RNA (ribonucleic acid), are fundamental biomolecules that encode, transmit, and regulate genetic information in all known forms of life. These macromolecules play crucial roles in biological systems, serving as the repository of genetic blueprints for protein synthesis and regulation.[1,2]

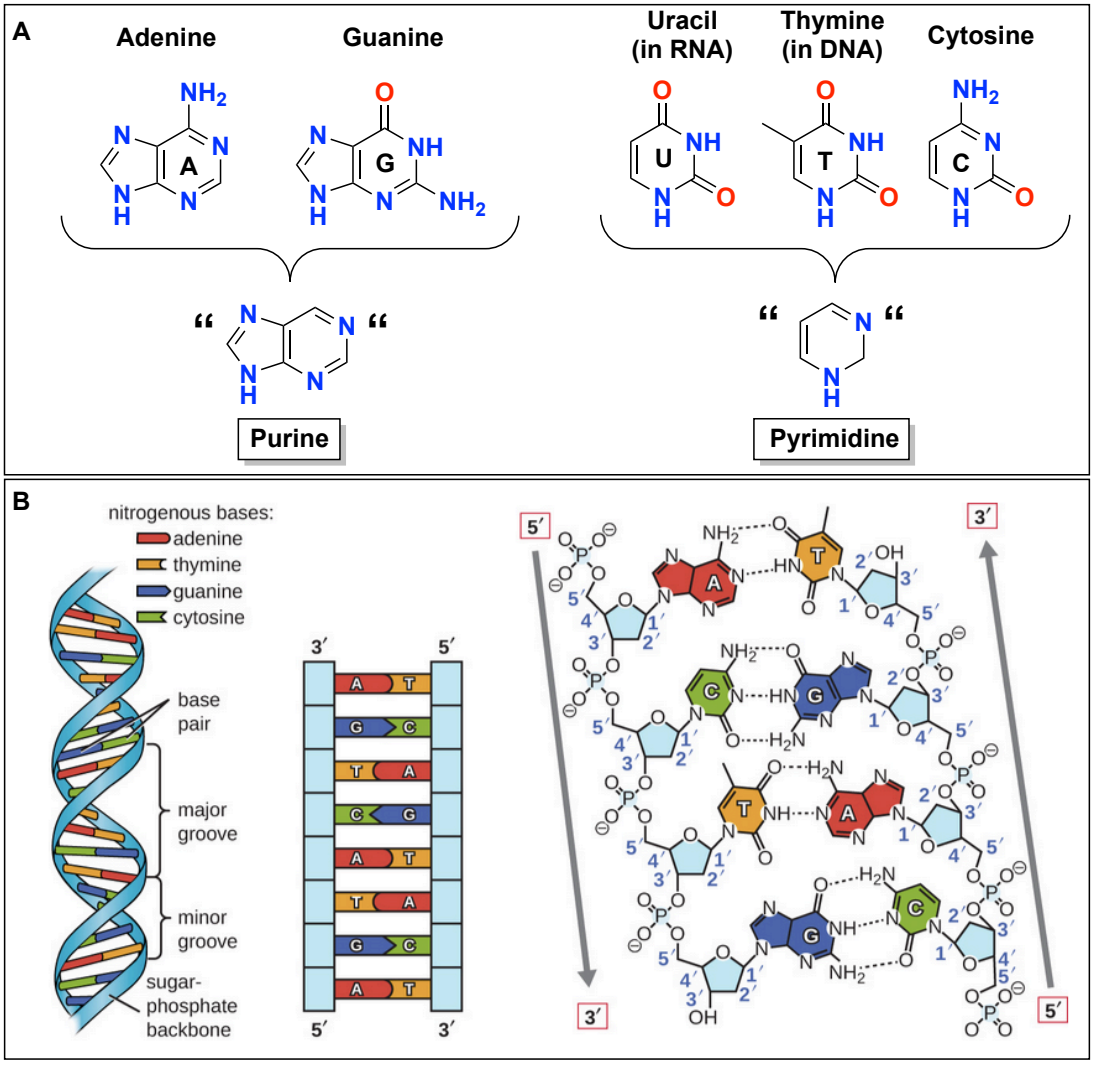

Figure 1-1: A – The structure of the canonical nucleotides of DNA and RNA; B – Base-pairing in DNA, showing the anti-parallel helix structure, where each strand runs in the 5' → 3' direction (from Parker et al. Microbiology (2016) from Openstax)

DNA primarily exists as a double-stranded helical polymer composed of billions of nucleotides in a set sequence (**Figure *1-1***). A nucleotide is made up of three components: a phosphate group, a deoxyribose sugar, and a nucleobase: either a purine base, adenine (A) and guanine (G), or a pyrimidine base thymine (T) and cytosine (C). Nucleic acid polymers are connected through phosphodiester bonds. A deoxyribose sugar connects the phosphate backbone to the nucleobase, which extends into the interior of the β-helix structure. The β-helix itself is made of two strands of DNA running antiparallel to each other. That is, both strands run from the 5' end to the 3' end, but the strands interact with each other in the opposing directions (**Figure *1-1B***). The bases form pairs with the opposite strand in the helix through hydrogen bonding interactions: adenine (a purine) pairs with thymine (pyrimidine), and guanine (purine) with cytosine (pyrimidine). While the discovery of DNA dates back to 1869, the double-helix structure was only elucidated by Watson and Crick in 1953, with indispensable X-ray contributions from Rosalind Franklin (***Figure 1-2***).[2–4]

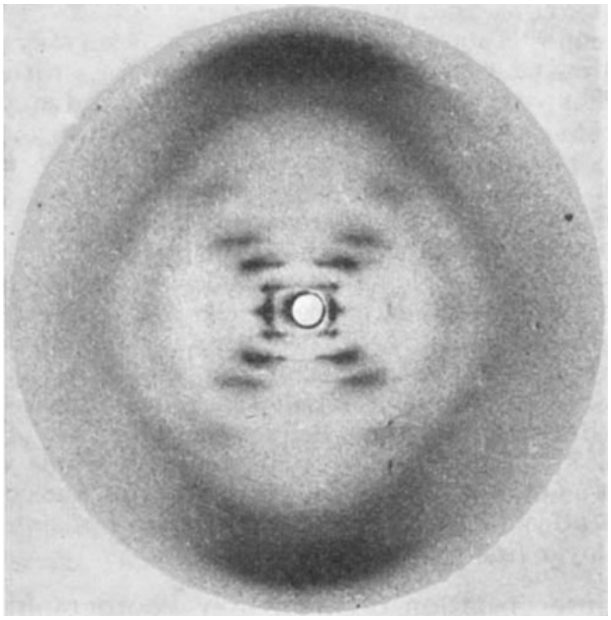

Figure 1-2: Photo 51, displaying the double-helical structure of a DNA strand[4]

1.2 Canonical functions of nucleic acids

The primary function of DNA is the storage and transmission of genetic information for a given organism. In eukaryotic cells, DNA is contained within the cell nucleus. The flow of genetic information is termed 'the central dogma' in biology: DNA is transcribed to RNA, and RNA is translated into protein.[1]

RNA shares many similarities with DNA, though there are important differences: RNA is typically single-stranded; contains a ribose sugar instead of a deoxyribose sugar; and RNA replaces thymine (T) with uracil (U) in the nitrogenous base canon, but otherwise use the same bases (**Figure *1-1A***). Owing to its single-stranded nature, RNA can take on a diversity of secondary structures and additional functionality when compared to DNA. The three major roles of RNA are: mRNA (messenger RNA), which is synthesized during transcription and carries genetic code to ribosomes where it is translated into proteins; tRNA (transfer RNA), used for amino acid delivery during protein synthesis; and rRNA (ribosomal RNA) which forms the core structural and catalytic components of ribosomes.[5] Additionally, regulatory RNA, such as microRNAs (miRNAs) and small interfering RNAs (siRNAs) play significant roles in gene expression modulation and RNA interference pathways.

1.3 Nucleic acid modifications

All living organisms experience natural chemical modifications of their DNA and RNA.[6,7] Numerous, naturally occurring reversible modifications have been discovered, especially in the past 15 years, as novel methods for identifying the locations of these modifications have been developed.[8–10] While it has been known for decades that modified nucleotides exist, their importance and the specific roles these modifications play had been quite underappreciated. Over 160 unique nucleobase modifications have been reported to date, of which the simplest and most studied is *N*-methylation, where one or more methyl groups are added to a nitrogen atom on a particular nucleic acid base.[7] Of all known epigenetic markers in RNA, *N*-methylation accounts for over 60% of those reported. Indeed, all nitrogen atoms of all nucleobases have been observed to undergo some methylation activity in particular circumstances (the only exception being the N^3 position of guanine).[11] Additionally, these methylations are regulated dynamically, through

complex interplay between DNA/RNA, and proteins known as methyltransferases and demethylases. This results in an ongoing process of addition and removal of methyl groups to nucleobases.[12] The most studied of these *N*-methylations is of adenosine, at the *N*6 position, known as m^6A (**Figure *1-3***).

1.3.1 m^6A

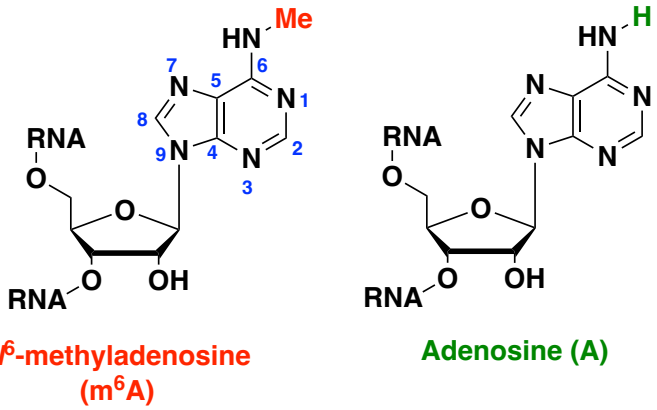

Figure 1-3: The structures of N^6-methyladenosine (with position numbering) and adenosine

The m^6A modification was first discovered in 1974.[13,14] The naturally-occurring modified adenosine base has proven to be integral to RNA stabilization, localization, translation, splicing, and transport.[15–20] This modification is often located near stop codons, as well as in the 3'-untranslated region (UTR), which suggests a regulatory role in cellular processes. The dynamic and reversible nature of methyl addition and subtraction from adenosine within RNA indicates the pivotal role the modification plays in cell signaling networks.[21–23] m^6A expands the chemical diversity of nucleic acids without altering the genomic/proteinogenic nature of them, and allows for an array additional features to be conveyed, especially as it relates to the major roles of RNA, and especially mRNA. In fact, when methyltransferase like 3 protein (METTL3) is removed from cell lines (removing the ability for m^6A to be generated), apoptosis is observed in humans, and other deleterious effects such as developmental arrest and defects in gamete formation were observed, illustrating the quintessential role of this modification.[21] Over the past couple decades, methods have been and continue to be developed to detect m^6A locations in RNA. Understanding the location of these modifications will enhance understanding of the role m^6A plays, and its

vitality to our nucleic acid makeup, especially in how its presence or absence affects human health and disease.

1.3.1.1 Reading, writing, and erasing proteins of m6A in humans

In eukaryotic cells, methyltransferase proteins (such as METTL3, METTL5, WTAP, ZC3H13, and VIRMA) and demethylase proteins (such as ALKBH5 and FTO) interact with each other to write and erase, respectively, methyl groups from adenosine in RNA. Reader proteins (such as YTHDF1/2/3) are responsible for interpreting the methylation event and responding.[24,25] Due to the association of m^6A and the writer and eraser proteins in cell signaling networks, dysregulation of these proteins is frequently seen and associated with many cancers and other diseases.[23,26–30] Thus, these proteins present themselves as promising targets for therapeutic design. One important class of demethylase proteins is the AlkB family, which consist of *e. coli* AlkB, and the nine human homologues, ALKBH1-8, and fat mass and obesity-associated protein (FTO).

1.3.1.1.1 AlkB demethylase family

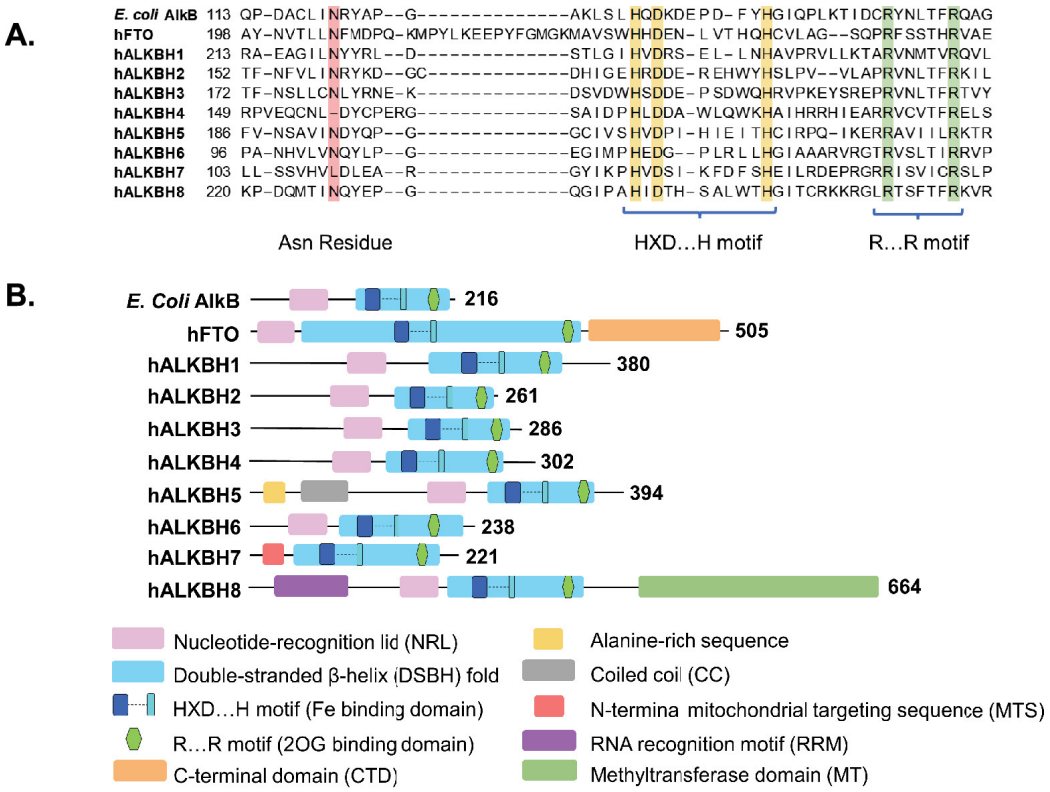

Figure 1-4: AlkB family of nucleic acid demethylases. A – alignment of sequences in the catalytic domain of the AlkB family, showing the highly conserved 'HXD…H' and 'R…R' motifs; B – Domain architecture of the AlkB family (figure from reference [11])

The AlkB family of demethylases are part of the iron(II) and 2-oxoglutarate (2-OG)-dependent oxygenases, a class of enzymes catalyzing reactions involving the oxidation of an organic substrate using O_2.[31] Each AlkB homologue efficiently demethylates specific nucleobases in either single- or double-stranded (ss or ds) DNA or RNA. ALKBH5 and FTO are the only human enzymes currently known to demethylate m^6A in mRNA, though they likely target different m^6A-containing mRNA transcripts as evidenced by distinct physiological functioning, and their relative associations with different diseases.[32,33]

Indeed, the up-regulation and down-regulation of ALKBH5 has been implicated in a plethora of cancerous and non-cancerous diseases, including pancreatic cancer,[34] colon cancer,[35] breast cancer,[36] lung cancer,[37] ovarian cancer,[38] glioblastoma,[39] and reproductive system diseases.[40] Due to the association with m^6A, the enzyme has recently become a novel target in disease research. Selective inhibition of the protein would greatly accelerate knowledge generation

in the role it plays in these and many other pathologies. Inhibiting a protein and observing the downstream effects on cell lines is an important tool researchers have in knowledge generation of a particular target. Unfortunately, due to structural similarities within the ALKB family, selective inhibition is a challenging prospect (**Figure *1-4***).

The ALKB family has generally been well characterized, with more than 100 crystal structures reported.[11] The demethylases all contain a central catalytic domain which is formed by eight β-strands folding into a double-stranded β-helix (DSBH) structure, colloquially referred to as the 'jelly roll' fold (**Figure *1-4B***).[41] Two highly conserved structural elements, essential for demethylase activity, are folded within the jelly roll: i) the 'HXD…H' motif, representing two bookending histidine residues with an aspartate residue between them, allowing for a tridentate binding of iron, and ii) 'R…R' arginine motif, which stabilizes 2OG binding (**Figure *1-4A***).[11,41] Owing to the conserved nature of these motifs, no selective inhibitors for ALKBH5 have been developed to date.

1.4 Nucleic acid polymers

Nucleic acid polymers (DNA and RNA) are most thought of in terms of their roles in genetic information storage and cellular instructions. However, there are naturally occurring instances where RNA can fold into three-dimensional structures (known as ribozymes) to catalyze reactions,[42] communicate cellular response,[43] mediate protein synthesis,[44] and control gene expression.[45,46] Pioneering advances in nucleic acid chemistry, solid-phase synthesis and the polymerase chain reaction (PCR), allowed researchers the capability to produce large populations of nucleic acid polymers (oligonucleotides) with non-biological function.[47,48] These discoveries pre-empted the Szostak, Joyce, and Gold labs to concurrently but independently develop a method which evolves synthetic oligonucleotides into high-affinity (tight-binding) ligands for protein targets; this method is now known as SELEX (Systematic Evolution of Ligands by EXponential enrichment).[49–51]

1.4.1 SELEX

Briefly, SELEX is an iterative process wherein a target (typically a protein) is incubated with a large library of short synthetic oligonucleotides (40-80 bases). The non-binding sequences are washed away after the incubation, and the binding members are eluted and PCR-amplified, producing a new, more 'fit' library of oligonucleotides, which undergo the next cycle of target incubation. This process is generally repeated 5-10 times, and the sequences should converge on a handful of enriched sequences (**Figure 1-5**). When successful, SELEX produces a functional, high-affinity, highly specific, three-dimensionally binding oligonucleotide, known as an 'aptamer' (from the Latin *aptus*, meaning 'to fit' and the Greek *meros*, meaning 'part' or 'portion').[52]

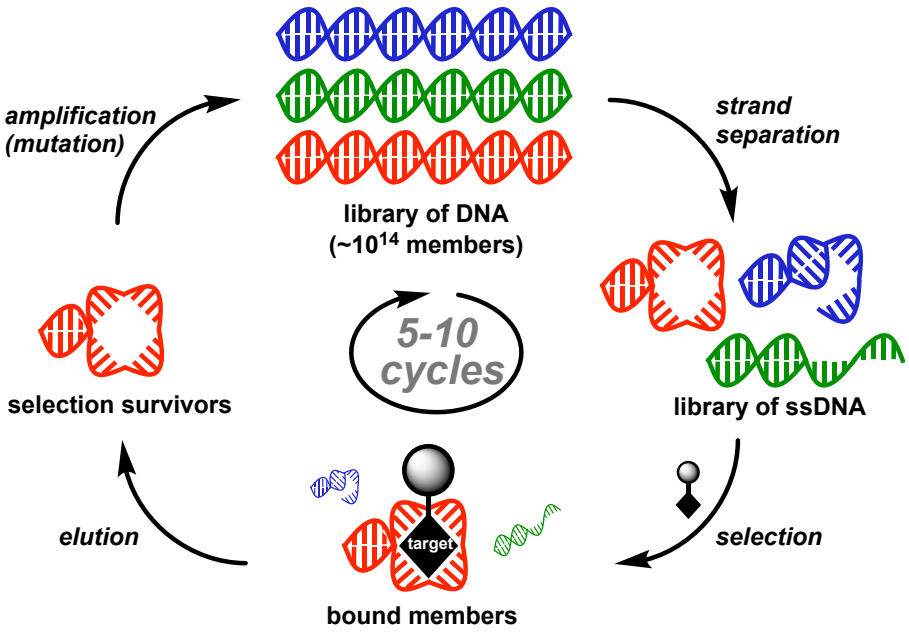

Figure 1-5: A SELEX cycle for aptamer evolution towards an immobilized target

1.4.2 Aptamers

As of 2020, nine oligonucleotide-based therapeutics have been approved by the FDA., and more than 180 clinical trials are underway. Of the approved therapeutics, two of them are aptamers: Macugen (approved in 1998, the first aptamer approved by the FDA), and the other, Defitelio (approved in 2016).[53] Thus, aptamers have matured into important tools in biotechnological and

medicinal chemistry toolboxes, with reported uses in therapies, drug delivery, and biosensing, among others.[54–60] They can be thought of as analogous to antibodies (which are typically evolved to target a particular protein), but with several distinct advantages: bench stability over long periods of time, reproducible renaturation, low-to-no immunogenicity, relatively larger scale of production, and the ability to incorporate modifications to enhance stability and affinity, leading to enhanced pharmacokinetic and pharmacodynamic properties.[54,55,61–63] The addition of covalent modifications to nucleobases within an aptamer framework, or on the ribose sugar, or even the phosphate backbone, are a further boon to molecular recognition, affinity, catalytic activity of functional nucleic acids, and even prolonged stability of the oligonucleotide *in vivo*.[62]

1.4.2.1 Aptamer modification

There are numerous methods to modify aptamers, both pre- and post-SELEX. Post-SELEX modifications can sometimes negatively impact the aptamer; altering the structure of the aptamer after a successful evolution can nullify the binding affinity.[64] However, in many cases, post-SELEX modifications can further enhance stability, solubility, or affinity to the target. For example, Macugen was appended with polyethylene glycol (PEG) post-SELEX, which increases the half-life of the therapeutic *in vivo*. PEGylation is considered safe, though there is some evidence suggesting the addition of PEG could produce unwanted side effects.[64] Common base modifications include pseudouridine, and modifications to the *C*-5 position of uridine, primarily seen in slow off-rate modified aptamers (SOMAmers).[65] Base modifications are typically used for mimicking protein-like functionality in aptamers. Some common ribose modifications include 2'-O-Methyl, locked nucleic acid (LNA), 2'-fluoro, 2'-arabino (ANA), and 2'-fluoroarabino nucleic acid (2'-FANA); these modifications often improve the stability of aptamers. Finally, modifications of the phosphodiester backbone include the addition of PEG groups, replacement of the linkage with methylphosphonate, or phosphothiorate. These modifications tend to confer additional thermal stability (**Figure *1-6***).[64]

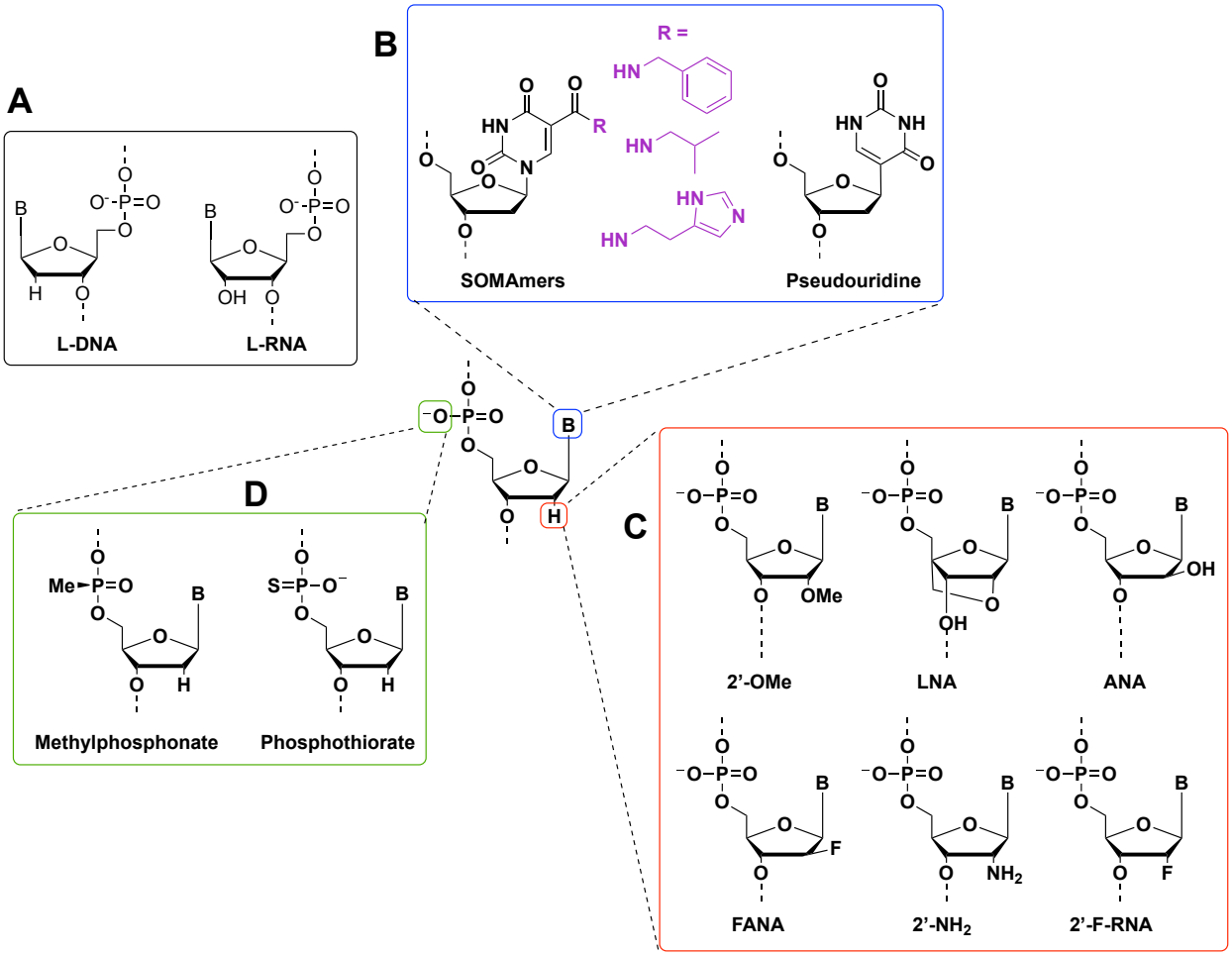

Figure 1-6: Some examples of common modifications at each component of a nucleotide. A – Mirror image nucleic acids (Spiegelmers);[66] B – SOMAmer modifications off the C-5 position in Uridine, and pseudouridine; C – several modifications to the ribose sugar, including arabinose substitution; D – phosphodiester modifications

Since post-SELEX modifications can occasionally negatively impact an aptamer, a frequently employed method to avoid these potential complications is to evolve aptamers directly with the modified nucleotides. This requires the use of a specialized polymerase for the amplification process, either naturally occurring or engineered. One method to access modified oligonucleotides, developed in the Hili lab, is Ligase-catalyzed OligOnucleotide PolymERization, or LOOPER.

1.4.2.2 LOOPER

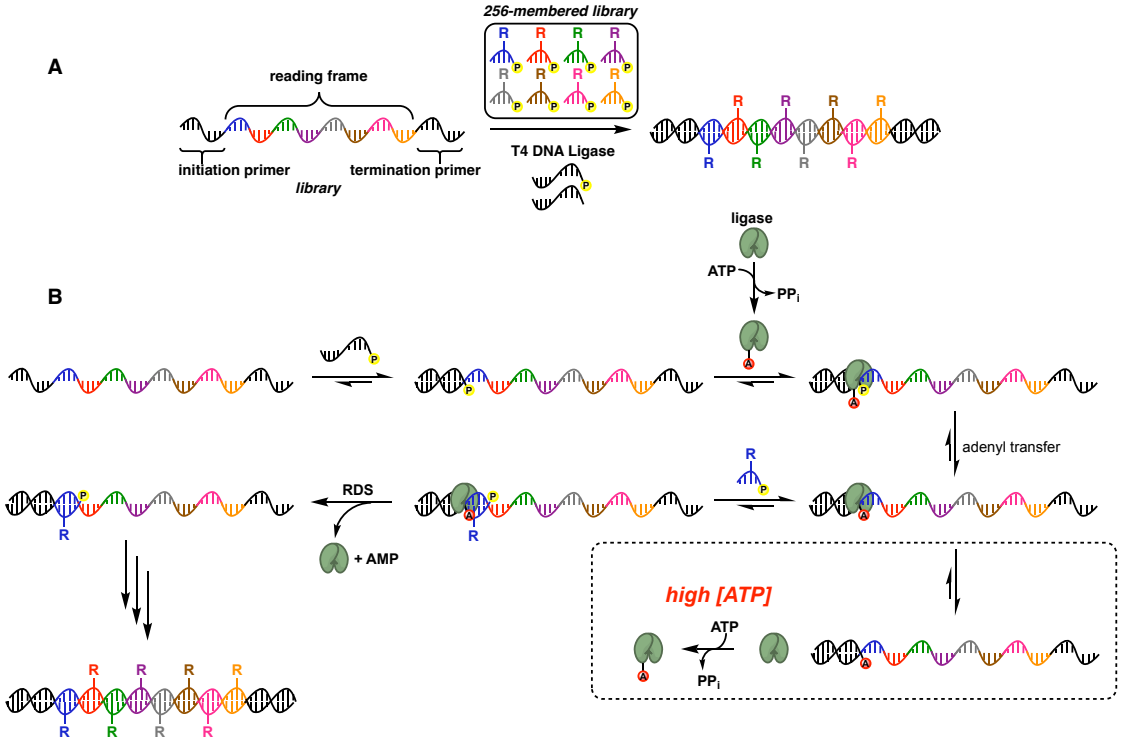

Figure 1-7: A – A general schematic of LOOPER showing the template strand, codon library, and chemically modified DNA duplex; B – Mechanism of LOOPER polymerization with T4 DNA ligase

LOOPER is a method to access heteromultivalent (**Figure *2-1***) modified aptamers.[67,68] The method relies upon DNA-template strands and T4 DNA ligase to catalyze the polymerization of these modified aptamers (**Figure *1-7***). To start, a 256-member pentanucleotide codon library was developed and optimized, each member consisting of a 5'-phosphorylated chemically modified adenosine, appended sequentially to a two-nucleotide random sequence, followed by two coding nucleotides at the 3' end, which encode one of 16 modifications extending off the 5'-adenosine (**Figure *1-8B***). Upon completion of the codon libraries, the fidelity of LOOPER was optimized with the DNA template sequence to ensure a robust system which could easily tolerate the selected modifications of the codon library and be polymerized with T4 DNA ligase. The template strand, starting at the 3' end, contains an initiation primer, a randomized 40 nucleotide reading frame, followed by a termination primer. A 5'-phosphorylated primer anneals to the template strand, which is then adenylated by T4 DNA ligase. Corresponding 5'-phosphorylated functionalized codons are ligated iteratively along the template DNA reading frame, with the DNA ligase

catalyzing the formation of the phosphodiester bond. Upon formation of the full-length DNA duplex, the sequences are strand-separated, yielding the diversely modified single-stranded DNA (ssDNA) polymer (**Figure *1-7B***). The sequence-defined incorporation of the chemically modified codons was found to be quite successful, proceeding with high efficiency and a fidelity of 94%.[67] LOOPER was able to produce corresponding modified nucleic acid polymers from a library of template DNA strands, yielding access to a library from which an aptamer could be evolved through SELEX.

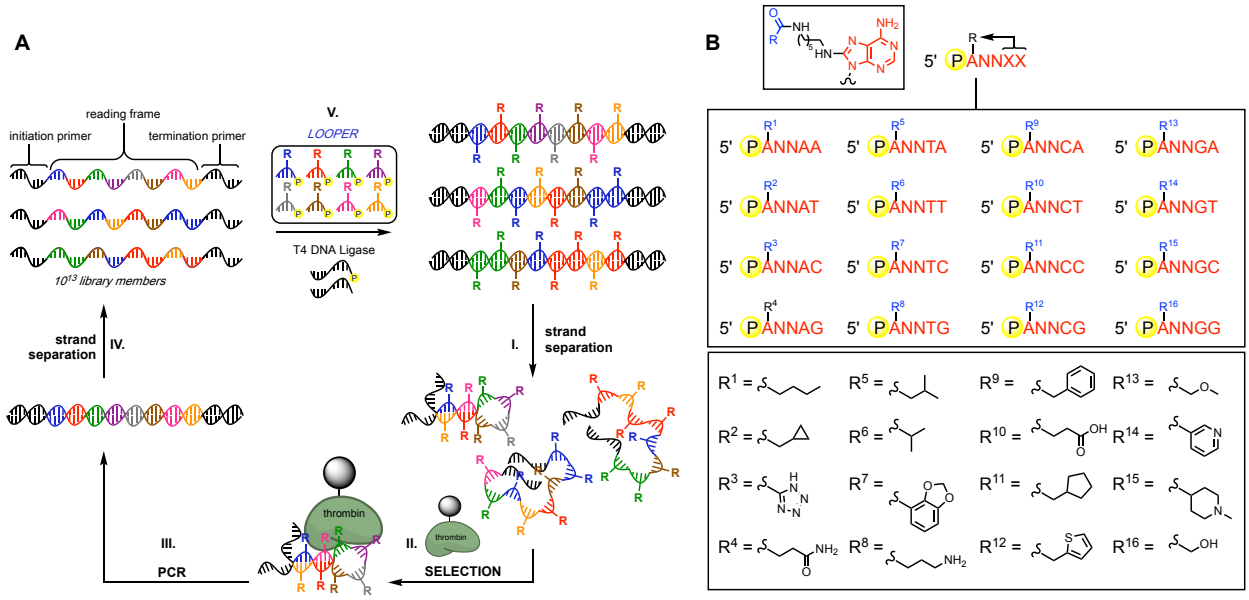

Figure 1-8: A – a LOOPER-SELEX cycle for an evolutionary aptamer selection for human α-thrombin; B – a 16 x 16 library of pentanucleotide codon members, containing the 5'-phosphorylated modified adenosine, random 'NN' dimer, and coding bases, corresponding to each chemical modification listed

LOOPER-SELEX incorporates LOOPER ssDNA generation into a SELEX aptamer evolution cycle (**Figure *1-8A***). Human α-thrombin was chosen as a model protein target because of its history of successful evolution of well-studied aptamer being evolved towards it. Briefly, a library of DNA templates were subjected to LOOPER, generating a DNA duplex of chemically modified sequences; this duplex was strand separated and the modified oligonucleotides were incubated with the target protein, human α-thrombin. The non-binding sequences were washed away, and the binders were eluted and PCR-amplified to produce a new duplex of oligonucleotides. These were then strand separated, yielding a new, more 'fit' library of template strands towards thrombin. This cycle was repeated 6 times until the library was of significantly

diminished sequence diversity. The surviving library members then underwent high-throughput DNA sequencing to determine their identities, and the chemical modifications contained within.

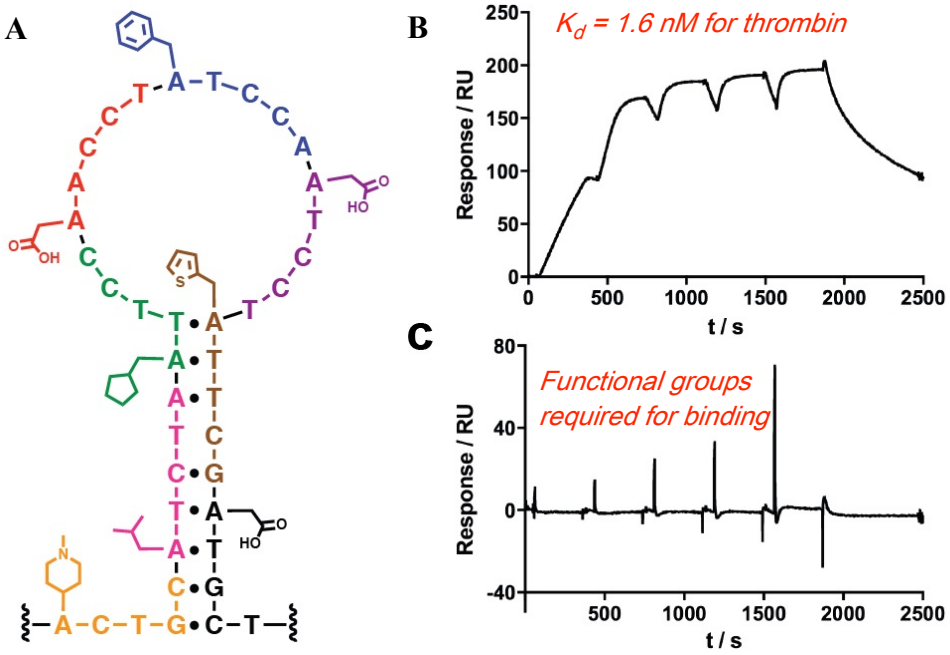

Figure 1-9: TBL-1 chemically modified aptamer structure and thrombin binding data. A – Stem-loop structure of TBL-1 aptamer, with chemical modifications; B – Single-cycle SPR data showing a Kd of 1.6 nM for the aptamer; C – SPR data showing no binding for the DNA sequence without the modifications

An aptamer named TBL-1 was identified from the sequencing data (**Figure *1-9A***). Surface plasmon resonance (SPR), an instrument used to test for target-binding with a ligand, indicated a dissociation constant (K_d) of 1.6 nM (**Figure *1-9B***). Importantly, an SPR experiment of the same DNA sequence but without the chemical modifications, showed that no binding occurred between the aptamer and the target (**Figure *1-9C***). Thus, the chemical modifications were essential to binding.[68]

However, LOOPER is not without its limitations. Since the process is enzymatic, it is an expensive methodology. Additionally, it is a slow process to carry out, SELEX notwithstanding. Finally, the yields are prohibitively low, allowing for only limited characterization and study of the aptamers, and no way to produce the aptamer at scale. Indeed, a strategy to produce larger amounts of LOOPER-derived aptamers would be essential for the technology to take on more utility.

1.5 Thesis project

There are numerous methods, both naturally occurring and synthetic whereby nucleic acids are modified for a variety of different functions. The work presented in this thesis aims to explore chemical methods of synthesizing LOOPER-derived modified nucleic acid polymers, and to explore the inhibitory chemical space of demethylase protein ALKBH5. The development, implementation, pitfalls and limitations of these methods will be discussed, and an outlook will be provided for the future of these projects.

Chapter 2 – Towards Solid-Phase Synthesis of Modified DNA Aptamers

2.1 Introduction

Inherently, nucleic acid polymers are functional group deficient (**Figure *1-1A***). The canonical bases are purine and pyrimidine rings, so aptamer binding primarily involves tertiary structures.[57] The expansion of chemical diversity elements in aptamer libraries can facilitate stronger binding affinity as well as access to novel folding motifs.[69,70] When heteromultivalency is considered (**Figure 2-1**), improved target-binding properties have been reported.[71]

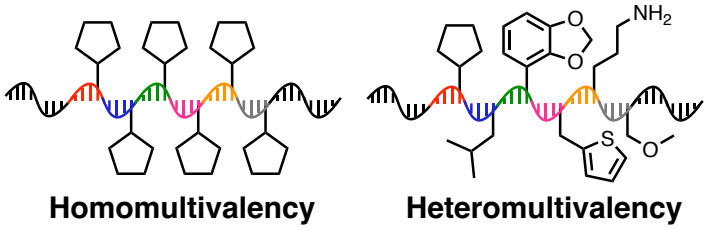

Figure 2-1: Homomultivalency and heteromultivalency

Our lab has recently developed LOOPER, a method to produce heteromultivalent sequence-defined nucleic acid polymers.[67,68,72,73] The 256-member pentanucleotide codon library was designed to allow for the incorporation of 16 different functional groups throughout a nucleic acid polymer.[67] The functional groups covered a wide substituent range, including aliphatic and aromatic groups, and Brønsted acids and bases (**Figure *1-8B***). LOOPER was ported into SELEX protocols for aptamer evolution, where a highly functionalized aptamer was successfully evolved against human α-thrombin after 6 rounds of LOOPER-SELEX. Upon kinetic evaluation, the aptamer (TBL-1) was found to exhibit a K_d of 1.6 nM by SPR to the target, and the modifications were confirmed to be essential to target binding.

While LOOPER is an effective strategy to access heteromultivalent aptamers, it has some associated limitations. The process is time-consuming, costly to perform, and low yielding. These limitations make further characterization and further study of these aptamers impossible. It also limits the technique's adoption to wider settings, since the produced aptamers cannot presently be synthesized to scale. Clearly, a strategy was required to produce larger amounts of LOOPER-derived aptamers.

The standard method to produce large quantities of DNA is through automated solid-phase synthesis on a synthesizer. Oligonucleotides can be synthesized from nanomole scale for

laboratory purposes, to massive kilogram-scale syntheses for use in therapeutics. Solid-phase synthesis is so successful at this because it is automated and drives reactions to completion by use of excess reagents, while impurities are washed away at each step, and unsuccessful couplings are capped to prevent deletion mutations in the final product. The chemistry used by solid-phase synthesizers was developed by Marvin Caruthers, and uses the phosphoramidite method to generate the phosphodiester linkage in a 3'-to-5' direction on solid support.[47,74] There are two options for solid-support in DNA synthesis: controlled-pore glass (CPG) particles and polystyrene (PS) particles. CPG is rigid, with deep pores where oligonucleotide synthesis occurs. Glass supports with a 50 nm pore are robust and used routinely for short synthesis. Larger pore sizes are needed where synthesis exceeds 40 bases, since the 50 nm pores tend to get blocked up beyond this length. However, larger pore sizes can compromise the structural integrity of the bead. PS beads are better at moisture exclusion than CPG beads, and they are efficient for synthesis on small scales (≤40 nmol). PS beads can be more densely loaded with nucleosides per gram, so they become more attractive for larger scale syntheses, though in these cases the efficiency drops due to steric hindrance between adjacent DNA chains.

The automated synthetic process of DNA synthesis on solid support occurs through several key steps (**Figure *2-2***): detritylation through trichloroacetic acid liberates the 5'-OH group from the 5'-DMT (4,4'-dimethoxytrityl) protecting group. The incoming nucleoside phosphoramidite monomer is activated with tetrazole and coupled to support-bound nucleoside. Where unsuccessful coupling occurs, the free 5'-OH group is acetylated to prevent further coupling. The next step is the oxidation (*P*(III) → *P*(V)) of the phosphite ester bond formed with the incoming nucleoside to stabilize the linkage between the monomers. Finally, the cycle returns to detritylation of the newly coupled base, preparing the oligonucleotide for the next base in the sequence. Coupling efficiency at each step is monitored by trityl absorbance, and average stepwise coupling of >99% is possible where fresh anhydrous solvents and reagents are used; the phosphoramidite cycle is very sensitive to moisture. After a full-length oligonucleotide has been synthesized, it must be cleaved from the solid support. This is commonly done using either ammonium hydroxide, or a 50:50 (v/v) mixture of Ammonium hydroxide and 40% aqueous MethylAmine (AMA),[75] and heat (65°C); this strategy also deprotects the requisite protecting groups on the bases and reveals the phosphodiester backbone.

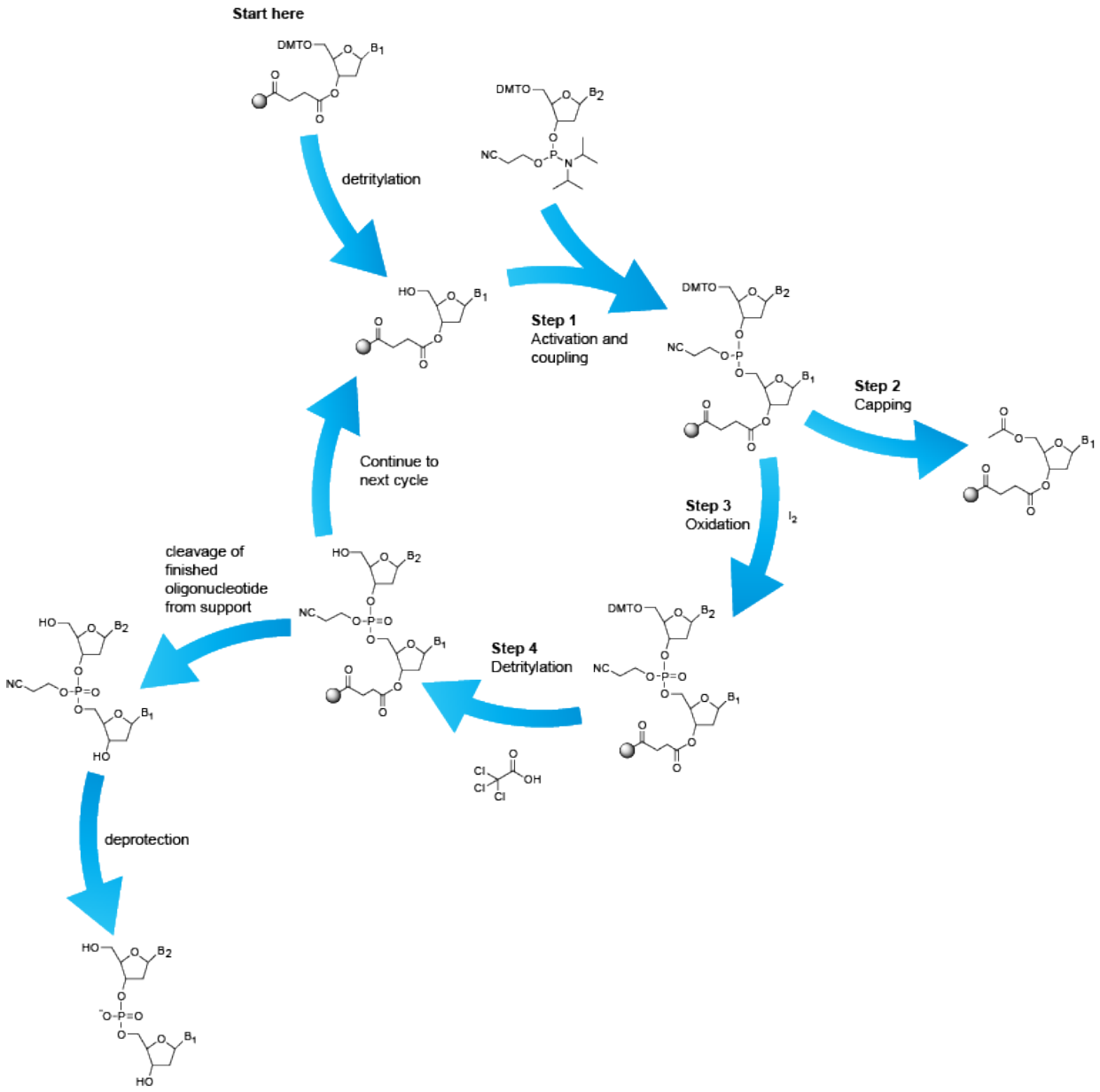

Figure 2-2: Automated solid-phase DNA synthesis cycle using the phosphoramidite method. Detritylation proceeds via trichloroacetic acid. Activation occurs with a tetrazole base. Capping uses N-methylimidazole to convert acetic anhydride to a strong electrophile for capping of the 5'-hydroxide. The oxidation step uses iodine and pyridine with water to convert the P(III) atom to a stable P(V). Cleavage from the solid support occurs through ammonium hydroxide or AMA, and heat.

To significantly increase yield, and decrease the cost and time, we envisioned an orthogonal deprotection and coupling method to synthesize LOOPER-derived aptamers by way of solid-phase oligonucleotide synthesis. This would provide the capability to produce up to thousands of orders of magnitude larger amounts of the aptamer and facilitate further study and

characterization of the evolved species.

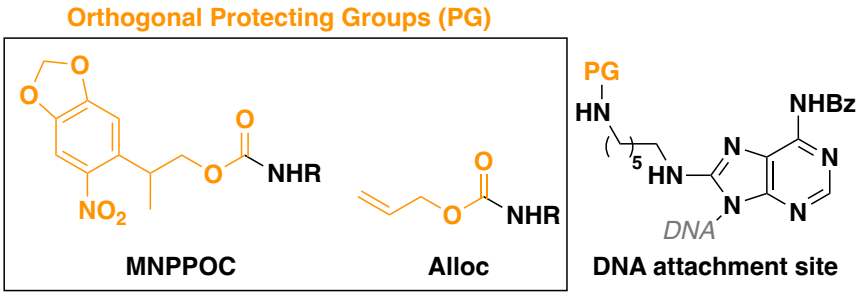

Figure 2-3: Orthogonal protecting groups and their attachment site on deoxyadenosine in solid-phase synthesis

However, solid-phase DNA synthesis involves both acids and bases in the coupling cycle. As such, conventional acid- and base-labile protecting groups must be excluded from use. 2-(3,4-Methylenedioxy-6-NitroPhenyl)PropylOxyCarbonyl (MNPPOC) and allyloxycarbonyl (alloc) are both orthogonal protecting groups. MNPPOC was developed as a photolabile protecting group for DNA oligonucleotides.[76] It is cleaved with UV light (365 nm). Alloc has been used for orthogonal deprotection in solid-phase peptide synthesis, and is cleaved with Pd(0) (**Figure *2-3***).[77,78] The protecting group would be installed at the terminal end of hexamethylenediamine (HMDA) linker, itself attached to the *C*-8 positions of adenine. The method would proceed as follows: the TBL-1 aptamer would be synthesized in sequence. The protecting-group-modified 2'-deoxyadenosine (modA) would be installed at the 5' end of pentamer codon. The entire column of beads would be removed from instrument, subjected to orthogonal deprotection, followed by EDC/NHS coupling of the chemical modification acid to the liberated amine. The column would then be put back on the DNA synthesizer, and extension of the oligonucleotide would be undertaken. The chemical diversity elements of TBL-1 would be incorporated where required until the synthesis of the LOOPER-derived aptamer was complete (**Scheme *2-1***).

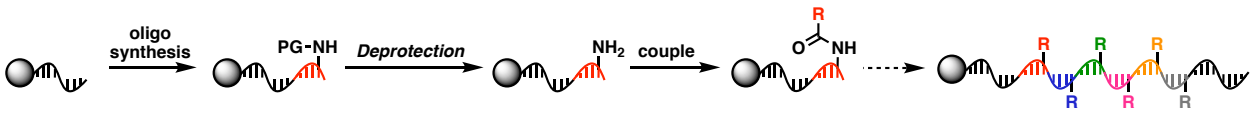

Scheme 2-1: Workflow of the orthogonal deprotection strategy

2.2 Results and Discussion

2.2.1 MNPPOC synthesis

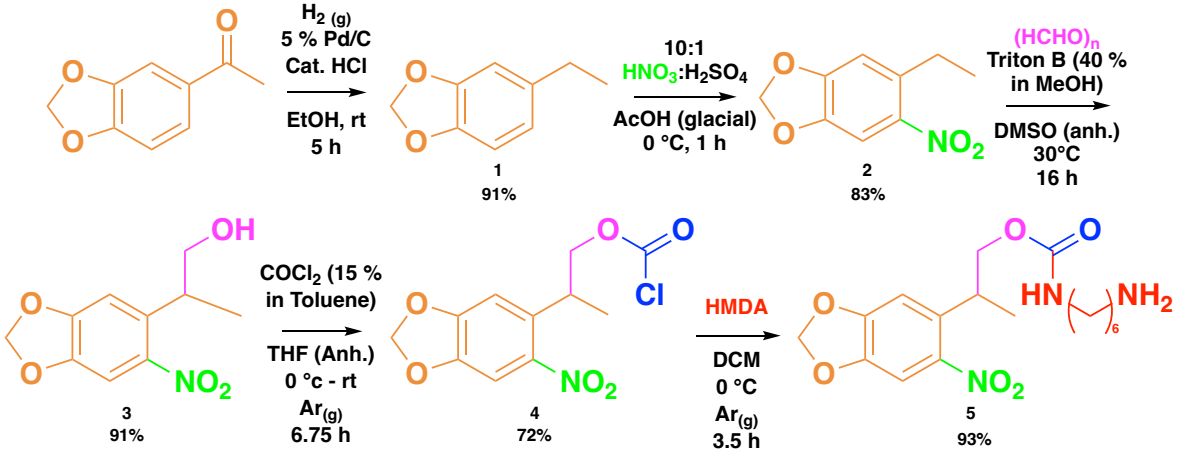

Scheme 2-2: Synthesis of HMDA-coupled MNPPOC. The overall yield across 5 synthetic steps was 46%

My first in this project was to synthesize the photolabile protecting group, MNPPOC (**Scheme *2-2***). The first step of that synthesis was the reduction of 3,4-(methylenedioxy)acetophenone to form **1**. The reported protocol for this reduction however posed some issues. The initial MNPPOC synthesis protocol employed the Huang-Minlon variant of a Wolff-Kishner reduction.[76] In practice, multiple product spots appeared by TLC, indicating incomplete reduction and by-product formation. I tried another protocol, calling for 10% palladium on carbon (Pd/C) in acetic acid with ammonium formate as the hydrogen source.[79] Unfortunately, I saw no starting material conversion to product, potentially due to acetic acid competition with ammonium formate on the Pd. My next attempt was to use H_2 (g) directly with 10% Pd/C in anhydrous THF. This protocol showed conversion of starting material to another compound, but I found that it was not the desired product. I hypothesized that the product I was seeing was a partial reduction of the ketone to the alcohol. In the interest of moving forward, a previously established protocol for MNPPOC synthesis within our research group was undertaken, which split the Huang-Minlon reduction into two parts, first by preparing the hydrazone and isolating it, then reducing it with potassium hydroxide. Since that procedure was performed over two days and based in the suspected hypothesis that partial reduction was being observed by the H_2 (g) reduction, another reaction was conducted simultaneously, this time using a catalytic amount of HCl with the belief

this would protonate the ketone and promote reduction; it would also facilitate reduction of the benzylic alcohol by protonation. This acid-catalyzed reduction was quite successful, yielding 91% of **1** on a 5 g scale.

The initial reported protocol for the nitration step, as with the reduction, was not a clean reaction and did not appear to produce product. The conditions called for 40% nitric acid (aqueous) in dichloromethane (DCM), two immiscible liquids. Despite vigorous stirring, starting material conversion was essentially absent. The procedure was attempted with unconcentrated nitric acid, which supplied a modest amount of product, but showed contamination. Another method was sought, wherein all reactants and reagents were miscible. A protocol[80], performed in acetic acid with a catalytic amount of sulphuric acid mixed with the nitric acid (1:10, respectively) was found, which quickly and thoroughly furnished the nitrated product **2** with an 83% yield at a 2.5 g scale.

Table 2-1: Optimization for preferential 3 formation

Entry	Triton B equivalents	Paraformaldehye equivalents	Product:by-product:starting material ratios	Approx. product yield, %	Time, h	T, °C
1	0.55	4.3	1:0.76:0.73	40	3	90
2	1	3.7	1:1:1	33	3	90
3	1	3.7	1:0.14:0.15	78	**22**	**30**
4	1	**5**	1:0.05:0.22	79	5.75	30
5	1	10	1:0.09:1	48	4.4	30
6	1	5 (batch add'n)	1:0.74:0.52	44	4.5	30
Experimental results of optimized conditions						
7	1	5	1:0.09:0.07	86	16	30

The most challenging step of the synthesis was the formaldehyde addition reaction to formaldehyde. The initial reported conditions, using paraformaldehyde with Triton B in methanol as base, were ineffective at converting the starting material, being left for days with only slight product formation (by TLC). It was seen that paraformaldehyde, due to the reaction heat (~80°C) was evaporating out of the reaction mixture and precipitating above on the flask walls. Thus, another protocol[81] was implemented, using the same reagents, but adding in DMSO to maintain mixture homogeneity. After two hours I observed all starting material had been consumed. After purification by column chromatography (35% EtOAc/Hex), two spots very close together appeared by TLC, and NMR confirmed the presence of two distinct products. A second run of this

reaction, followed by column separation of these spots indicated the desired product, as well as a by-product were synthesized. Through 2D NMR analysis of the second spot, the by-product was identified (**Figure *2-4***). Optimization, summarized in **Table 2-1**, was performed to find the greatest starting-material-conversion and by-product-minimization conditions. My first thought was the by-product, presumably formed through nucleophilic aromatic substitution (S_NAr) attack with methanol, required more energy than the C-C bond formation. I devised a temperature gradient experiment, wherein the reaction was started at room temperature, and every hour temperature would be increased until product formation (as determined by TLC) was observed; once product formation was seen at a given temperature, no further increases were implemented. This experiment was also left overnight to facilitate starting material conversion. My next optimization parameter, paraformaldehyde equivalents, were then examined (**Table 2-1, entries 4-6**). The first alteration was increasing paraformaldehyde equivalents to 5. These results displayed minimized by-product formation at the expense of a decrease in starting material conversion compared with **entry 3**. The reaction appeared to be complete after 2 hours, but was allowed to continue further to validate that hypothesis. **Entries 5** and **6** were performed simultaneous to examine paraformaldehyde effects on the reaction. The experiment shown in **entry 5** used 10 equivalents of paraformaldehyde, the results of which showed that a large excess hampered the reaction progress. The experiment for **entry 6** started with 1 equivalent of paraformaldehyde, and an additional equivalent was added every 25 minutes until 5 equivalents had been added; I monitored the reaction by TLC before each addition. Before the second equivalent had been added, TLC indicated significant by-product formation, providing further insight into the role of paraformaldehyde in the reaction: too much inhibits starting material conversion, while too little coerces by-product formation. As such, paraformaldehyde, above all other reaction components, appears to dictate the reaction pathway. The optimized reaction conditions, taken collectively from **entries 3** and **4**, are shown in **entry 7**; compound **3** was produced in a 91% yield on a 1.9 scale.

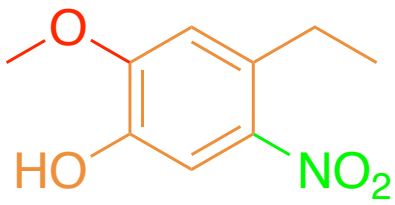

6

Figure 2-4: By-product 6 formed during the synthesis of 3

The chloroformate-forming step proceeded as initially reported without optimization or alternative protocols, giving **4** in 72% yield through employ of phosgene and THF (anhydrous). Monitoring the reaction by TLC, however, did not show obvious starting material conversion, even when the reaction was worked up and complete product formation was confirmed by NMR. I hypothesized that the acidic nature of the TLC plate hydrolyzed the product, so that both starting material and product appeared by TLC, even when starting material was likely entirely converted. Large scale reactions for this product were not performed; I observed stability of the product over 2 days at 4°C, however the potential for this reactive product to hydrolyze back to **4** was too much of a concern, so chloroformate production would only be performed as needed.

I synthesized **5** by injecting a solution of chloroformate **4** in DCM dropwise over 1.5 hours into a large equivalents of an HMDA solution in DCM stirring at 0°C.[82] Coupling MNPPOC to HMDA in this manner significantly reduced the chances of coupling to both free amines bookending the HMDA linker. By TLC, all starting material was converted to product. I confimed the successful synthesis by ^{1}H, ^{13}C NMR, and MS, with a 93% yield at a 60 mg scale. Finally, I had successfully synthesized compound **5** (MNPPOC appended to one end of HMDA linker) for attachment to modified 2'-deoxyadenosine (dA). **5** was synthesized at an overall yield of 46% across the 5 steps.

2.2.2 Alloc-HMDA coupling

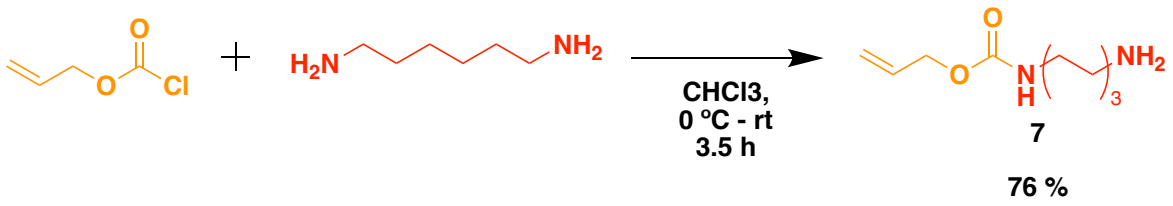

Scheme 2-3: Allyl chloroformate-HMDA coupling

To couple the allyl chloroformate to HMDA, I followed the same procedure as with MNPPOC (**Scheme *2-2***), but without an inert atmosphere. Successful synthesis of **7** was confirmed by ^{1}H, ^{13}C NMR, and MS.[83] It is interesting to note that the ^{1}H NMR did not show the proper number of protons; experimentally, 17 protons were observed. From another report of HMDA coupling to alloc, 21 protons were reported.[84] **7** should display 20 protons, which suggests that the carbamate may affect proton visibility on an NMR timescale. When I tried switching deuterated solvents for NMR, I saw no clearer resolution of the protons. Nonetheless, with synthetic validation from ^{13}C NMR and MS, including no double-addition product, both HMDA-linked protecting groups awaited coupling to modified dA.

2.2.3 Synthesis of modified phosphoramidite

The next part of this project was the synthesis of the modified dA phosphoramidite. **Scheme 2-4** outlines the synthetic route to this phosphoramidite.

I started with bromination of the *C*-8 position of 2'-deoxyadenosine. The reaction was performed in a 1 M pH 4 sodium acetate buffer at room temperature. Formation of **8** was complete after 3 hours by TLC monitoring, and product was precipitated out of solution by the addition of 10 M NaOH to pH 10. **8** was confirmed successfully synthesized by ^{1}H NMR, with an 55% yield at 5 g scale. I formed **9** with 4,4'-dimethoxytrityl chloride (DMT-Cl) in pyridine, using 4-dimethylaminopyridine (DMAP) as a catalyst. The crude material was then subjected to column purification using silica deactivated by 1% TEA in DCM. **9** was eluted with a 0-5% MeOH/DCM solvent gradient, and the pure product was isolated at an 86% yield at a 3.5 g scale. The formation

of **10** proceeded through transient protection of the 3'-hydroxyl group with trimethylsilyl chloride (TMS-Cl), followed by overnight benzoylation of the *C*-6 amino group. The TMS group was removed with 2M methanolic ammonia, and I performed column chromatography on the crude material using a 0-3% MeOH/DCM gradient. Purified **10** was relinquished at 71% yield at a 3.5 g scale.

At this stage of the synthesis, I had to decide on which protecting group I would move forward with. I considered the conditions by which both orthogonal deprotections would proceed, relative to the practicalities of their use. For MNPPOC, the beads in the column of the DNA synthesizer would need to be exposed to UV light in such a way that all amines were 100% exposed to the light to achieve 100% deprotection. To me, this was risky, since the column would need to be opened to expose the beads, and it would be difficult to be totally confident that all beads had been significantly exposed/deprotected. The deprotection of alloc is solution-phase. To perform the deprotection, 1 mL syringes could be easily attached to either end of the synthesizer column, creating a sealed, makeshift reactor. The syringes could be inversely pumped back and forth to mix the solution and the beads, and the column can then be replaced on the DNA synthesizer to continue oligonucleotide synthesis. I decided to move forward with the alloc protecting group, **7**.

Next was the synthesis of compound **11**. An S_NAr was performed in ethanol at reflux for 5 hours to insert **7** at the *C*-8 position of adenosine in a 78% yield after column chromatography purification (0-5% MeOH/DCM). I confirmed **11** was successfully synthesized by ^{1}H and ^{13}C NMR, and mass spec data.

Finally, I performed the phosphitylation reaction to produce the final modified phosphoramidite **12** (modA). 2-cyanoethyl-N,N-diisopropylchloro phosphoramidite was stirred for 3 hours with **11** in DCM after which TLC indicated the total consumption of starting material. Column purified of the **12** proved difficult due to poor resolution of the product spot relative impurities just surrounding the desired spot. However, pure product was isolated (**$modA_1$**), as well as some mostly pure, but somewhat mixed product (**$modA_2$**). By NMR and mass spec data, the product was confirmed synthesized in both cases, and no notable impurities were observed. I found an 80% yield for this step, at a 65 mg scale. I assumed that any impurity would not participate in DNA synthesis, and the only coupling would occur between phosphoramidite **12** and the incipient oligonucleotide.

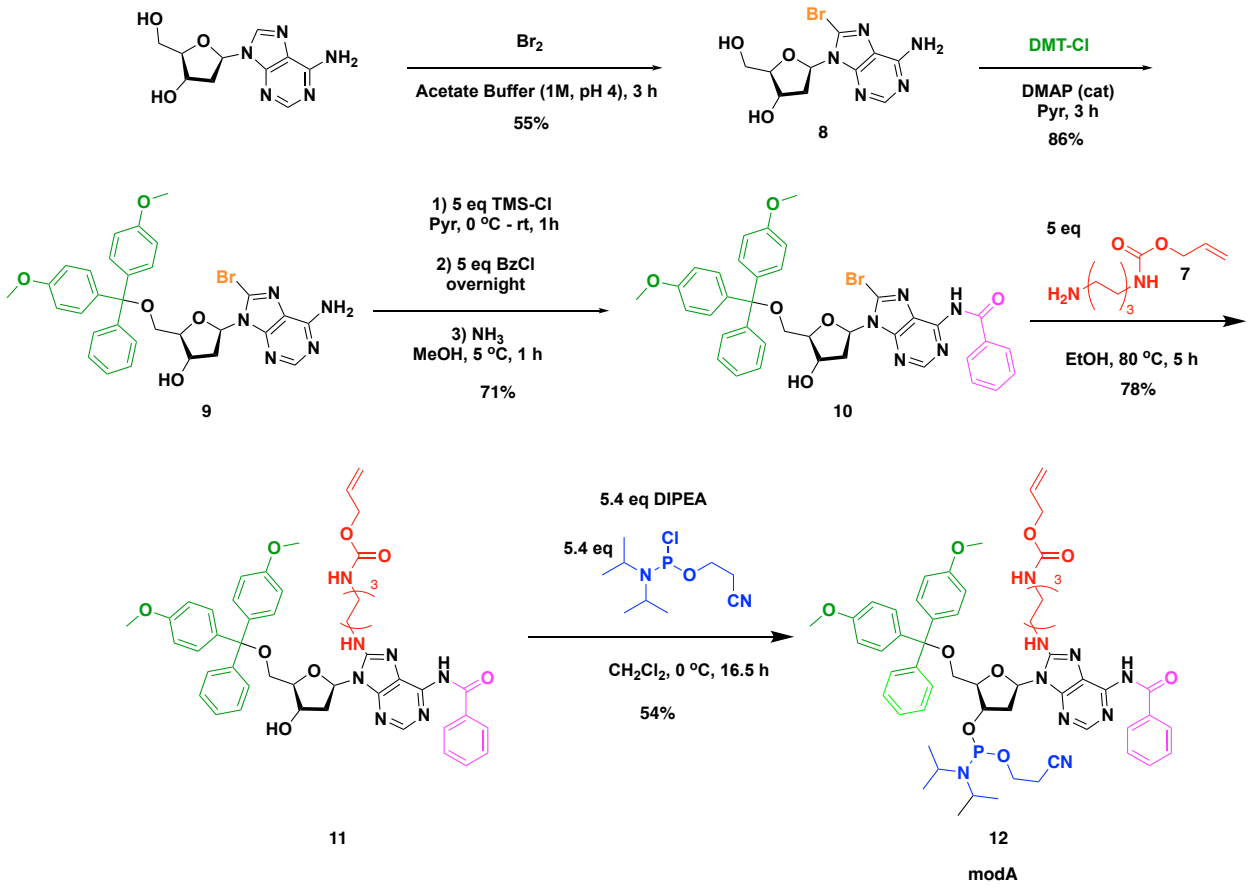

Scheme 2-4: Synthetic route to alloc-protected 2'-deoxyadenosine phosphoramidite

2.2.4 Pentamer synthesis

Solid-phase DNA synthesis is performed in small columns loaded with CPG beads which are pre-immobilized with one of the four canonical. For all synthesizer runs, oligonucleotides wer synthesized at a 0.2 µmole scale. To make sure the synthesizer was functioning properly, and that the reagents were fresh, I set up a synthesis of a test pentamer oligo. For most experiments run on the synthesizer, I often ran test pentamers first for this reason.

Test pentamer 5'-ACTAG-3' was synthesized. After AMA cleavage off-bead and deprotection, I purified the sequence using High-Performance Liquid Chromatography (HPLC), and the sequence was confirmed successfully synthesized by mass spectrometry. The next step was to synthesize a pentamer with modA, **12**.

When conducting solid-phase DNA synthesis, the only way to confirm the results are HPLC and mass spectrometry data. To analyse the pentamer, the sequence must be cleaved off bead, which means no additional experimentation can be performed on it (i.e., oligonucleotide extension, or deprotection). Alloc deprotection must be performed before any analysis can be conducted on the pentamer, and no information can be gleaned about whether the deprotection worked until the sequence is analyzed.

Several slightly different alloc deprotection methods exist in the literature. The first involves tetrakis(triphenyphosphine)-palladium(0) ($Pd(PPh_3)_4$) at 0.24 equivalents, Phenylsilane ($PhSiH_3$) at 20 equivalents as the nucleophile, with 40 mL of dichloromethane (DCM) with stirring for 1 hour.[85] The next used 0.10 equivalents of $Pd(PPh_3)_4$, and 24 equivalents of $PhSiH_3$, in 4 mL of DCM with stirring for 10 minutes.[86] The third variant used 0.25 equivalents of $Pd(PPh_3)_4$, 24 equivalents of $PhSiH_3$, in 8 mL of DCM, stirred for 30 minutes.[87] Since the deprotection must occur within the synthesizer column, I reduced the volume to 1 mL. My initial deprotection protocol was thus adapted from the preceding methods, to use 0.24 equivalents of $Pd(PPh_3)_4$, 20 equivalents of $PhSiH_3$, 'stirring' for 15 minutes (which involved mechanically pumping the syringes back and forth on either end of the column).

A sequence, 5'-modAGCTA-3', was synthesized on two columns using **$modA_2$**. Upon completion of synthesis on instrument, oligonucleotide extension of column 2 was performed to elongate the sequence to 5'-TACGmodAGCTA-3' (**T2**). A small amount of column 1 beads were removed (**T3**), and the rest of the beads were subjected to the adapted alloc deprotection protocol (**T4**). **T2** beads were cleaved off bead with AMA, as well as the **T3** and **T4**. After purifying the sequences by HPLC, I submitted the sequences for analysis by mass spec. Elongated oligonucleotide **T2** was observed as an octamer, instead of the expected nonamer synthesized. Additionally, sequence **T3** was observed as the n-1 tetramer, not the expected modA pentamer. Correspondingly, **T4** was also confirmed as the n-1 tetramer.

Since these results were not known right away (due to typical delays in receipt of mass spec results), I wanted observe whether the non-incorporation of **12** was just a one-off occurrence; I made another attempt to synthesize the modified pentamer. Using $modA_2$, I attempted another modified pentamer synthesis with the sequence 5'-modACGAT-3' (**T5**). The beads were then subjected to the on-column alloc deprotection protocol. I then cleaved all sequences off-bead with AMA and purified them by HPLC. Unfortunately, I again observed entirely truncated products in

the HPLC trace. It became clear that whatever impurity existed within $modA_2$ was causing catastrophic failure in coupling. The next modified pentamer synthesized would use the pure fraction $modA_1$.

I set up a synthesis of sequence 5'-modATGCA-3' (**T6**) using $modA_1$ phosphoramidite. After AMA cleavage and HPLC purification, I saw that again **T6** showed only truncated products. Even though this synthesis had used a pure fraction of the phosphoramidite **12**, coupling was still being inhibited. The coupling of this class of phosphoramidite produced following this synthetic pathway had already been reported within our lab, so I found it bizarre that oligonucleotide synthesis involving this specific phosphoramidite was experiencing such problems.[88]

Having used up all my stock of **12**, I subjected the remainder of my stock of **11** to phosphitylation. Upon column purification, ^{1}H NMR analysis and mass spec data confirmed the synthesis of **12**, **$modA_3$**. I tried pentamer synthesis again with this newly formed phosphoramidite.

I set up the synthesis of **T7**, 5'-modATCGA-3' using phosphoramidite **$modA_3$**. A small number of beads were removed from the modified pentamer column (**T7-pre**), and the rest of the beads were subjected to on-bead alloc-deprotection (**T7-post**). All beads were then subjected to AMA cleavage and HPLC purification. By HPLC analysis, both **T7-pre** and **-post** were truncation products. Clearly, something relatively benign within the 'pure' phosphoramidite mixture was wreaking havoc within solid-phase DNA synthesis. By this point, all remaining stock of compound **11** had been consumed by these experiments.

2.2.5 Phosphoramidite ($modA_4$) synthesis revisited

I performed again the bromination of the *C*-8 position of 2'-deoxyadenosine. This time, I modified the conditions to a portion-wise addition of bromine in a 1 M sodium acetate buffer, pH 4.0, to a solution of dA in the same buffer over 20 minutes, followed by 3 hours of stirring. The reaction was quenched with sodium bisulfite, and the resulting solution was neutralized to pH 11 with 10 N sodium hydroxide, where the brominated product precipitated while stirred in an ice bath. Analysis of the ^{1}H NMR indicated successful synthesis of **8**, and agreed with previous experimental results, and the literature.[89]

The 5' alcohol of **8** was then subjected to dimethoxytrityl (DMT) protection. After column purification, I confirmed the synthesis by ^{1}H NMR, and comparison of that spectrum with

previously synthesized product at 46% yield. Transient protection of the 3'-alcohol by TMS-Cl, followed by the benzoylation of the *C*-6 amine group afford **10** in a 78% yield after column purification. Next, I coupled alloc-HMDA **7** to **10** via S_NAr, and produced **11** at a 65% yield after purification. Finally, phosphitylation was performed to produce **12**. I tried to find a better solvent system to purify the compound, attempting 5% MeOH/Hexanes, 20% Ethyl Acetate/Hex, 5% MeOH/$CHCl_3$, and 10% MeOH/DCM. However, I found no better resolution from any of these solvent systems over 5% MeOH/DCM, so proceeded to purify the compound with the previously used system. I ended up with **12** in a 59% yield after purification. **modA$_4$** was ready for the next attempt at pentamer synthesis. Additionally, I was told by an expert during a conference that in-house synthetic phosphoramidites need to be used at a higher concentration for use on DNA synthesizers, so I took that information forward for the pentamer synthesis as well.

2.2.6 Modified pentamer deprotection and coupling

After a successful test pentamer synthesis, **modA$_4$** was dilute to 0.2 M (bases for DNA synthesis are usually at a 0.1 M concentration) and installed on the DNA synthesizer. I synthesized a hexamer **T8** (5'-TmodAGCAC-3') modA in the 5th position, so that I could observe base-coupling on modA, instead of that base being terminal. After AMA cleavage off bead, the sample was purified by HPLC, which produced figure 100. From the HPLC trace, it was immediately clear that full-length oligonucleotide was produced. After DMT cleavage, and HPLC purification, I analyzed the oligo by mass spec and found that the hexamer had been successfully synthesized. Having *finally* incorporated the base into an oligonucleotide, the next step was to attempt on-bead deprotection of the alloc group.

Another pentamer (**T9**) was synthesized of sequence 5'-modACTGT-3'. The beads were then subjected to alloc deprotection protocol. Following deprotection, the oligonucleotide was cleaved off-bead by AMA, and purified by HPLC. After DMT removal, **T9** was purified by HPLC. The sequence was again submitted for mass spec analysis. Excitingly, a mass of 1590.4086 was found. The expected mass for the deprotected amine in the modA pentamer was 1590.4085, which meant the alloc deprotection had been successful in liberating the amine on-bead (***Figure 2-5***). Finally, I could move forward with examining amide bond formation with chemical modifications acids to produce TBL-1.

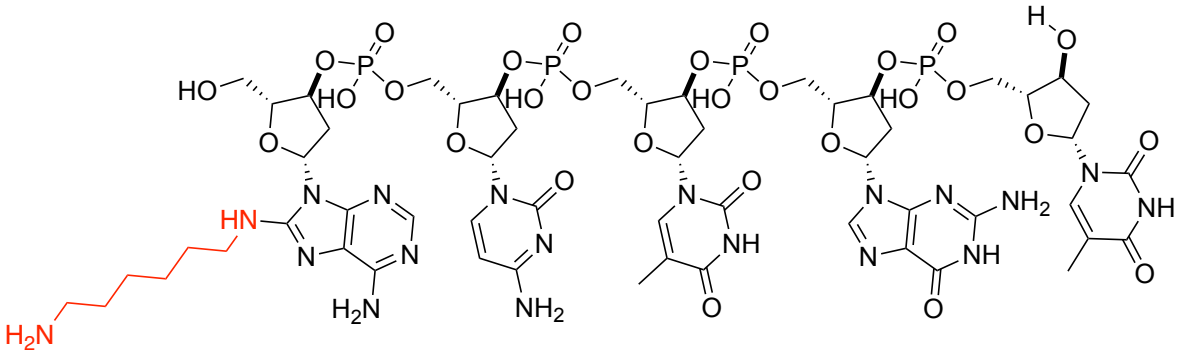

Figure 2-5: The successfully deprotected modified pentamer T9

Within TBL-1's reading frame are eight chemical modifications coming off the modified adenosine base; they are summarized in **Table 2-2**. Before proceeding with the solid-phase synthesis of TBL-1, I needed to verify the successful coupling of each acid to the modified phosphoramidite. During the full synthesis of the aptamer, there would be no way to validate each step coupling step since the oligonucleotide would have to remain on-bead. So, to feel confident moving forward with the synthesis, each acid would need to couple with ~100% yield.

Table 2-2: TBL-1 chemical modification acids

Pentamer Codon (5'-ANNNN-3')	**Chemical Modification**	**Chemical Structure**
ACTGC	1-methylpiperidine-4-carboxylic acid•HCl	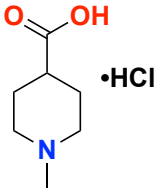
ATCTA	Isovaleric acid	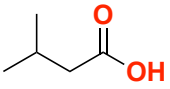
ATTCC	Cyclopentylacetic acid	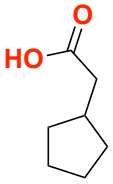
AACCT	Succinic anhydride	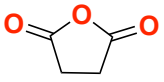

ATCCA	Phenylacetic acid	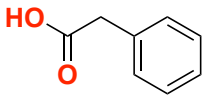
ATCCT	Succinic anhydride	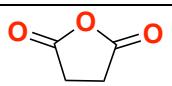
ATTCG	3-thiopheneacetic acid	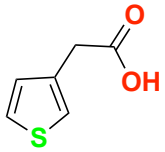
ATGCT	Succinic anhydride	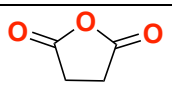

I first attempted the coupling of 1-methylpiperidine-4-carboxylic acid to the deprotected amine. **T10**, the corresponding TBL-1 codon sequence 5'-modACTGC-3' was synthesized and subjected to alloc deprotection protocols. I then applied an adapted EDC/NHS coupling from the protocols reported in the TBL-1 study:[68] a 1M solution of the acid in DMSO was activated for coupling with a 1M solution of NHS (in a 1:1 DMSO:water mixture) and a 1M solution of EDC in DMSO for 30 minutes with gentle agitation. In the same fashion as the alloc deprotection, this activated acid solution was taken up in a 1 mL syringe, and in another, a 500 mM sodium carbonate (Na_2CO_3) buffer in water, pH 9. The syringes were inserted into either end of the synthesizer column, and the contents were mixed. The reaction was incubated for 1 hr with gentle agitation every ~10 minutes, followed by quenching with 500 mM Tris•HCl buffer in water. After the reaction, I dried the beads, cleaved the DNA off-bead with AMA, and purified the oligonucleotide by HPLC. Through LC/MS analysis, the coupling was unsuccessful.

I made another attempt at coupling on a chemical modifier acid to the deprotected amine, this time following a coupling protocol reported by Glen Research, a chemical supplier of DNA synthesizer reagents and bases. **T11**, a sequence of 5'-modAACCT-3', corresponding to succinic anhydride modifier, was synthesized on the automated synthesizer. Alloc was deprotected, and the acid was activated by a modified protocol, adding mono-methylsuccinate, NHS, and EDC first to a vessel, solubilizing these components with DMSO and water, followed by 30 minutes of gentle agitation at room temperature. I took up the activated acid mixture, along with 1% DIPEA, and mixed both solutions on the synthesizer column. The reaction was left to incubate at 37°C for 2 hours. After the reaction finished, I washed off the beads on synthesizer, added a G base to the 5'

end of the sequence, then subjected the sequence to AMA cleavage off-bead for HPLC purification and evaluation. Unfortunately, the coupling was again unsuccessful.

I made a final attempt at coupling mono-methyl succinate by the Glen method. I synthesized **T12**, corresponding to 5'-modATGGA-3', performed alloc deprotection, and activated the acid to form the NHS ester. The activated acid solution was mixed with 1% DIPEA on the DNA synthesizer column, and the reaction was incubated for 3 hours at 37°C. After removal of the reaction mixture and rinsing of the beads, I coupled a T base onto the sequence, cleaved the oligonucleotide off-bead by AMA, and purified by HPLC. Disappointingly, the acid did not couple to the amine.

2.3 Conclusions

I successfully synthesized and coupled two orthogonal protecting groups to an HDMA linker. Practical limitations of both methods were considered, and I opted to move forward with the alloc protecting group for the synthesis of a modified aptamer on an automated DNA synthesizer. I synthesized and characterized the alloc-protected 2'-deoxyadenosine phosphoramidite for to use as a base on the DNA synthesizer. A protocol was established for successful deprotection of the amine on-column and coupling methods for the functionalization of the liberated amine were attempted, though were ultimately unsuccessful. Alternative methods for amine functionalization on-column should be sought, attempted, and verified. Once the method shows it couples for ~100% yield, all functionalized acids found in TBL-1 should be examined for compatibility. Finally, the full-length TBL-1 LOOPER-derived aptamer should be synthesized and tested to verify kinetic activity against thrombin, using SPR or BLI.

2.4 Experimental details and supporting data

2.4.1 General information

^{1}H NMR spectra were recorded at 400 MHz on a Bruker spectrometer. Processing of the spectra was performed with MestReNova software. Analytical thin-layer chromatography (TLC) was

performed on aluminum plates pre-coated with silica gel $60F_{254}$ as the adsorbent. The developed plates were air-dried and exposed to UV light. Column chromatography was performed using Silicycle SiliaFlash® F60 silica, 40-63 μm (230-400 mesh). All materials and reagents used for oligonucleotide synthesis were purchased from Glen Research™. Oligonucleotide synthesis was performed on an ABI 394 synthesizer using a (DiMethoxyTrityl) DMT-ON protocol on a 0.2 μmol scale (1000 Å CPG column). Oligonucleotide cleavage off-bead was performed by submerging the beads under 400 μL AMA (50:50 (v/v) mixture of Ammonium hydroxide and 40% aqueous MethylAmine) solution in a 1.5 mL tube. After vortex and centrifugation, the tube was heated at 65°C for 15 minutes. Upon cooling, the tube was centrifuged, and the supernatant was carefully collected and transferred to a second tube. The second tube underwent 35°C SpeedVac evaporation, leaving a dry residue at the bottom of the tube. DMT-ON oligonucleotide products were purified by reverse-phase high-performance liquid chromatography (HPLC, 1260 Infinity II LC System) using a C18 stationary phase (Eclipse-XDB C18, 5 μm, 4.6 × 150 mm) and an acetonitrile (solvent B)/0.1 M triethylammonium acetate (TEAA buffer, solvent A) gradient (**Table *2-3***). Purified products were lyophilized using a FreeZone 2.5 L -84 °C Benchtop Freeze Dryer. Purified oligonucleotides were subjected to DMT removal by reconstitution of the purified residue in 1 mL of 40% acetic $acid_{(aq)}$, incubation for 1 hr, followed by lyophilization. Purification of the DMT-OFF samples were again performed by RP-HPLC. Oligonucleotide product concentrations were quantified from A_{260} values using a Nanodrop One UV-Vis Spectrophotometer. Mass spectrometry of coupled products was carried out using the Velos Pro Mass spectrometer (Orbitrap Elite MS). The mass accuracy of Velos Pro Orbitrap ranges from 0-6.62 ppm.

Table 2-3: HPLC DMT-ON (collection at 15 min) and DMT-OFF (collection at 3 min) protocol

Time (min)	Solvent A (%)	Solvent B (%)	Flow (mL/min)
0	90	10	4
10	80	20	4
20	20	80	4
25	20	80	4
28	90	10	4
30	90	10	4

2.4.2 Synthetic procedures and supporting data

5-ethylbenzo[*d*][1,3]dioxole, 1

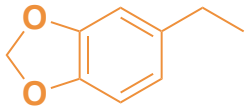

Compound **1** was synthesized following a procedure adapted from literature.[90] 3',4'-(methylenedioxy)acetophenone (5.0125 g, 30.5342 mmol) was dissolved in 86 mL ethanol and heated to 35°C for 5 min. 0.35 mL of conc. HCl were added to solution, and the flask was purged under argon. 5% Pd/C (0.5 g, 4. 7 mmol, 0.1 equiv.) was added, followed by flask atmosphere evacuation under vacuum. Three cycles of filling the flask with $H_{2\,(g)}$, then evacuating under vacuum were performed, then the solution was stirred for 5 hours until starting material was consumed by TLC (20% EtOAc/Hex). The reaction mixture was gravity filtered and concentrated to yield a yellow oil. NMR was matched with literature values. ^{1}H NMR (400 MHz, $CDCl_3$) δ 6.74 (t, J = 8 Hz, 2H), 6.65 (d, J = 8 Hz, 1H), 5.91 (s, 2H), 2.60 (q, *J* = 7.6 Hz, 2H), 1.22 (t, *J* = 7.3 Hz, 3H)

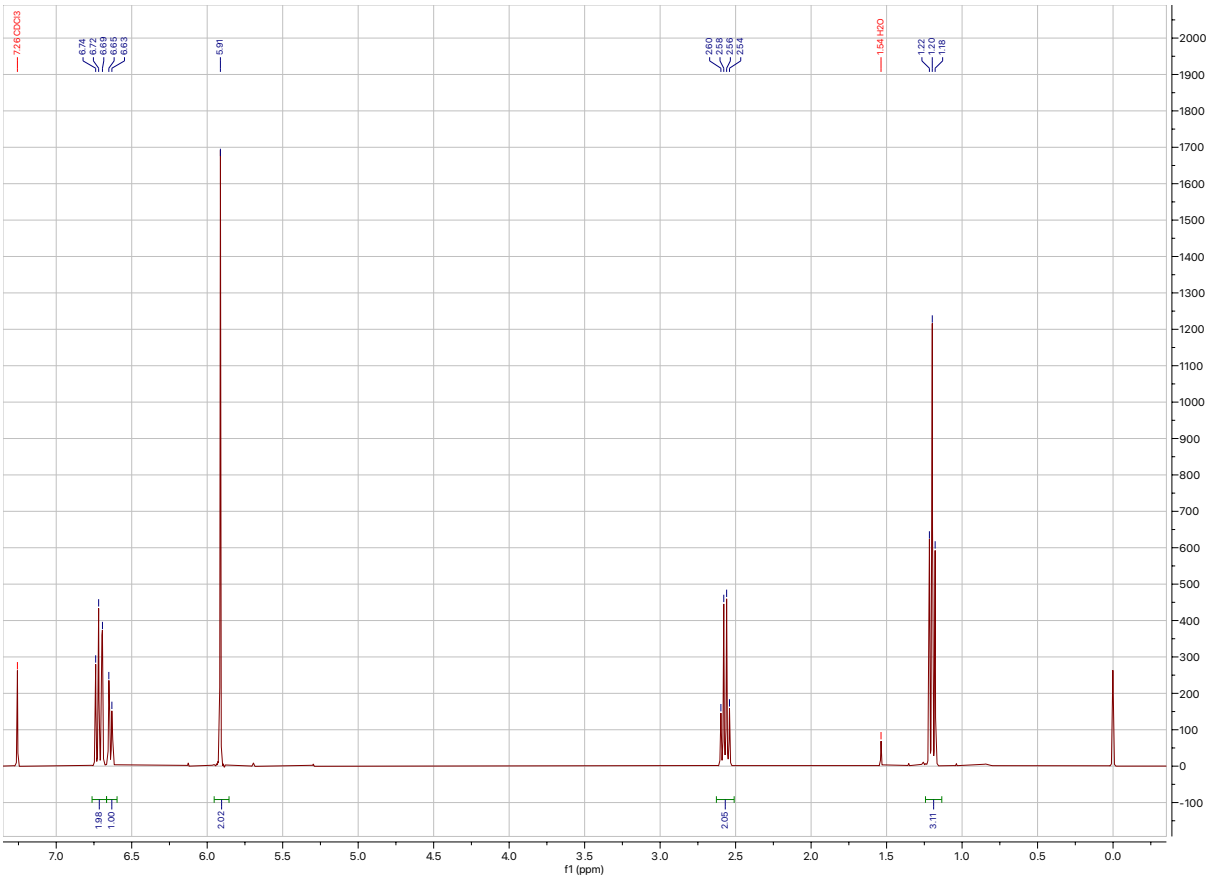

5-ethyl-6-nitrobenzo[*d*][1,3]dioxole, 2

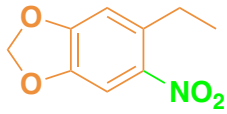

Compound **2** was synthesized following a procedure adapted from literature.[91] **1** was dissolved in glacial acetic acid (11 mL) at 0°C. A 10:1 HNO_3:H_2SO_4 mixture was added dropwise, and the reaction was stirred for 1 hour, after which TLC indicated the starting material had been consumed (20% EtOAc/Hex). The reaction mixture was extracted with 4 x 15 mL ethyl acetate, and the combined organics were washed with 4 x 15 mL dH_2O. The organic layer was washed with 2 x 15 mL sat. $NaHCO_{3\ (aq)}$, and the organic layer was dried over Na_2SO_4, filtered, and concentrated, yielding the product as a brown-red oil. NMR was matched with literature values. ^{1}H NMR (400 MHz, $CDCl_3$) δ 7.47 (s, 1H), 6.75 (s, 1H), 6.08 (s, 2H), 2.92 (q, J = 7.6 Hz, 2H), 1.28 (t, J = 7.6 Hz)

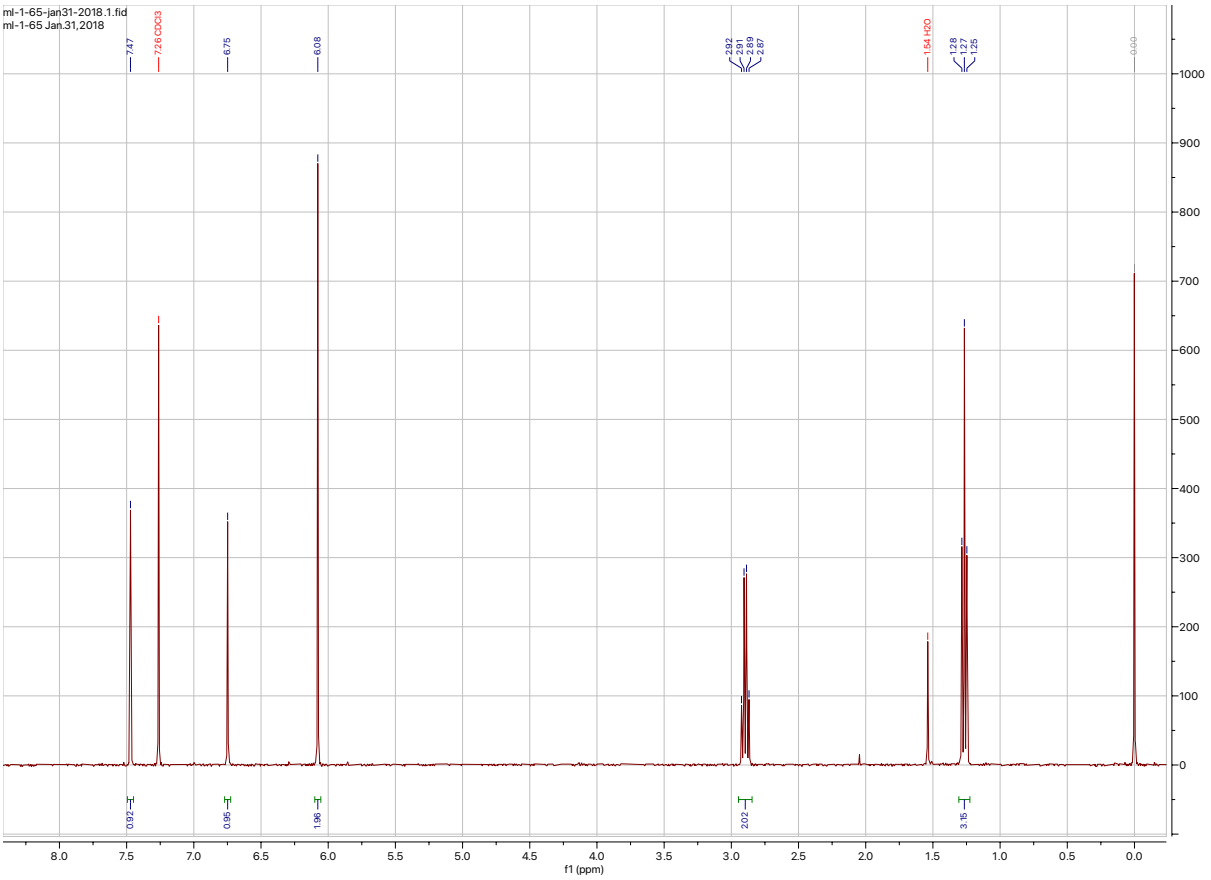

2-(6-nitrobenzo[*d*][1,3]dioxol-5-yl)propan-1-ol, 3

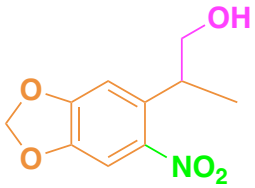

Compound **3** was synthesized following optimization of a procedure adapted from the literature.[92] **2** (1.867 g, 9.568 mmol) was dissolved in anhydrous DMSO (9.5 mL), followed by paraformaldehyde (1.450 g, 47.85 mmol, 5 equiv.) and Triton B (40% in methanol) (1.68 mL, 9.568 mmol, 1 equiv.) were then added, and the reaction was heated to 30°C and stirred for 16 hours, after which TLC indicated starting material had been consumed (20% EtOAc/Hex). The reaction mixture was quenched by the addition of 20 mL 5% $HCl_{(aq)}$. The aqueous layer was extracted with 4 x 15 mL ethyl acetate. The combined organics were washed with 2 x 20 mL brine, dried over Na_2SO_4, filter, and concentrated. The crude mixture was purified by column chromatography (20 – 40% EtOAc/Hex), yielding pure **3** as yellow-brown solid. NMR was

matched with literature values. ^{1}H NMR (400 MHz, $CDCl_3$) δ 7.33 (s, 1H), 6.89 (s, 1H), 6.09 (d, J = 6.04 Hz, 2H) 3.83 (m, 2 H), 3.68 (m, 1 H), 1.62 (t, J = 5.72, 1H) 1.29 (m, 3H)

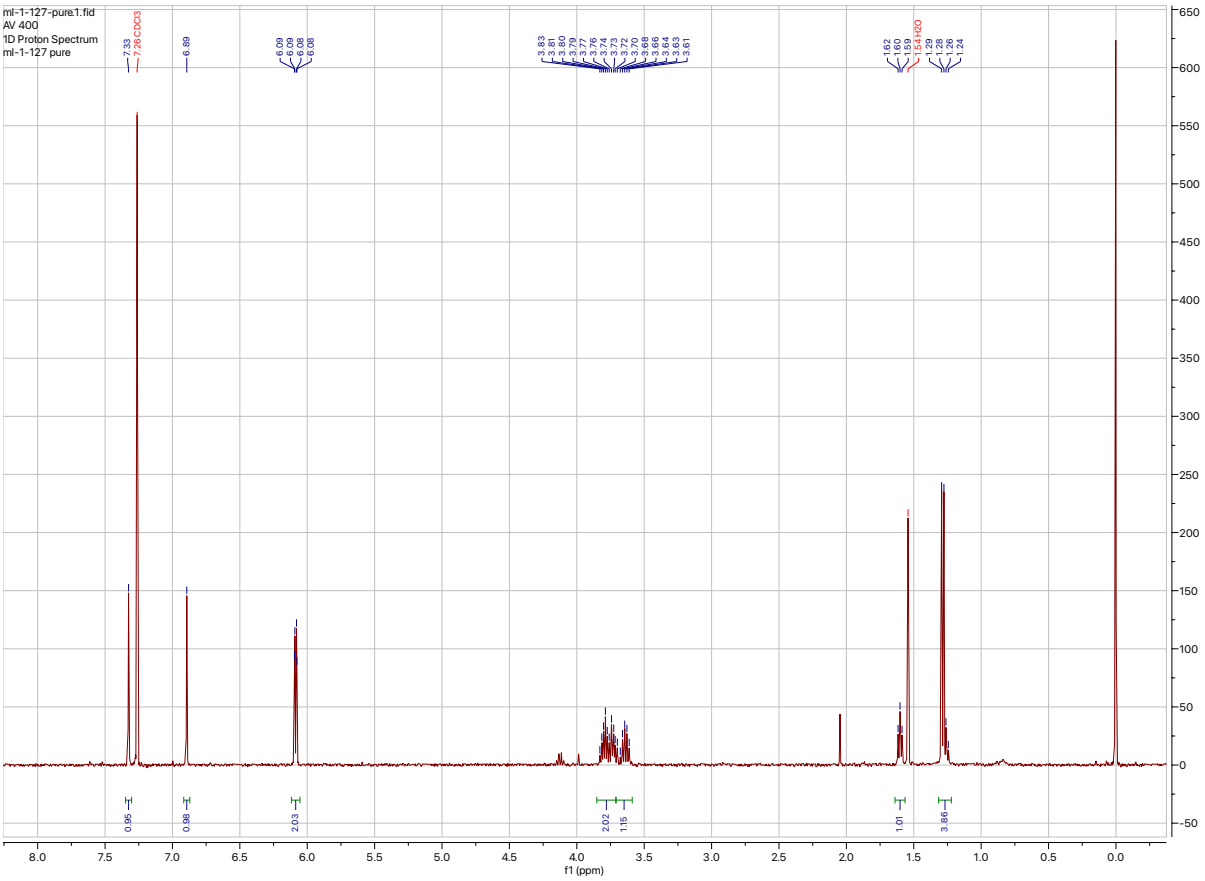

4-ethyl-2-methoxy-5-nitrophenol, byproduct 6

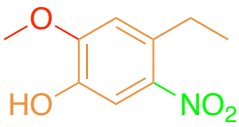

^{1}H NMR (400 MHz, $CDCl_3$) δ 7.61 (s, 1H), 6.72 (s, 1H), 5.61 (s, 1H), 3.99 (s, 3H), 2.92 (q, J = 7.4 Hz, 2H), 1.27 (t, J = 7.5 Hz, 3H) ppm. ^{13}C NMR (151 MHz, $CDCl_3$) δ 150.5, 143.7, 133.6, 112.0, 111.7, 56.4, 29.9, 27.0, 15.3 ppm.

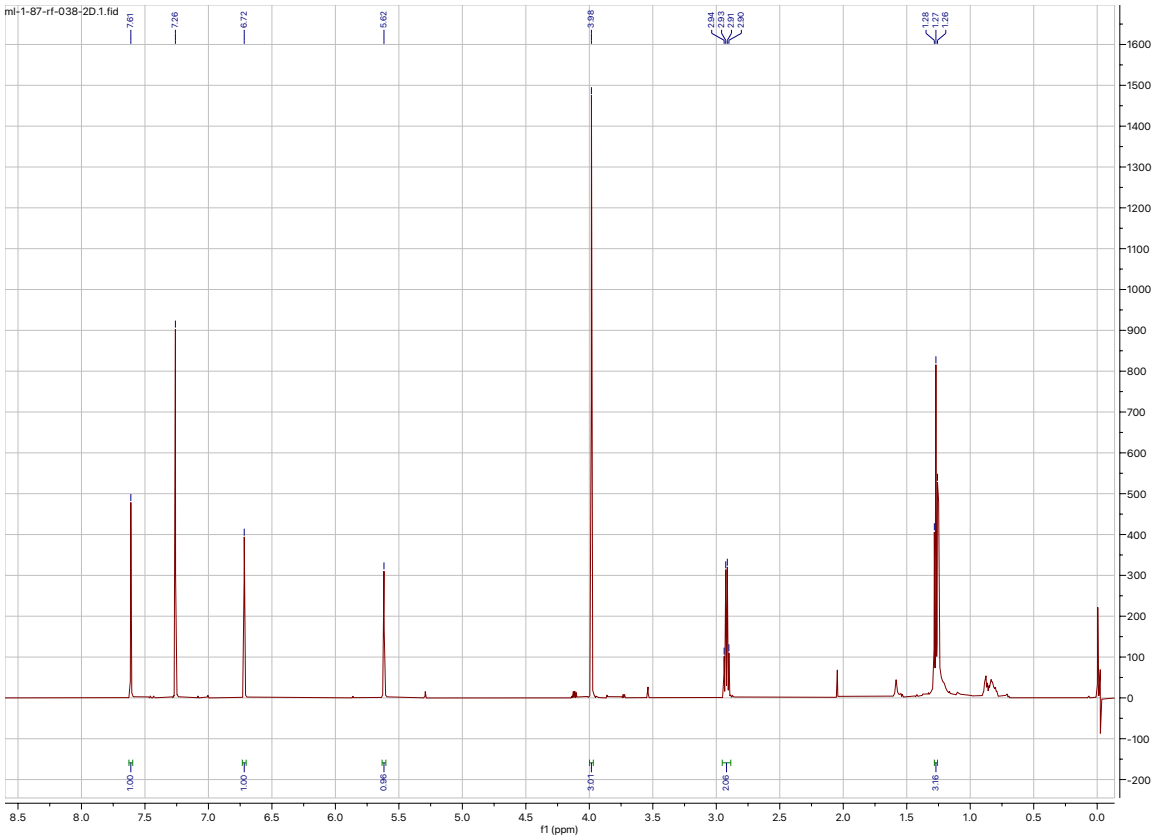
ml-1-87-rf-038-2D.1.fid
7.61
7.26
6.72
5.62
3.98
2.94
2.93
2.91
2.90
1.28
1.27
1.26
1.00
1.00
0.96
3.01
2.06
3.16
f1 (ppm)

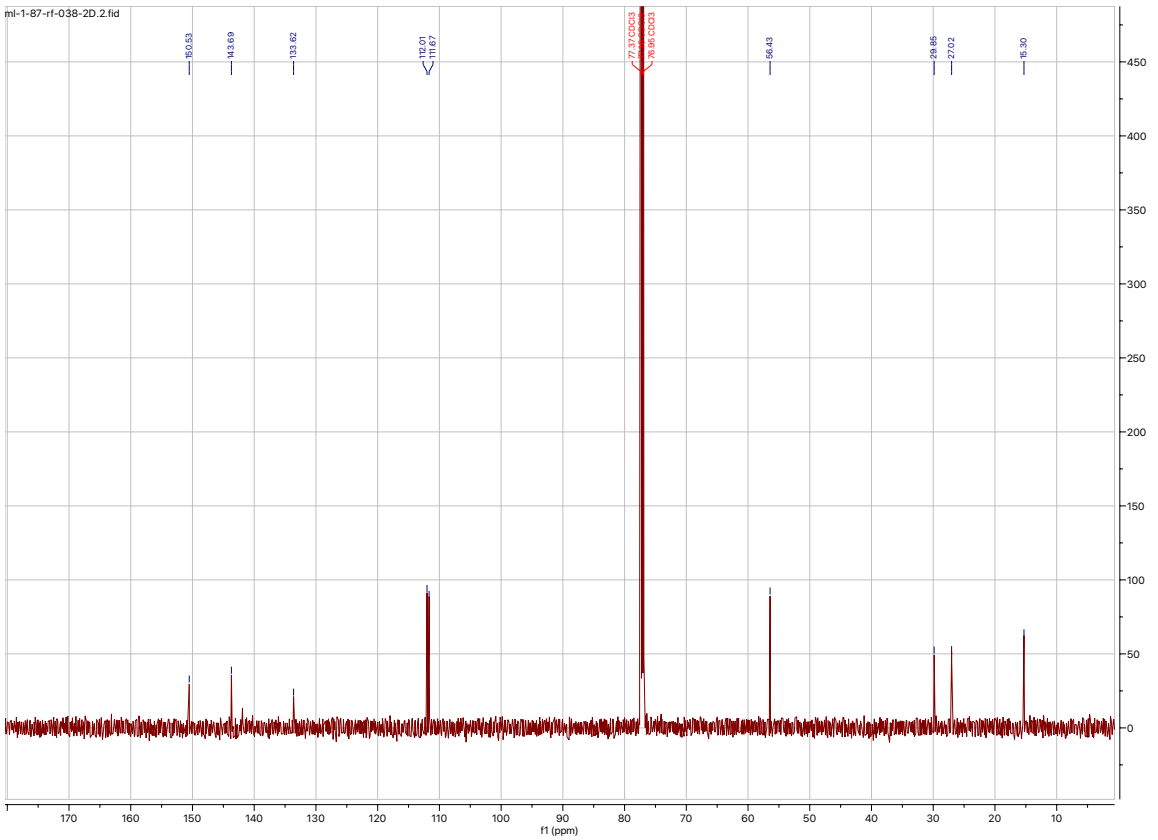
ml-1-87-rf-038-2D.2.fid
150.53
143.69
133.62
112.01
111.67
77.37 CDCl3
76.95 CDCl3
56.43
29.95
27.02
16.30
f1 (ppm)

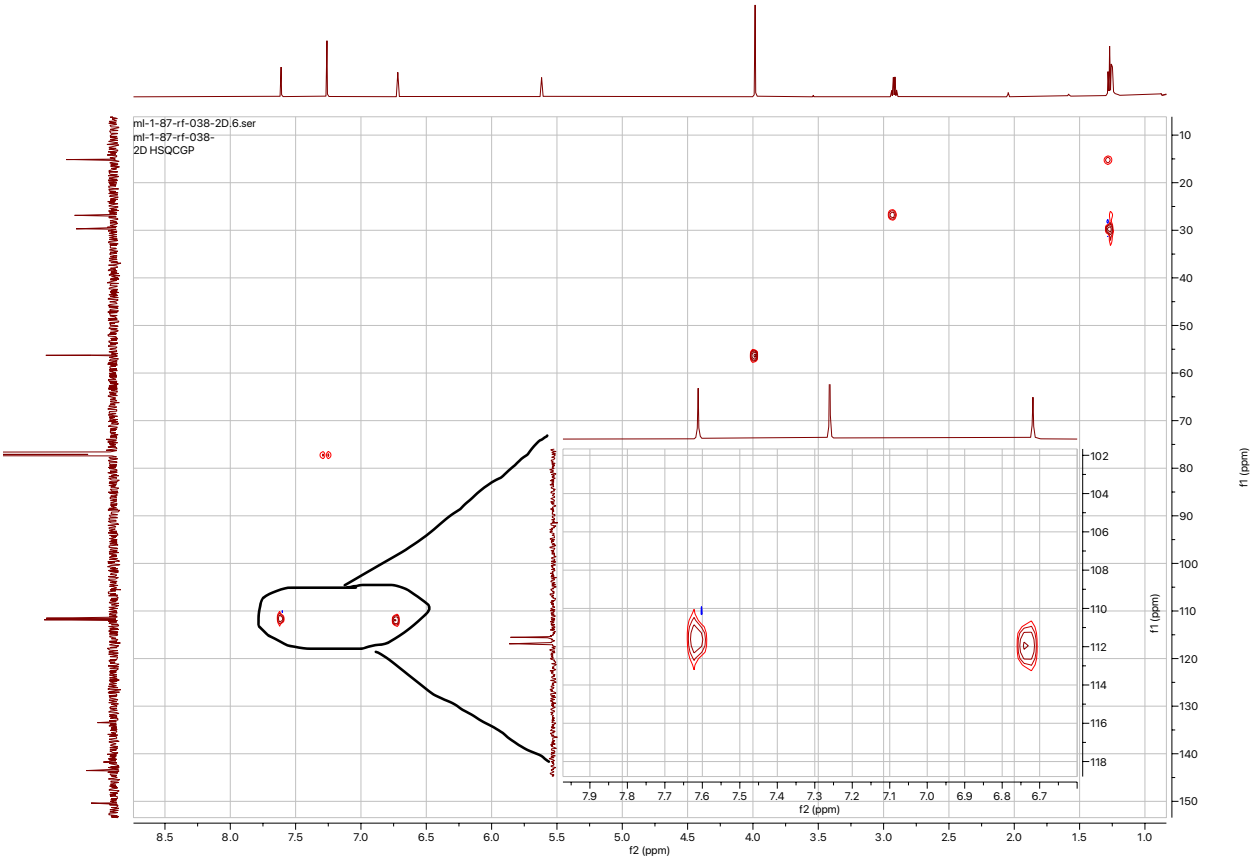

2-(6-nitrobenzo[*d*][1,3]dioxol-5-yl)propyl carbonochloridate, 4

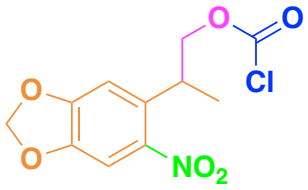

Compound **4** was synthesized following an adapted procedure reported in the literature.[76] Compound **3** (0.050 g, 0.2220 mmol) was dissolved in anhydrous THF (0.19 mL) in a flame-dried vial, which was then capped and purged under argon. The mixture was cooled to 0°C, and phosgene (15 wt. % in toluene) (0.19 mL, 0.2664 mmol, 2 equiv.) was injected dropwise over 15 minutes. After 45 minutes of stirring at 0°C, the mixture was allowed to heat to room temperature and stirring continued for an additional 4 hours. Argon was bubbled into the reaction mixture into a beaker of sat. $NaHCO_3$ solution for 20 minutes. The reaction was then concentrated yielding a black oil. NMR was matched with literature values. ^{1}H NMR (400 MHz, $CDCl_3$) δ 7.39 (s, 1H),

6.85 (s, 1H), 6.12 (s, 2H), 4.47 (d, J = 6.0 Hz, 2H), 3.93 (q, J = 6.6 Hz, 1H), 1.38 (d, J = 7 Hz, 3H) ppm.

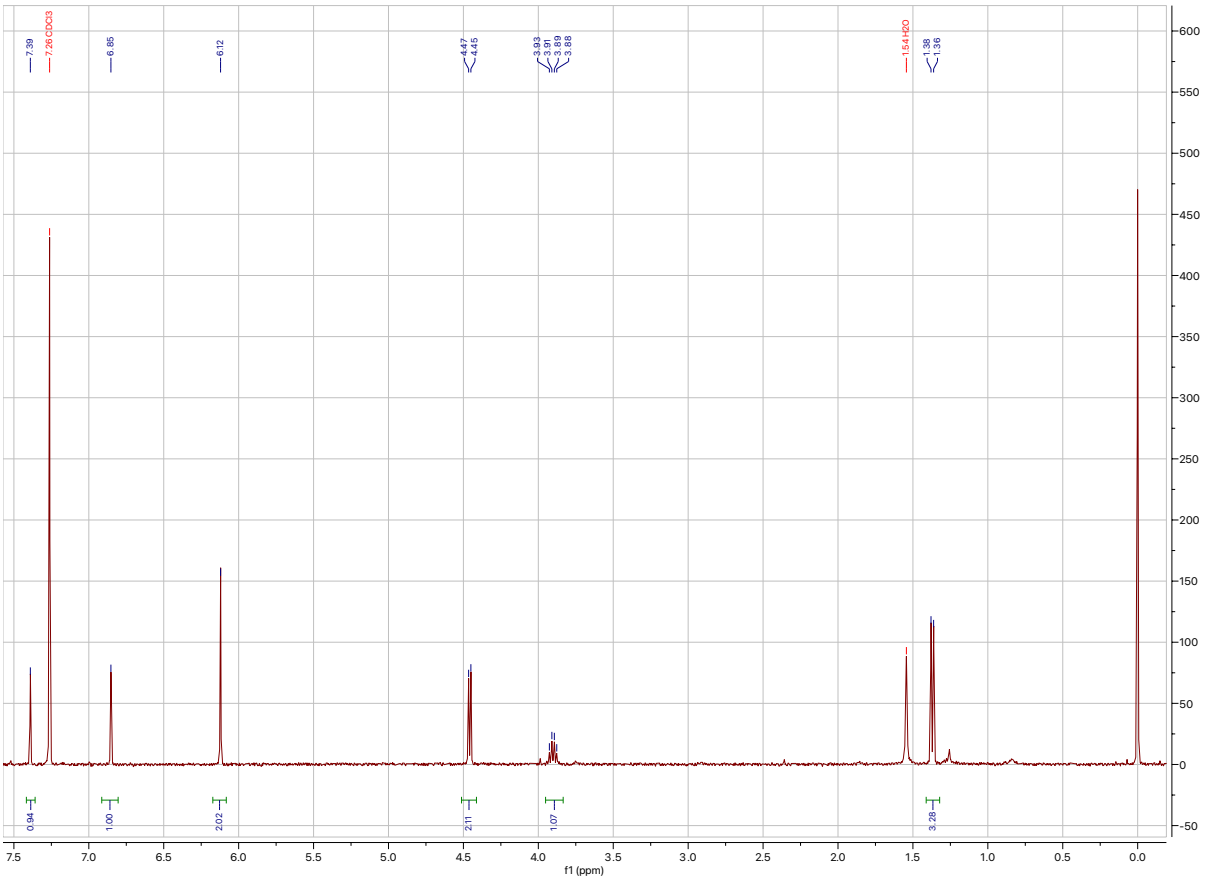

2-(6-nitrobenzo[*d*][1,3]dioxol-5-yl)propyl (6-aminohexyl)carbamate, 5

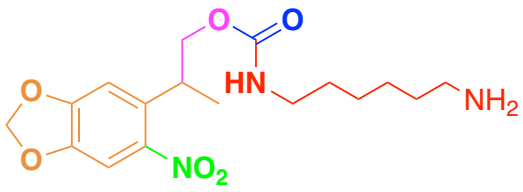

Compound **5** was synthesized following an adapted procedure reported in the literature.[93] A solution of **4** (0.05971 g, 0.2076 mmol) in degassed DCM (0.60 mL) was injected over 1.5 hours into a 0°C solution of hexamethylenediamine (0.24353 g, 2.096 mmol, 10 equiv.) in degassed DCM (2.1 mL). After the injection, the solution was stirred for 2.5 hours, then transferred to a separatory funnel. The organic layer was washed with 2 x 10 mL H_2O, 2 x 10 mL brine, and dried over Na_2SO_4, filtered, and concentrated. ^{1}H NMR (400 MHz, $CDCl_3$) δ 7.29 (s, 1H), 6.85 (s, 1H),

6.08 (s, 2H), 4.63 (m, 1H), 4.21 (q, J = 5.68 Hz, 1H), 4.07 (t, J = 8.84 Hz, 1H), 3.82 (m, 1H), 3.11 (br s, 2H), 2.69 (t, J = 6.88 Hz, 1H), 1.48 (m), 1.30 (m, 12 H in tandem with 1.48) ppm. ^{13}C NMR (75 MHz, $CDCl_3$) δ 156.2, 151.5, 146.2, 144.2, 134.4, 106.7, 105.3, 102.8, 68.5, 42.0, 40.9, 33.4, 29.8, 26.5, 26.2, 17.5 ppm. HRMS calcd for $C_{17}H_{25}N_3O_6$ $[MH]^+$: 368.1743 Found: 368.1791

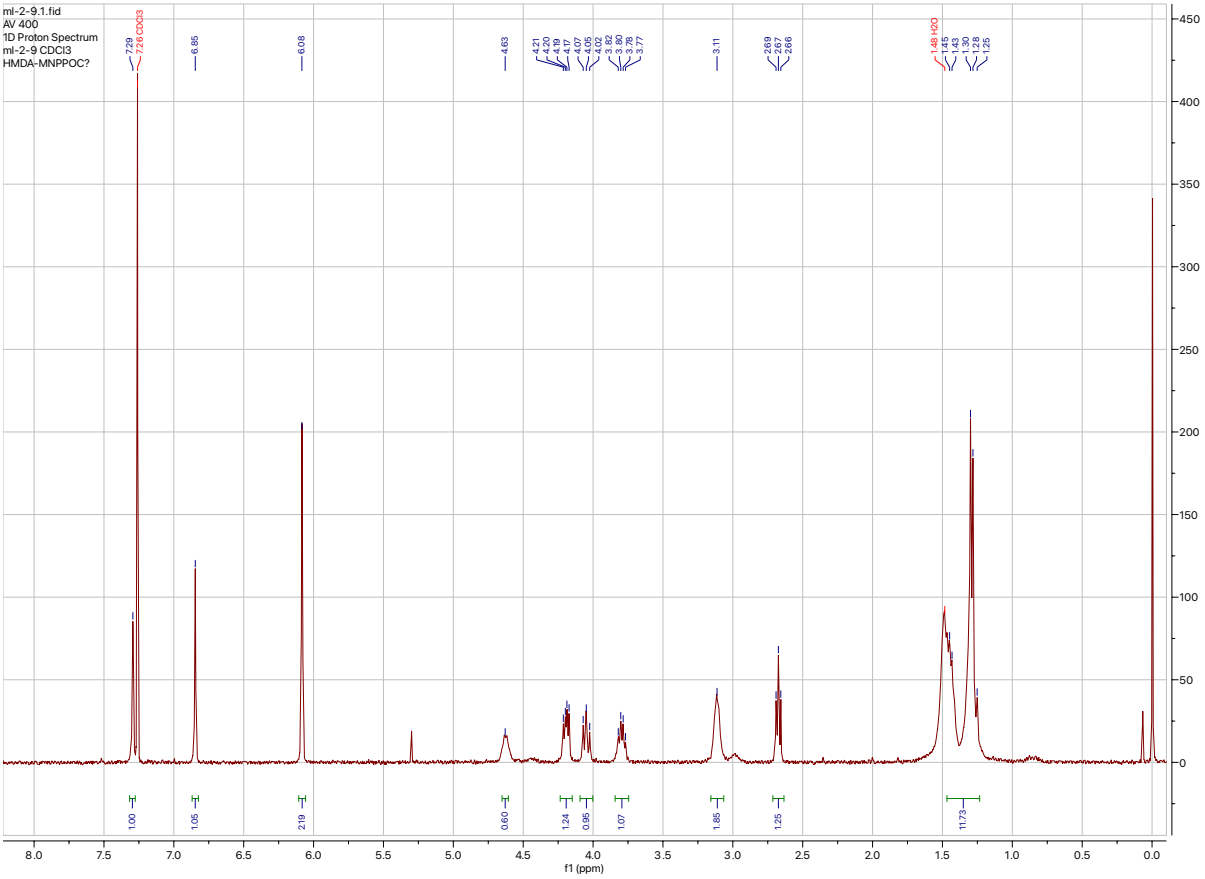

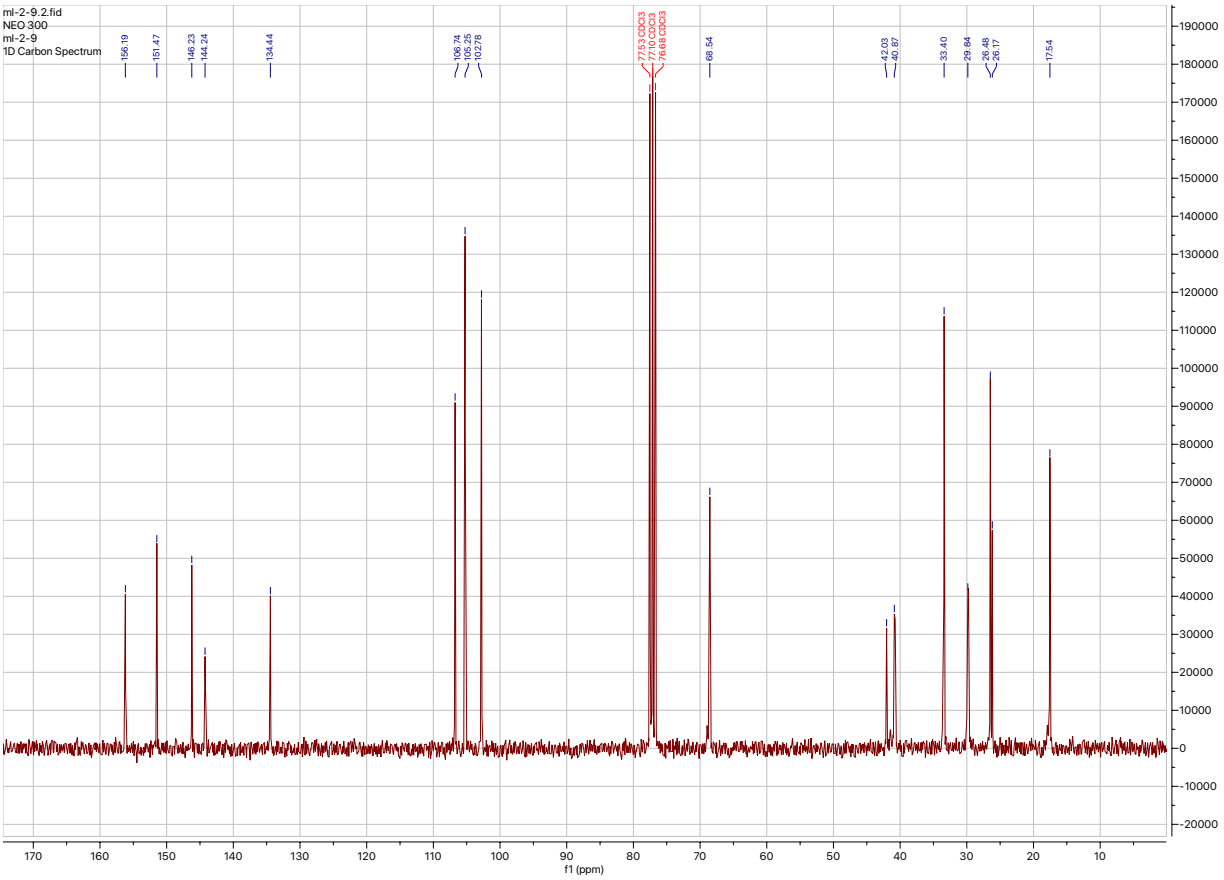
ml-2-9.2.fid
NEO 300
ml-2-9
1D Carbon Spectrum
156.19
151.47
146.23
144.24
134.44
106.74
105.35
102.78
77.53 CDCl3
77.21 CDCl3
76.88 CDCl3
68.54
42.03
40.87
33.40
29.84
26.48
26.17
17.54
f1 (ppm)

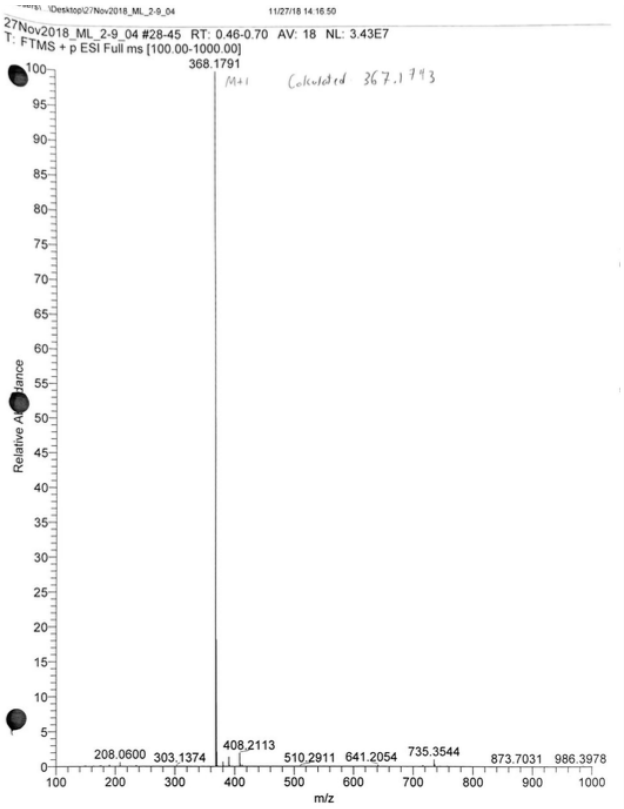
27Nov2018_ML_2-9_04 #28-45 RT: 0.46-0.70 AV: 18 NL: 3.43E7
T: FTMS + p ESI Full ms [100.00-1000.00]
368.1791
M+1
Calculated 367.1793
Relative Abundance
208.0600
303.1374
408.2113
510.2911
641.2054
735.3544
873.7031
986.3978
m/z

allyl (6-aminohexyl)carbamate, 7

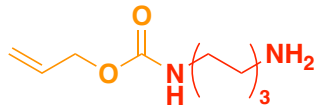

Compound **7** was synthesized following an adapted procedure from the literature.[83] A solution of allyl chloroformate (1.0 mL, 9.408 mmol) dissolved in ACS grade DCM (23 mL) was injected over 1.5 hours into a solution of hexamethylenediamine (11.30 g, 97.23 mmol, 10 equiv.) in DCM (97 mL) stirred at 0°C. The reaction subsequently allowed to stir at room temperature for an additional 3.5 hours. The crude mixture was washed with 3 x 120 mL dH_2O, 3 x 120 mL brine, dried over Na_2SO_4, filtered, and concentrated. ^{1}H NMR (400 MHz, $CDCl_3$) δ 5.93 (m, 1H), 5.28 (d, J = 17.2 Hz, 1H), 5.18 (d, J = 10.4 Hz, 1H), 4.89 (br s, 1H), 4.52 (d, J = 5.7 Hz, 2H), 3.17 (m, 2H), 2.64 (t, J = 7.0 Hz, 1H), 1.51 (br m, 7H). ^{13}C NMR (75 MHz, $CDCl_3$) δ 156.5, 133.0, 117.4, 65.3, 49.9, 41.7, 40.8, 33.0, 29.8, 26.4. MS calcd for $C_{10}H_{20}N_2O_2$ $[MH]^+$: 201.15 Found: 201.16

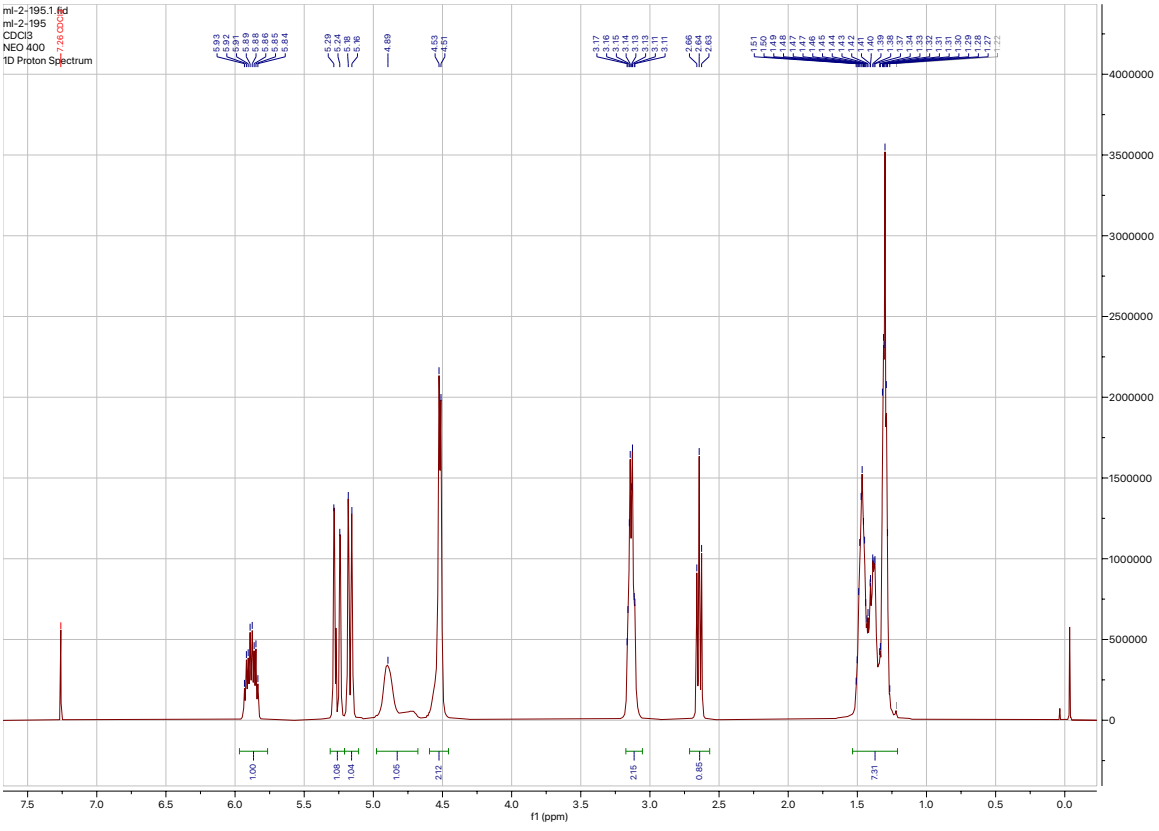

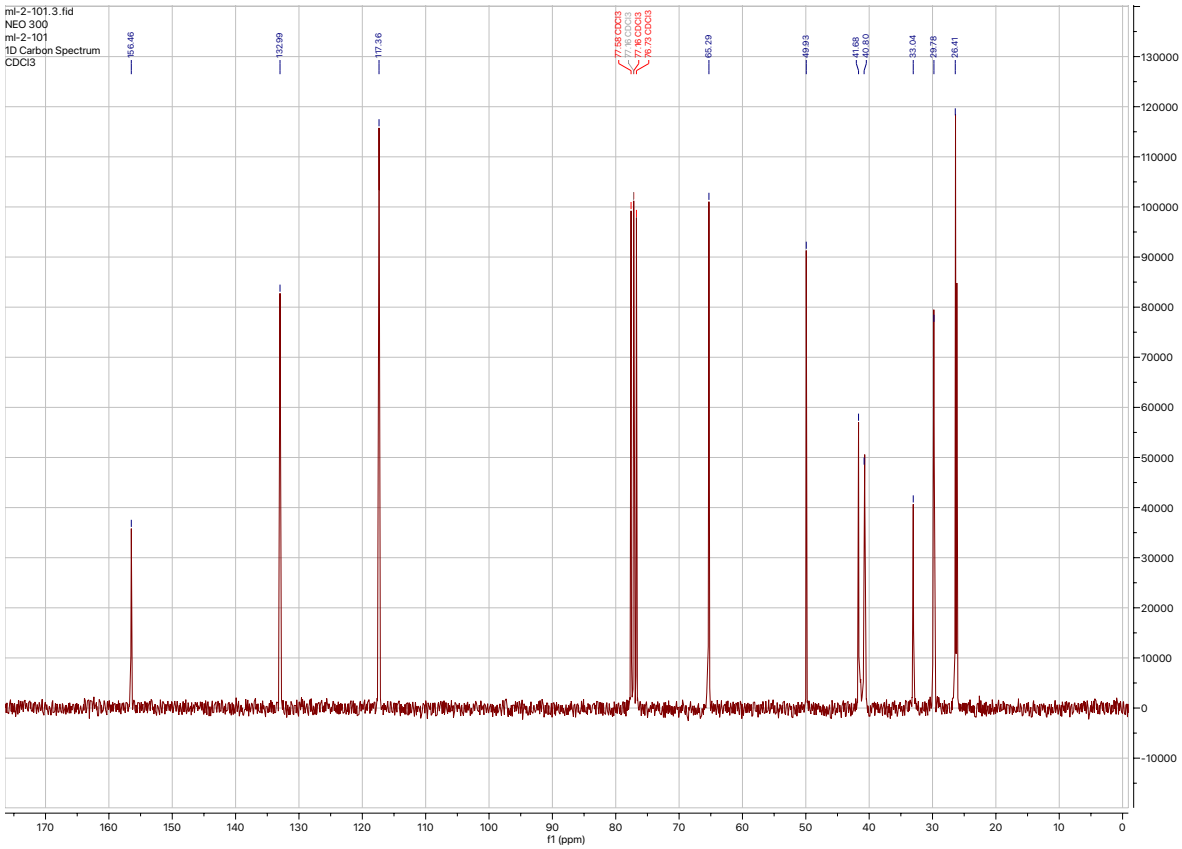
ml-2-101.3.fid
NEO 300
ml-2-101
1D Carbon Spectrum
CDCl3
156.46
132.99
117.36
77.58 CDCl3
77.16 CDCl3
76.73 CDCl3
65.29
49.93
41.68
40.80
33.04
29.78
26.41
f1 (ppm)

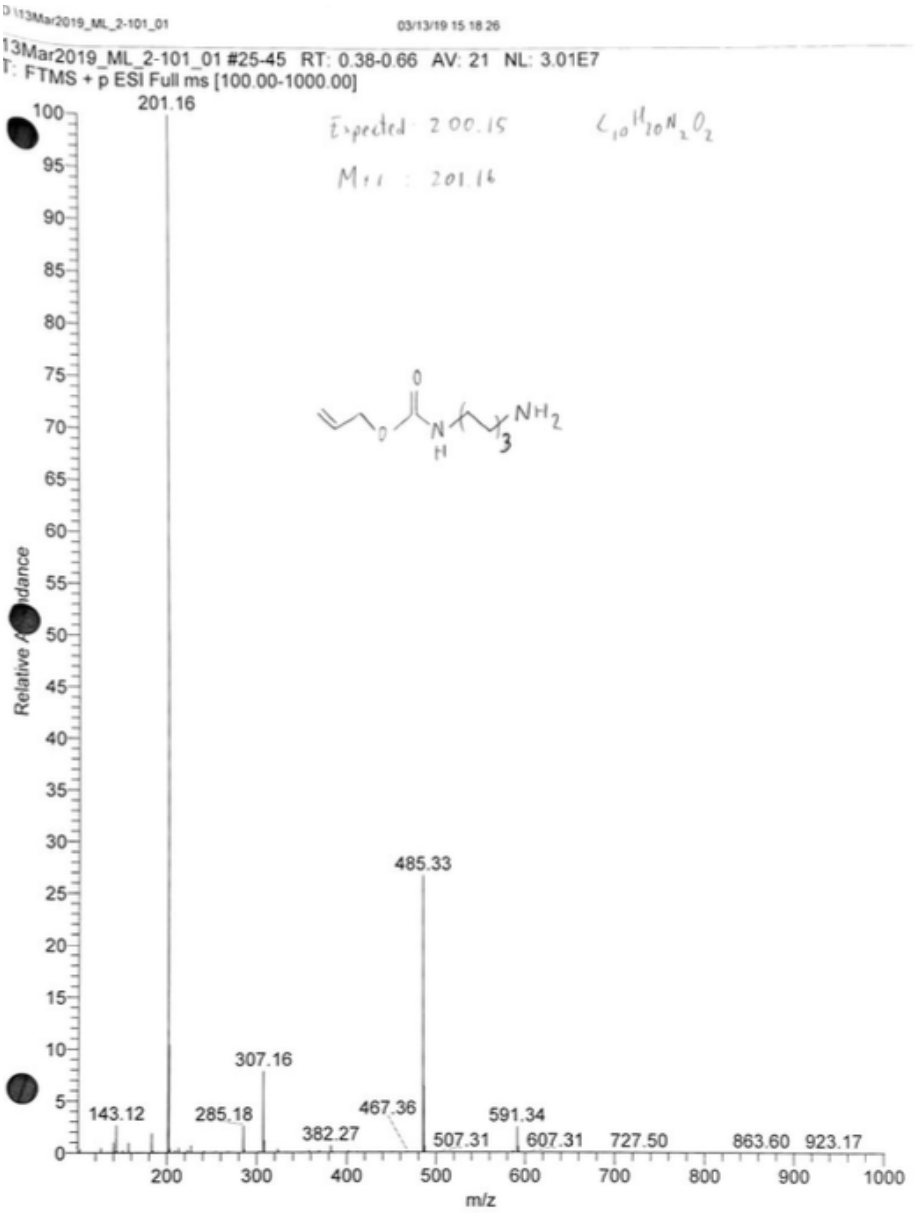

8-bromo-2'-deoxyadenosine, 8

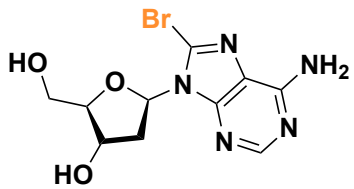

Compound **8** was synthesized following a procedure from the literature.[89] Bromine (1.30 mL, 24.88 mmol, 1.25 equiv.) was dissolved in freshly made 1 M NaOAc buffer, pH 4.0 (32 mL). The bromine solution was then added in portions via Pasteur pipet over 20 minutes into a suspension

of dA (5.00 g, 19.9 mmol) in the acetate buffer (80 mL). After 3 hours, the reaction was deemed complete by TLC (20% MeOH/$CHCl_3$). 30 mL of sat. $Na_2S_2O_5$ solution was added to quench the reaction, and the mixture was neutralized by addition of 10 N NaOH to pH 11. The product was allowed to precipitate while stirring in an ice bath for 1 hour. Finally, the precipitate was collected with a frit and washed with 60 mL of 0°C water. The solid was collected and dried under high vacuum. NMR was matched with literature values. ^{1}H NMR (400 MHz, DMSO) δ 8.11 (s, 1H), 7.49 (s, 2H), 6.29 (t, J = 7.08 Hz, 1H), 5.33 (d, J = 4.2 Hz, 2H), 5.26 (q, J = 4.32 Hz, 1H), 4.48 (s, 1H), 3.88 (m, 1H), 3.65 (m, 1H), 3.48 (m, 1H), 3.25 (m, 2H), 2.19 (m, 1H).

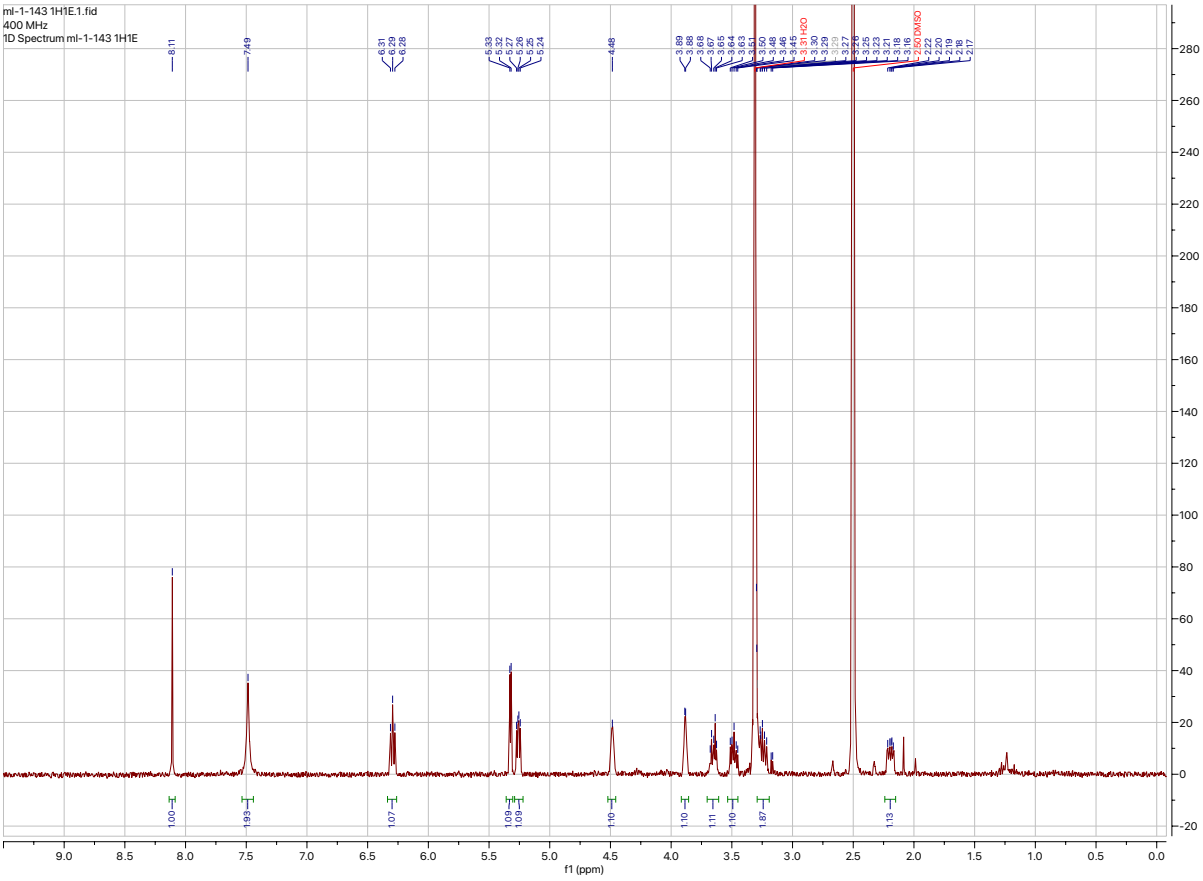

5'-O-(4,4'-dimethoxytrityl)-8-bromo-2'-deoxyadenosine, 9

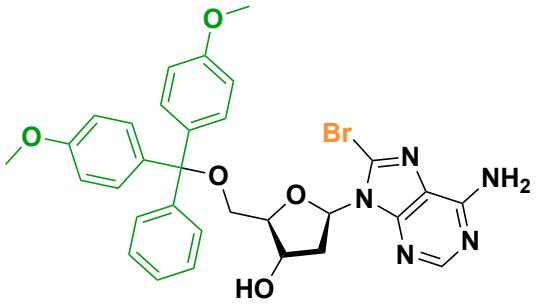

Compound **9** was synthesized following a procedure from the literature.[94] Compound **8** (3.23639 g, 9.80 mmol) was dried twice by addition, and subsequent evaporation of pyridine (10 mL) under vacuum at 55°C. Pyridine (18.5 mL) and 4-dimethylaminopyridine (0.14909 g, 1.22 mmol, 0.12 equiv.) were added to the solid residue. A solution of 4,4'-dimethoxytrityl chloride (3.65370 g, 10.78 mmol, 1.1 equiv) in pyridine (18 mL) was injected to the reaction over 3 hours. After the addition, methanol (20 mL) was added to the mixture, and the solution was concentrated. The residue was taken up in DCM (50 mL) and washed with water (2 x 50 mL), then brine (2 x 50 mL). The organic layer was dried over Na_2SO_4, filtered, and concentrated, yielding a green foam. The crude material was purified by column chromatography in a column pre-treated with 1% triethylamine in DCM (0-5% MeOH/DCM). NMR was matched with literature values. ^{1}H NMR (400 MHz, $CDCl_3$) δ 8.08 (s, 1H), 7.37 (m, 2H), 7.28 (d, J = 1.4 Hz, 3H), 7.26 – 7.15 (m, 4H), 6.77 (m, 4H), 6.39 (dd, J = 7.5, 5.9 Hz, 1H), 5.48 (s, 2H), 4.96 (dt, J = 6.8, 4.6 Hz, 1H), 4.09 (q, J = 5.9 Hz, 1H), 3.78 (d, J = 1.1 Hz, 7H), 3.56 (m, 2H), 3.40 (m, 2H), 2.53 (q, J = 7.2 Hz, 5H), 2.36 (ddd, J = 13.6, 7.5, 4.9 Hz, 2H), 1.46 (t, J = 7.3 Hz, 1H), 1.03 (t, J = 7.2 Hz, 7H) ppm.

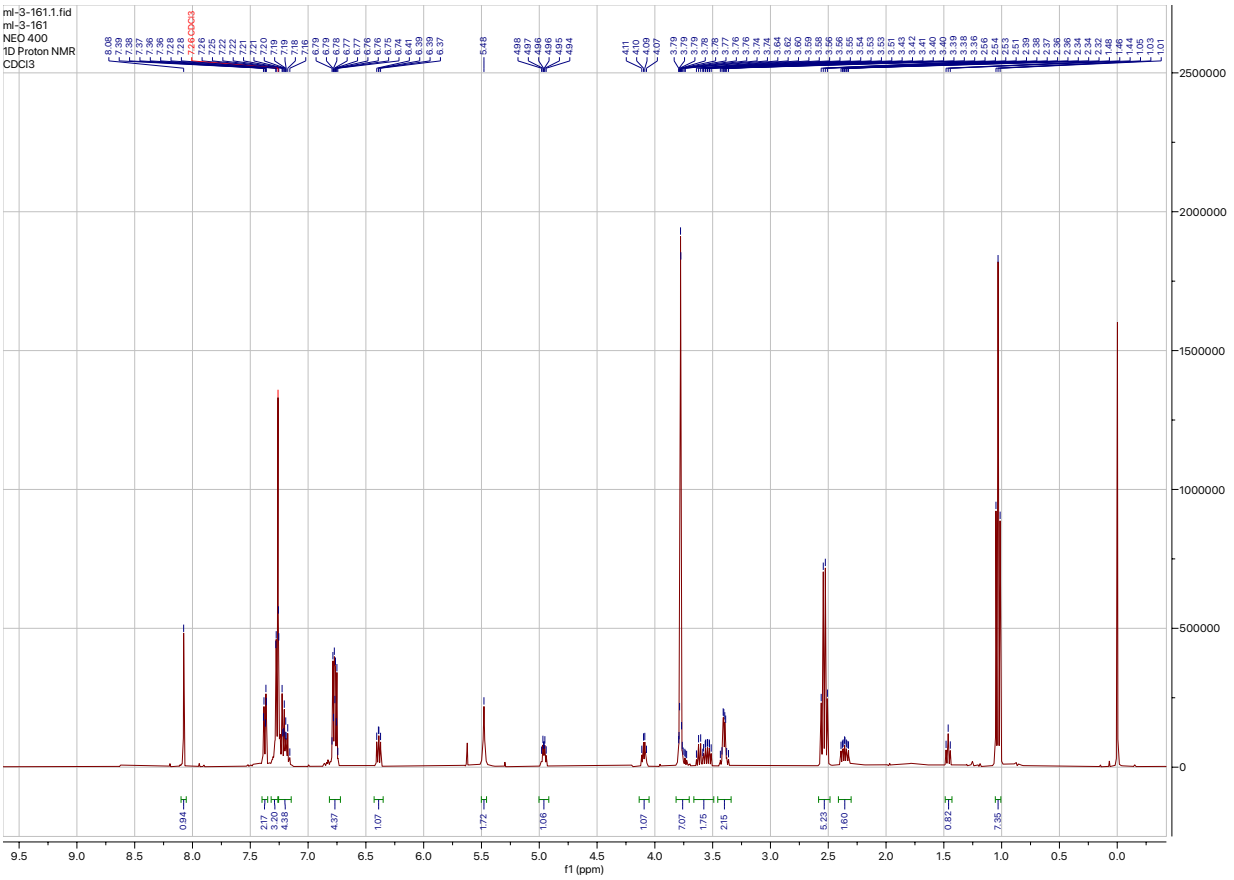

N-benzoyl-5'-O-(4,4'-dimethoxytrityl)-8-bromo-2'-deoxyadenosine, 10

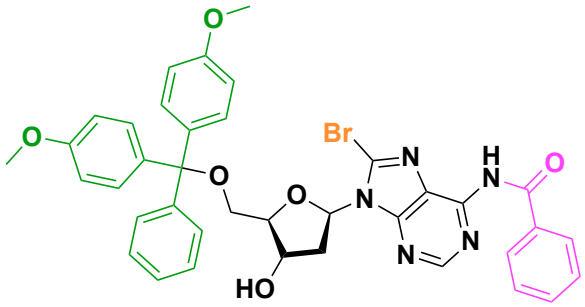

Compound **10** was synthesized following a procedure from the literature.[94] Compound **9** (2.86 g, 4.52 mmol) was dried twice by addition, and subsequent evaporation of pyridine (10 mL), followed by concentration under vacuum at 55°C. The solid residue was dissolved in pyridine (64.5 mL) and cooled to -5°C in a ~1:0.3 ice:ammonium chloride bath. Trimethylsilyl chloride (2.9 mL, 22.61 mmol, 5 equiv.) was added dropwise over 5 min, and the mixture stirred for 1 hour. The solution was warmed to room temperature, and benzoyl chloride (2.7 mL, 22.61 mmol, 5 equiv.) was added and the reaction stirred for 15.5 hours. The reaction was quenched by addition of methanol (20 ml)

and stirred for 5 minutes. The mixture was then concentrated. Methanolic ammonia (200 mL, 2M) was added to the yellow residue, and stirred for 1 hour. The yellow complexion gave way to an orange during this time. The mixture was again concentrated. The yellow solid was dissolved in a mixture of DCM (200 mL) and water (20 mL). The organic layer was isolated, washed with water (2 x 100 mL), and brine (2 x 100 mL), then dried over Na_2SO_4, filtered, and concentrated. The crude material was purified by column chromatography (0-5% MeOH/DCM) which had been pre-treated with 1% triethylamine in DCM, yielding a yellow solid. NMR was matched with literature values. ^{1}H NMR (400 MHz, CD_2Cl_2) δ 8.84 (s, 1H), 8.58 (m, 2H), 8.49 (s, 1H), 7.98 (d, J = 7.7 Hz, 3H), 7.80 (m, 2H), 7.66 (m, 3H), 7.55 (m, 4H), 7.46 (m, 2H), 7.37 (m, 3H), 7.24 (m, 13H), 6.75 (m, 6H), 6.46 (dd, J = 7.4, 5.7 Hz, 2H), 4.93 (br s, 1H), 4.13 (q, J = 5.6 Hz, 2H), 3.76 (m, 10H), 3.58 (m, 2H), 3.36 (m, 3H), 2.40 (ddd, J = 13.5, 7.5, 4.8 Hz, 2H), 2.15 (d, J = 3.8 Hz, 1H).

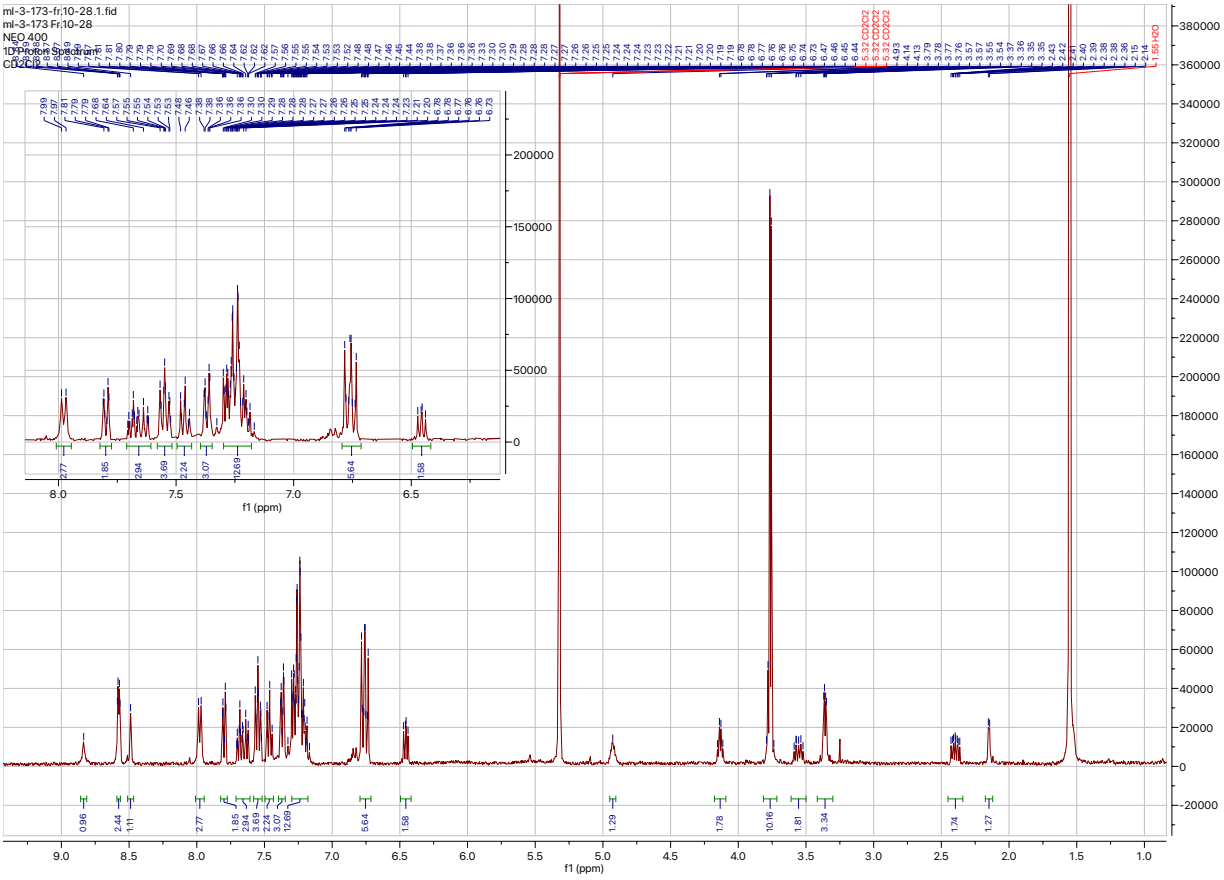

N^6-benzoyl-5'-*O*-(4,4'-dimethoxytrityl)-8-(allyl-(6-aminohexyl)carbamate)-2'-deoxyadenosine, 11

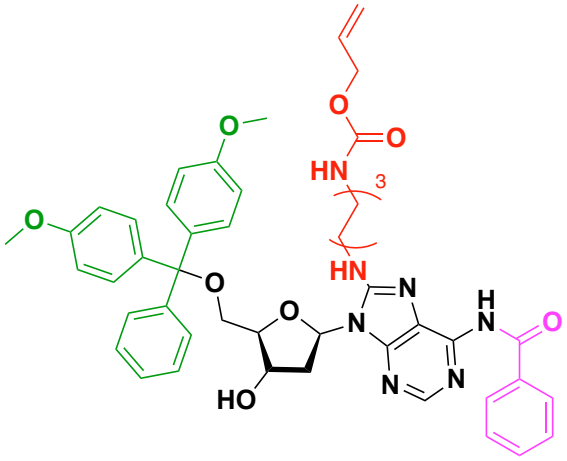

Compound **11** was synthesized followed adapted procedures from the literature.[88,95] Compound **10** (1.45 g, 1.966 mmol) was dissolved in 100% ethanol (65 mL), followed by **7** (1.95447 g, 9.832 mmol, 5 equiv.), and heated to reflux. After 4.25 hours, the starting material had been consumed by TLC (5% MeOH/DCM). The reaction was cooled and concentrated. The reaction was cooled and concentrated *in vacuo*. The product was purified by column chromatography, pre-treated with 1% triethylamine in DCM, and eluted (0-5% MeOH/DCM) yielding a yellow solid. ^{1}H NMR (400 MHz, $CDCl_3$) δ 8.85 (s, 1H), 8.60 (m, 1H), 8.51 (s, 1H), 7.80 (m, 1H), 7.50 (m, 3H), 7.32 (m, 3H), 7.24 (m, 2H), 6.81 (m, 2H), 5.92 (m, 2H), 5.30 (m, 1H), 5.22 (qd, J = 5.2 Hz, 1.4 Hz, 5H), 4.74 (m, 1H), 4.53 (m, 4H), 3.78 (m, 3H), 3.17 (q, J = 6.7 Hz, 3H), 3.07 (m, 2H), 1.69, (s, 3H), 1.50 (t, J = 6.9 Hz, 3H), 1.33 (p, J = 3.6 Hz, 4H), 1.15 (s, 1H) ppm. ^{13}C NMR (101 MHz, $CDCl_3$) δ 164.9, 158.9, 158.6, 156.4, 154.0, 152.8, 150.0, 148.8, 144.1, 136.1, 135.4, 135.3, 133.2, 132.4, 132.2, 130.3, 130.2, 130.2, 128.9, 128.8, 128.4, 128.1, 127.9, 127.5, 127.3, 123.9, 117.7, 113.4, 113.3, 86.9, 85.7, 83.7, 72.0, 65.6, 63.1, 55.4, 55.4, 53.6, 42.8, 41.0, 38.8, 30.0, 29.7, 29.3, 26.4, 26.2, 1.2 ppm. HRMS calcd for $C_{48}H_{53}N_7O_8$ $[MH]^+$: 856.3956 Found: 856.4019

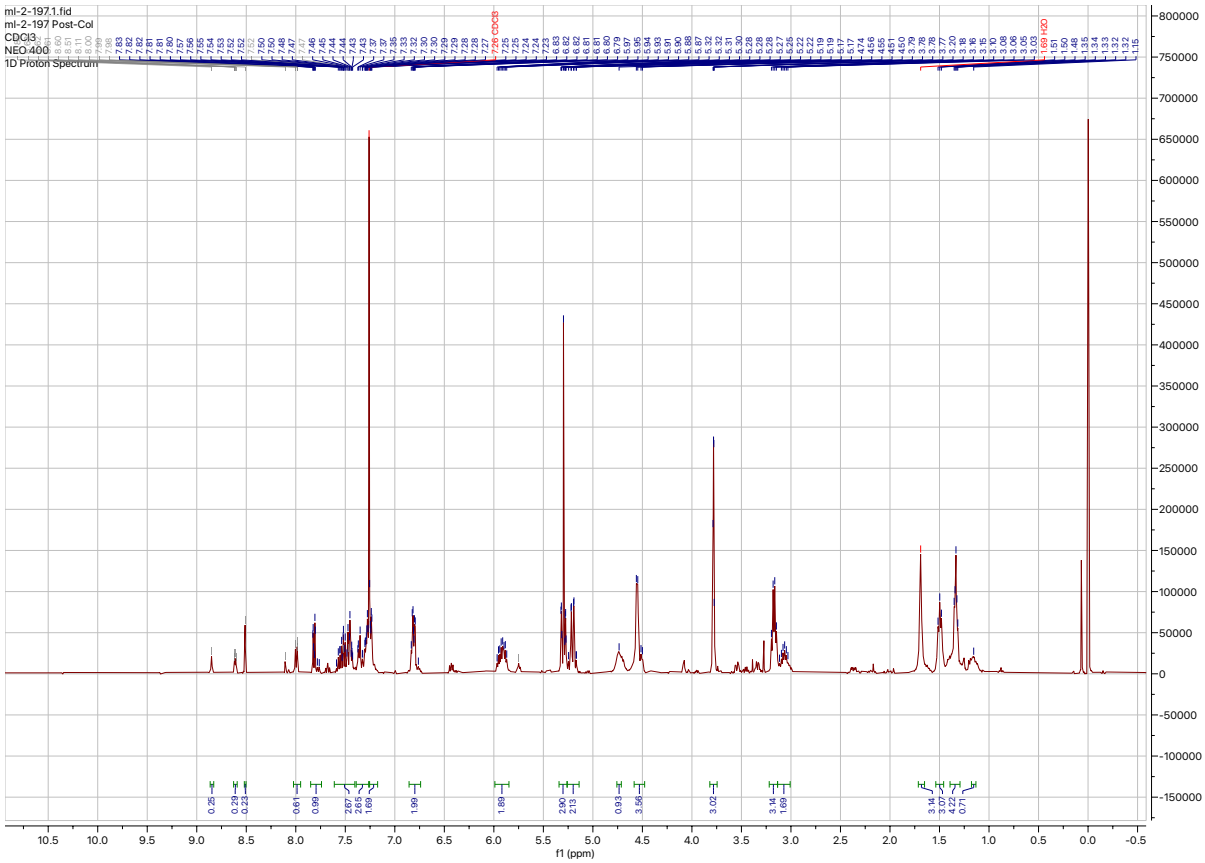
ml-2-197.1.fid
ml-2-197 Post-Col
CDCl3
NEO 400
1D Proton Spectrum
f1 (ppm)

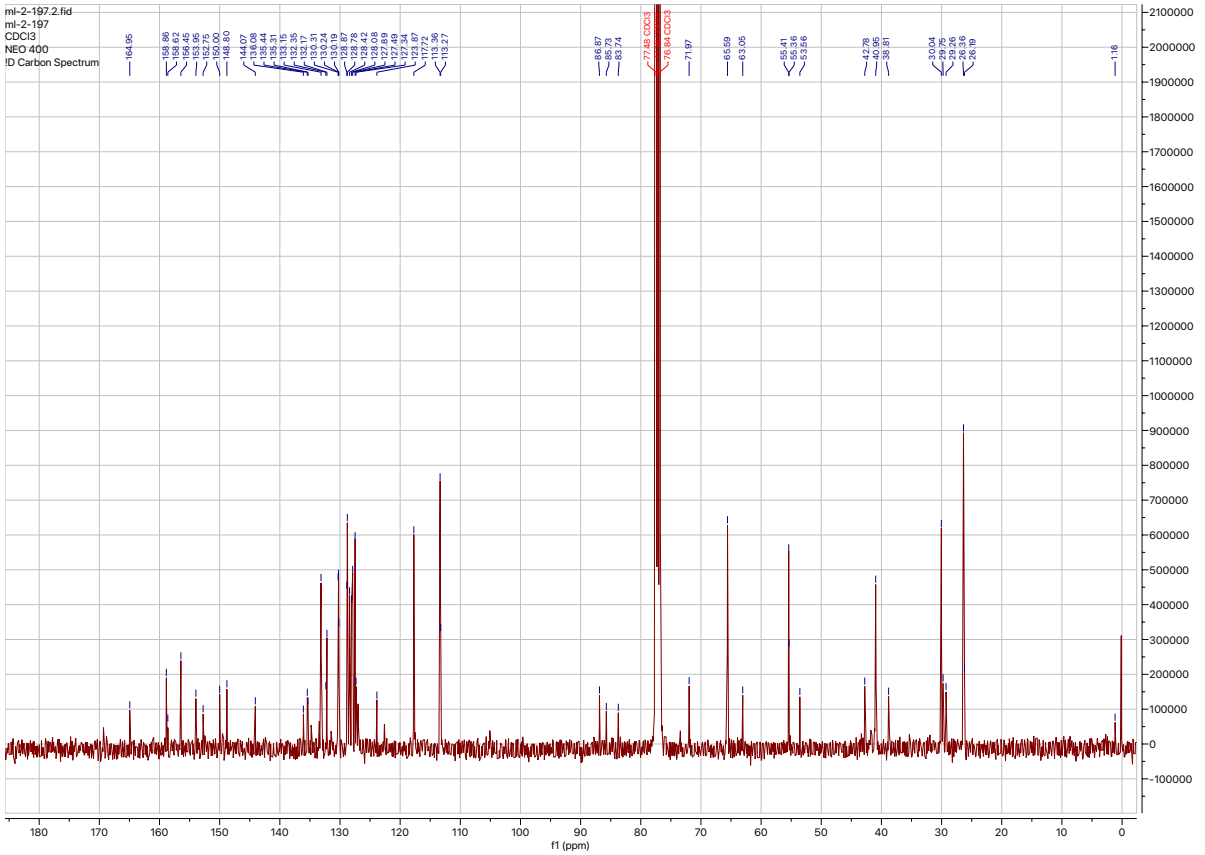
ml-2-197.2.fid
ml-2-197
CDCl3
NEO 400
1D Carbon Spectrum
f1 (ppm)

Sample Name	ML-2-197	**Data File**	191031_3008.d	**Acq Method**	AIMS_Default.m
DA Method	AIMS_Accurate_Mass.m	**Instrument**	Agilent 6538 UHD	**Acq Date, Time**	31-Oct-19 10:30:51 AM
Comment	ESI+				

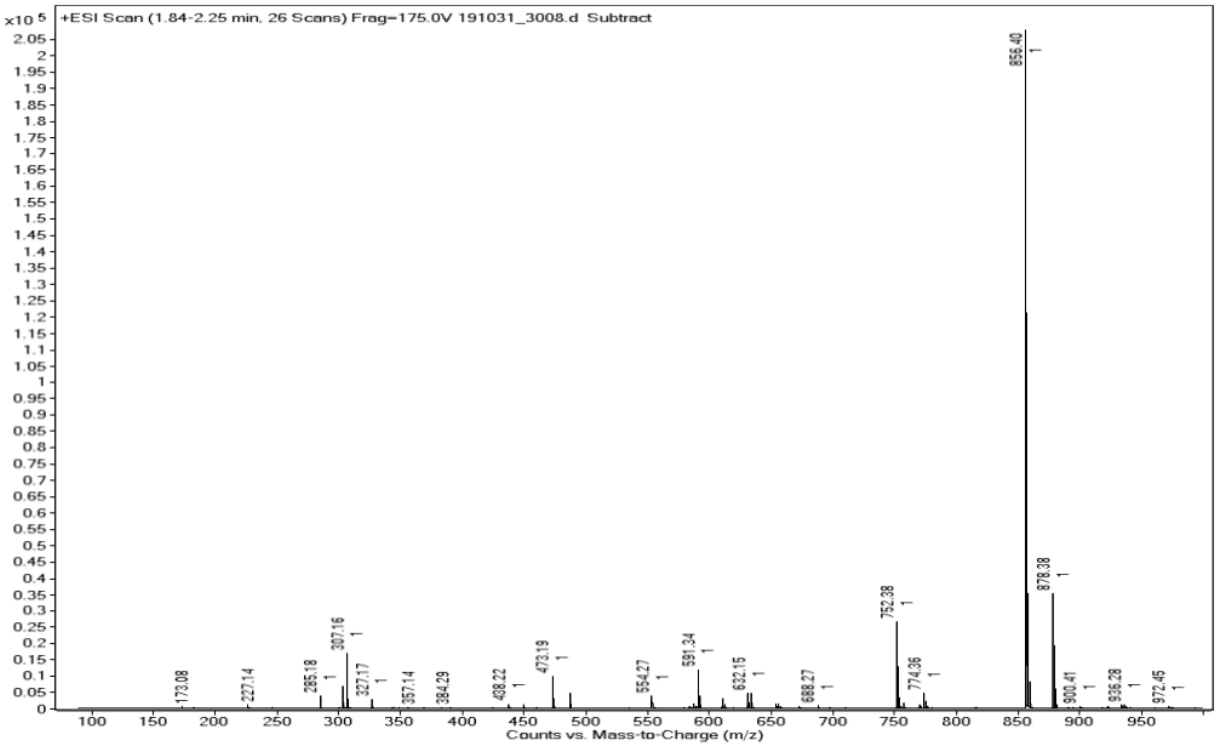

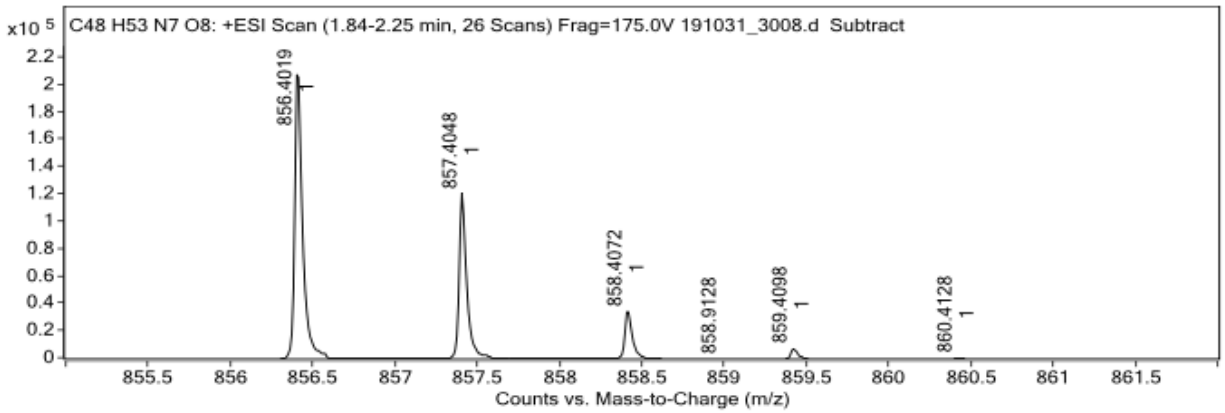

N^6-benzoyl-5'-*O*-(4,4'-dimethoxytrityl)-3'--(2-cyanoethyl-N,N-diisopropylphosphoramidite)-8-(allyl-(6-aminohexyl)carbamate)-2'-deoxyadenosine, 12

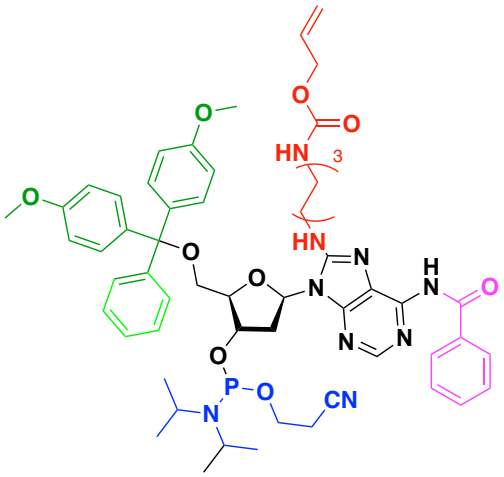

Compound **12** was synthesized following adapted procedures from the literature. Compound **11** (290 mg, 0.339 mmol) was dissolved in DCM (35 mL) under $Ar_{(g)}$ at 0°C. N,N-Diisopropylethylamine (DIPEA) (325 µL, 1.867 mmol, 5.4 equiv) was added, followed by dropwise addition of 2-cyanoethyl-N,N-diisopropylchlorophosphoramidite (417 µL, 1.867 mmol, 5.4 equiv.). The reaction was stirred for 3 hours at 0°C. TLC (5% MeOH/DCM) after 3 hours indicated total consumption of starting material. The reaction was quenched with 6 mL MeOH, and the crude mixture was concentrated until little only a small volume remained. 10% Et_2O/pentane (20 mL) was added to the mixture and swirled. The product oil crashed out, the supernatant removed, and the remainder was added to a separatory funnel, EtOAc (8 mL) was added to solubilize the mixture, which was washed with sat. $NaHCO_3$ (10 mL), then brine (10 mL). The organic layer was dried over Na_2SO_4, filtered, and concentrated. A column was pre-treated with 1% triethylamine (TEA) in DCM, and the product was eluted (0-5% MeOH/DCM) yielding a yellow foam. 1H NMR (400 MHz, CDCl3) δ 11.12 (s), 9.27 (s), 7.79 (m), 7.49 (m), 7.25 (m), 6.80 (m), 5.90 (m), 5.21 (m), 4.51 (m), 4.13 (m), 3.77 (d, J = 3.1 Hz), 3.66 (m), 3.46 (m), 3.11 (m), 2.75 (m), 2.63 (m), 1.95 (s), 1.53 (t, J = 7.4 Hz), 1.44 (t, J = 6.5 Hz), 1.32 (m), 1.25 (m). ^{13}C NMR (101 MHz, $CDCl_3$) δ 158.8, 158.5, 156.4, 133.1, 131.3, 130.1, 128.8, 128.6, 127.8, 127.0, 117.6, 117.0, 113.2, 113.2, 65.5, 58.2, 58.2, 55.3, 55.3, 45.4, 45.3, 40.9, 29.9, 26.3, 23.1, 23.0, 23.0, 22.9, 20.2, 20.1 ppm. HRMS calcd for $C_{57}H_{70}N_9O_9P$ $[MH]^+$: 1056.5034 Found: 1056.5067.

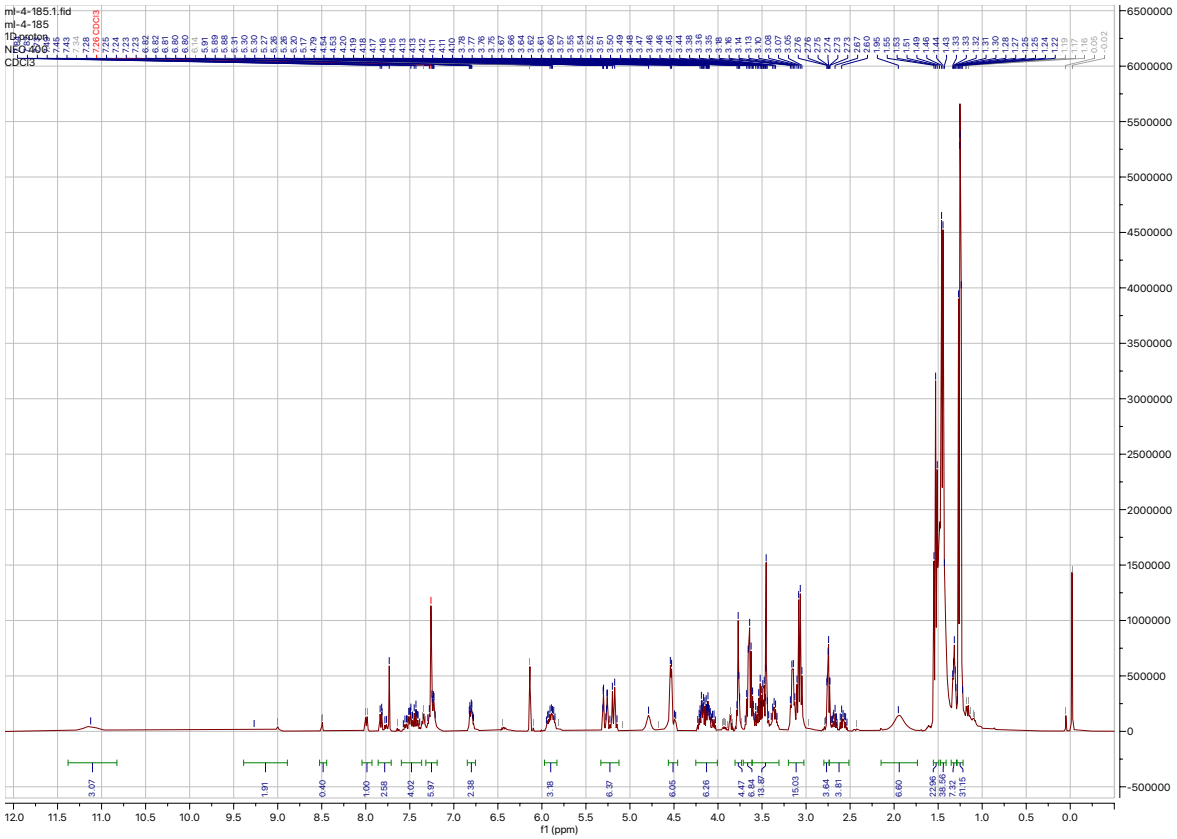
ml-4-185.1.fid
ml-4-185
1D proton
NEO 400
CDCl3
f1 (ppm)

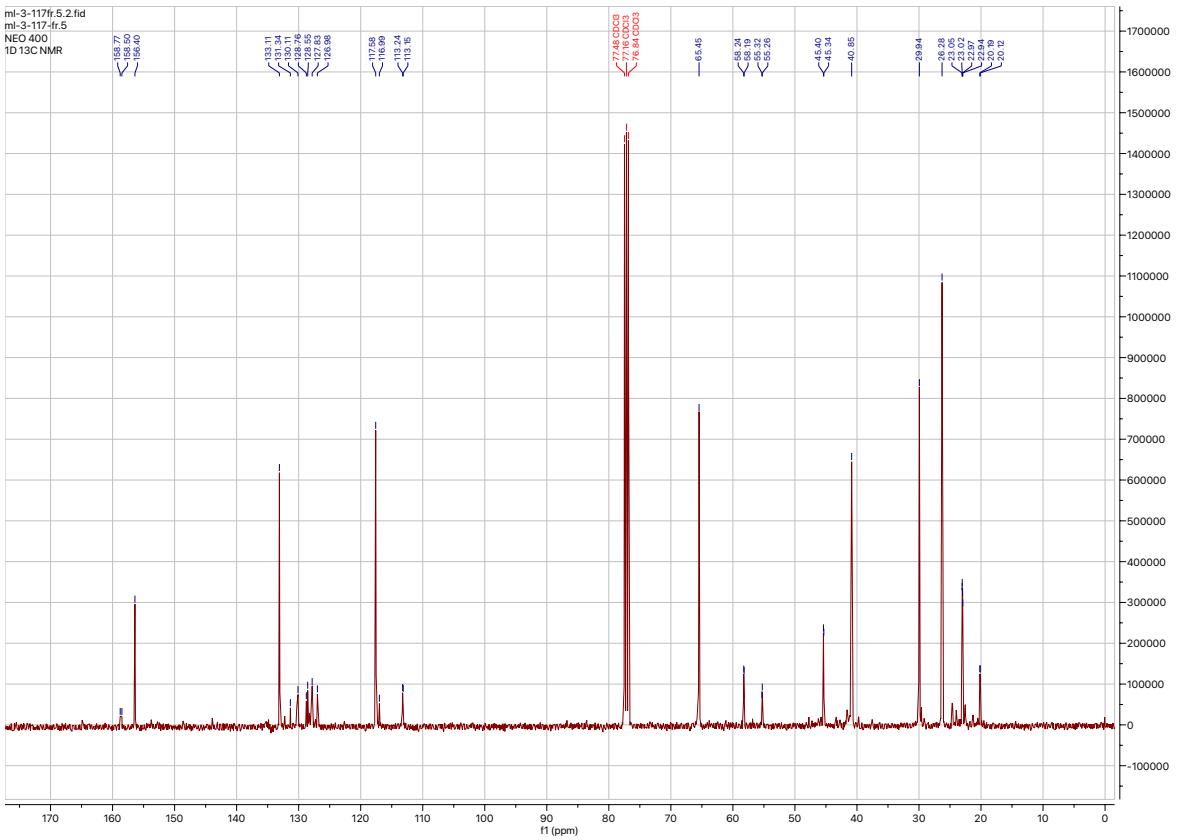
ml-3-117fr.5.2.fid
ml-3-117-fr.5
NEO 400
1D 13C NMR
f1 (ppm)

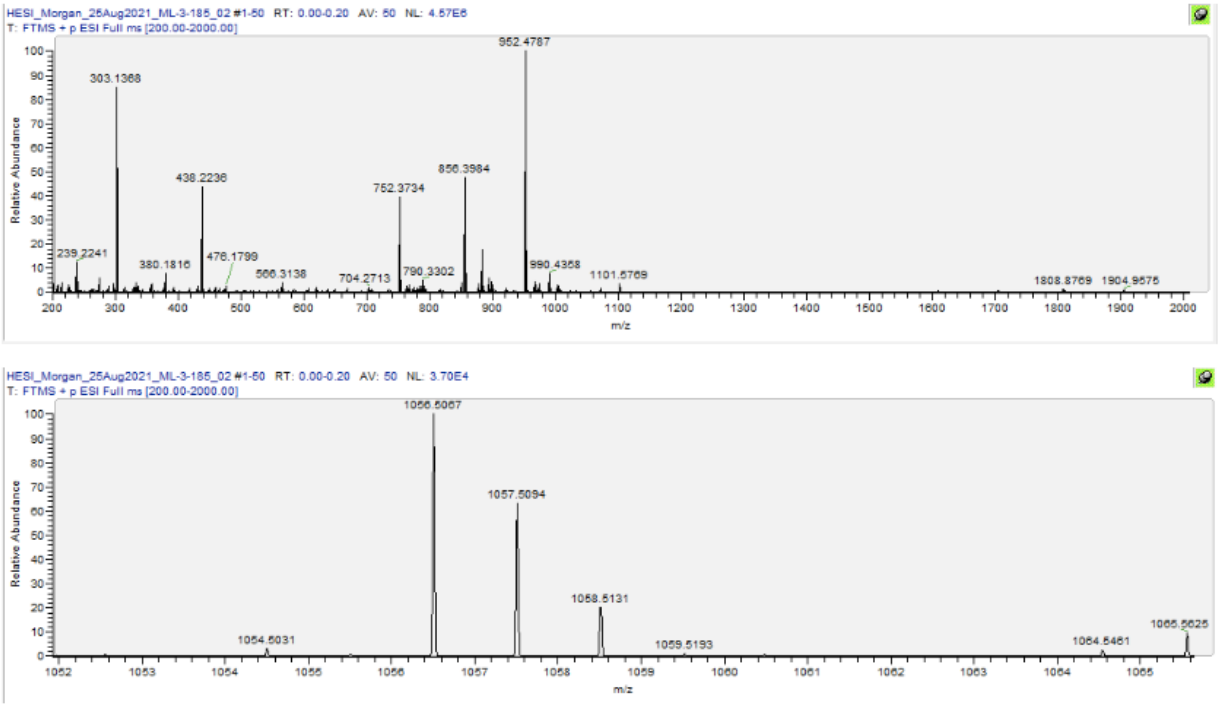

Table 2-4: Mass fragmentation of 12

Molecular Fragment	Expected mass [M]	Observed mass $[MH]^+$
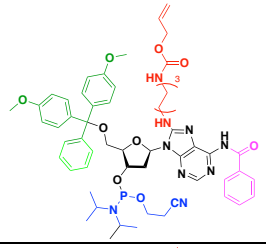	1055.5034	1056.5067
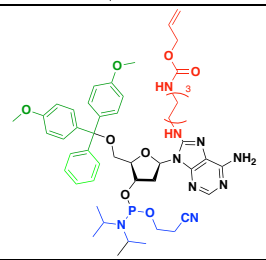	951.4772	952.4787
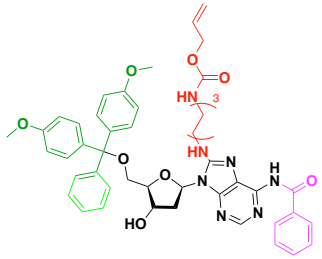	855.3956	856.3984

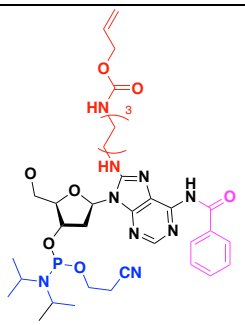	752.3649	753.3734

Solution-phase alloc deprotection protocol

All additions to the oligonucleotide column were performed using two 1-mL syringes, one on either end of the column to create a seal. All mixing was performed by 'injecting' one syringe while letting the other syringe 'fill up'. The beads were washed with anhydrous DCM (3 x 1 mL, 30 s/mL). A 16 mM solution of $PhSiH_3$ in DCM (anh.) (250 µL, 20 equiv.) was added to the beads, and mechanically stirred for 2 min. Then, a 64 µM solution of $Pd(PPh_3)_4$ in DCM (anh.) (750 µL, 2 equiv.) was added, and the whole mixture was stirred with the beads for 15 minutes (1-2 syringe pumps/s). The beads were then washed with DCM (anh.) (3 x 1 mL, 30 s/mL), and the column placed back on the DNA synthesizer and flushed with instrumental acetonitrile for 90s. The beads were then dried with $N_{2\,(g)}$ (70s).

T8 HRMS analysis

	M	$\frac{M-1}{1}$	$\frac{M-2}{2}$	$\frac{M-3}{3}$	$\frac{M-4}{4}$
Calcd	1973.4876	1972.4876	985.7438	656.4958	492.1219
Found	-	1972.4851	985.7383	656.8238	492.3660

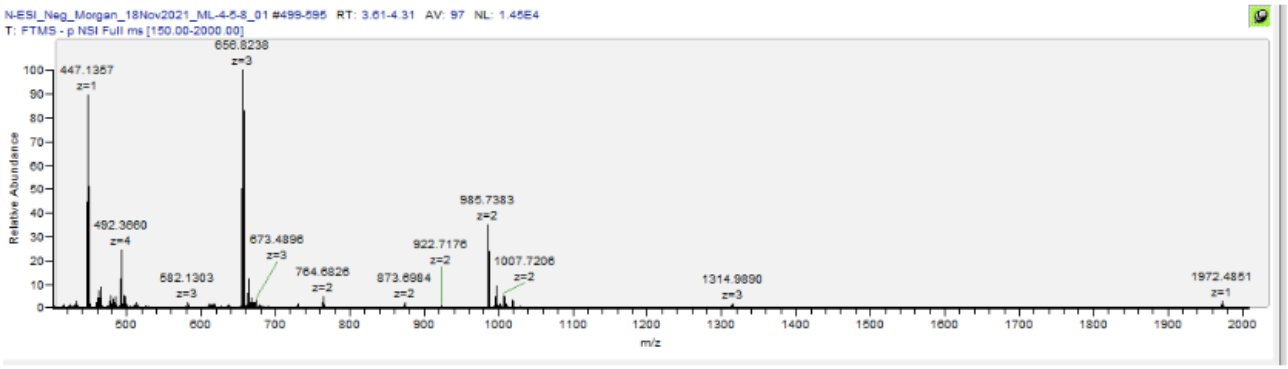

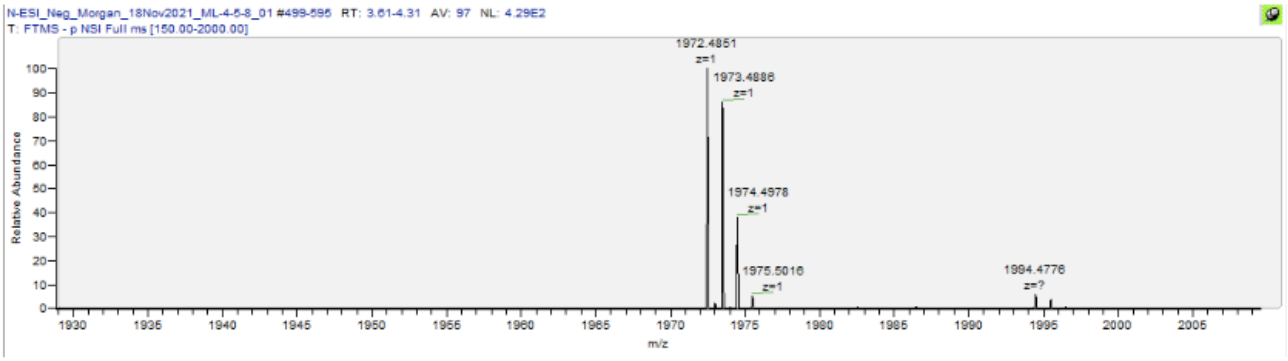

T9 HRMS analysis

	M	$\frac{M-1}{1}$	$\frac{M-2}{2}$	$\frac{M-3}{3}$
Calcd	1591.4085	1590.4085	794.7042	529.1361
Found	-	1590.4086	794.7067	529.4649

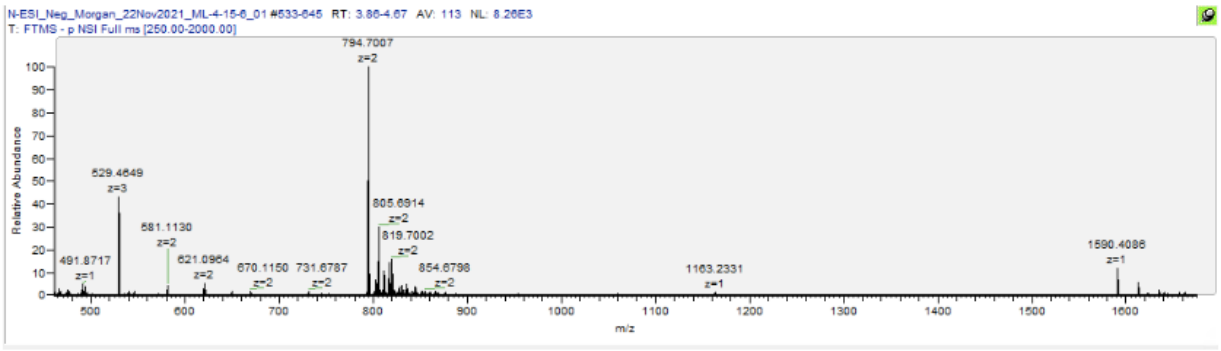

Chapter 3 – Hit compound optimization for selective inhibition of m^6A demethylase ALKBH5

3.1 Introduction

The reversible chemical modification of DNA or RNA nucleobases occurs within all living organisms. These enzyme-catalyzed modifications are essential for myriad biological processes, including gene expression and epigenetic regulation.[11] The most studied of this modification class is nitrogen methylation (*N*-methylation), which accounts for 60% of all known epigenetic RNA modifications;[6,7,11] methylation of the *N*-6 position on adenosine accounts for half of these (**Fig. 3-1**).[24,96] N^6-methyladenosine (m6A) regulates all major mRNA functions, including translational efficiency and stability.[97] RNA methylation is the result of dynamic interplay of between methyltransferases and demethylases, which add or remove the methyl substituent from the bases, respectively.[6,11,24,32]

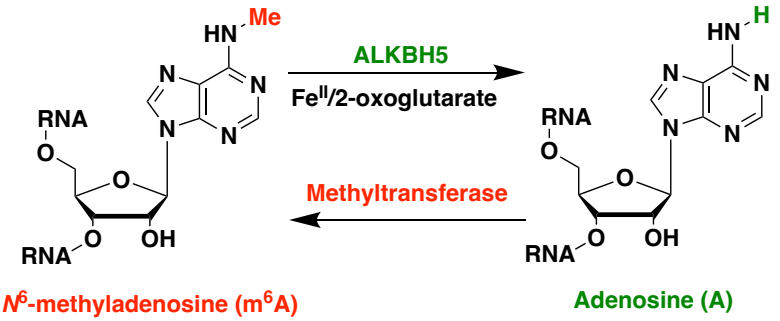

Figure 3-1: Demethylation of m6A by demethylase ALKBH5, and reverse process with a methyltransferase forms m^{6}A

One significant family of nucleic acid demethylases is that of AlkB, which are iron(II)/2-oxoglutarate (2OG)-dependent oxygenases, consisting of *E. coli* AlkB, and the nine human homologues, ALKBH1-9 (ALKBH9 is also known as fat mass and obesity-associated protein, FTO).[11,31]

The AlkB family is well characterized.[11] Due to the highly conserved structural elements within the catalytic domain of the demethylases (the 'HXD…H' motif, two bookending histidine residues with an aspartate residue between them, and the 'R…R' arginine motif (**Figure *1-4***)), no selective inhibitors for ALKBH5 have been developed to date. A high-throughput screening (HTS) of large molecular libraries could therefore be an effective method for selective inhibitor discovery.

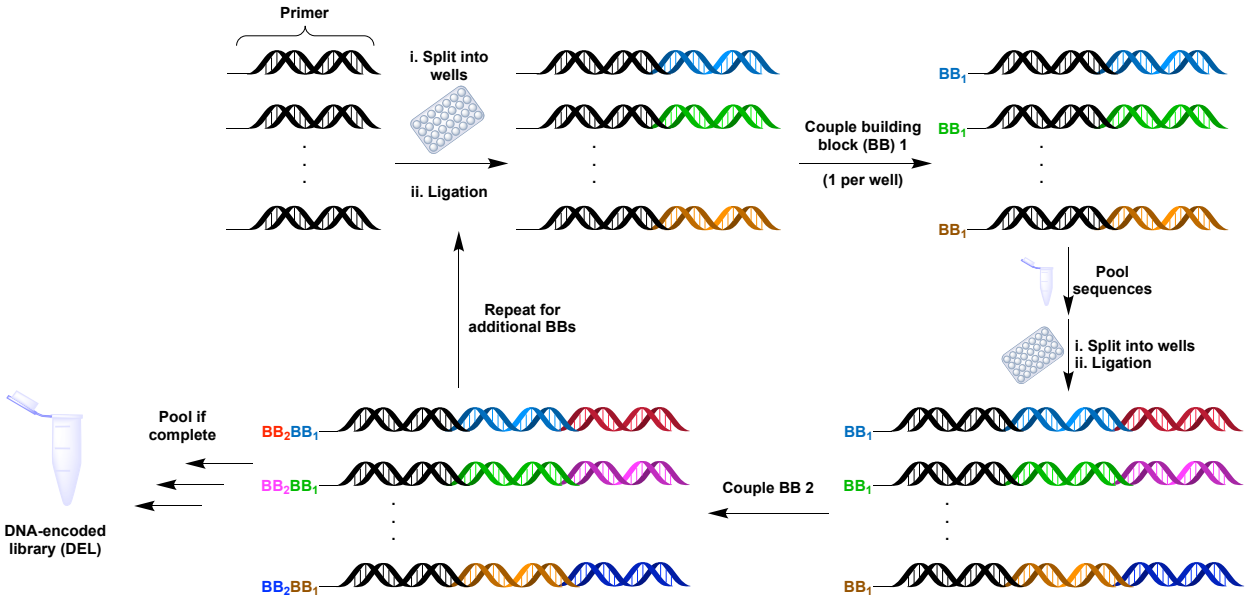

Figure 3-2: Split-and-pool construction of a two-cycle DNA-encoded library

Since first conceptualized by Brenner and Lerner in 1992, DNA-encoding of small molecule libraries has become a pioneering method for hit development in industrial and academic pursuits.[98–101] DNA-encoded chemical libraries (DELs) represent an economic method of HTS – they comprise mass libraries of small molecules (often $>10^6$ members) which are individually barcoded with a discrete DNA sequence. A library is screened against a target of interest, usually a protein, and hit molecules towards the target can be identified easily and unambiguously. DELs are built with simple, DNA-compatible chemistry using split-and-pool methodology, exponentially growing the size of the library (**Figure *3-2***). DEL construction starts with a DNA primer, appended with a functionalization 'handle'. This pool is split into a multi-well plate (one well for each chemical building block in the round, ***m***); a unique DNA barcode is ligated to the primer, corresponding to the building block for that well; the building block is then covalently attached to the handle, and the sequences are pooled again. This cycle is repeated for a set number of rounds (***n***) until sufficient library size is achieved ($\boldsymbol{m^n}$). Commonly, DEL constructs proceed through 2-3 rounds of construction, with each round using 100s of individual building blocks.

A HTS of a DEL occurs as follows: the library is incubated with an immobilized target, where hit molecules bind to the target; the non-binding members are washed away; the binding members are eluted from the immobilized target; PCR amplification and sequencing of the DNA

barcodes (of both pre- and post-selection libraries) generates an unambiguous molecular identity. The hit compound is synthesized off-DNA for further evaluation and optimization (**Figure *3-3***).[101–103] The *in vitro* selection of small-molecules from DELs has been very successful, both industrially and academically, for the identification of lead molecules from which potent inhibitors have been developed.[104–107]

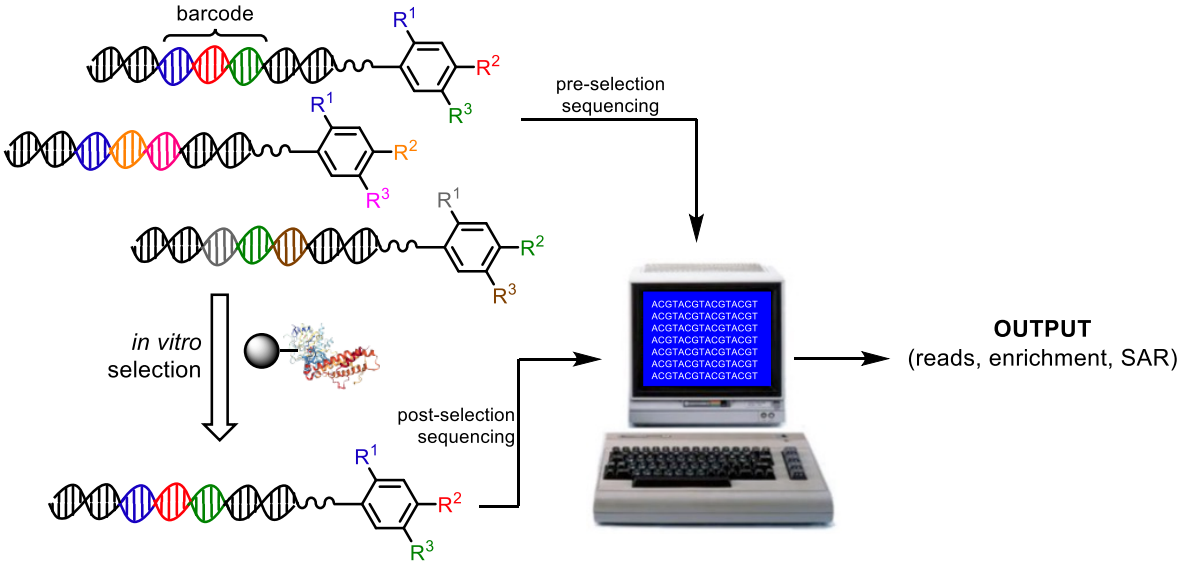

Figure 3-3: Workflow of DEL screening

This project started with a DEL screening for hits towards two demethylases and a methyltransferase, ALKBH5, FTO, and METTL3, respectively. Molly Hu, from the Hili lab, performed DEL selections against these proteins using pre-made libraries commercially available through WuXi AppTec. The company performed hit sequencing and analysis for the enrichment of members in post-selection libraries. They then synthesized the top five compounds from all three target screenings, and Molly performed chemiluminescent IC_{50} inhibition assays against the three FTO compounds and the two ALKBH5 compounds using commercially available kits from BPS Bioscience. The two ALKBH5 compounds and their IC_{50} data are shown in **Figure 3-4**.

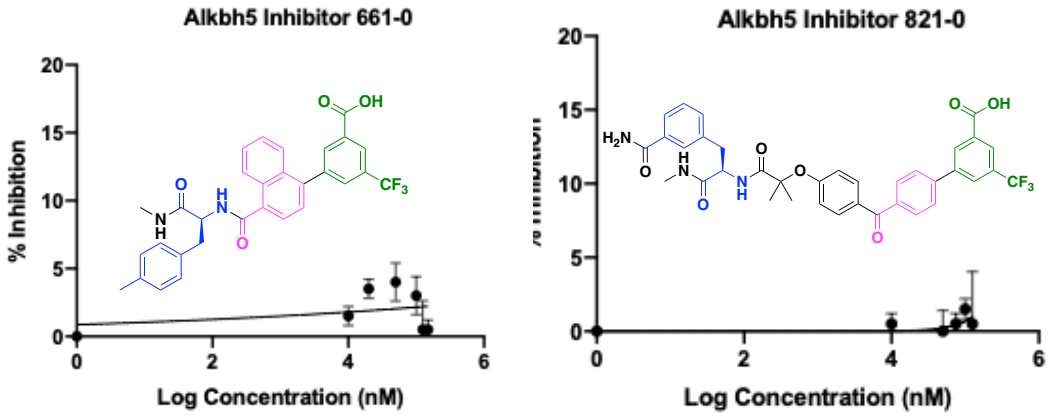

Figure 3-4: IC50 data from the 'hit' compounds for ALKBH5 inhibition

Both compounds contain a substituted phenylalanine residue (blue), an aromatic ketone (pink), and a terminating (trifluoromethyl)benzoic acid (green). Of particular interest is the presence of the trifluoromethyl group in both compounds, as there are a host of beneficial aspects for fluorine-containing drug molecules, including slower metabolism, better cell permeability, and solubility facilitation.[108]

To note, while the IC_{50} data for both molecules does not look particularly strong, both experiments were hampered by insolubility issues with the molecules themselves. I decided that because of the significant structural overlap, and that compound 661-0 seemed to produce slightly better inhibitory data of the two, this hit molecule would be synthetically optimized as a potential lead for selective inhibition of ALKBH5. Following the strategy for the optimization of DEL hits in a meta-analysis by Reihar *et. al.*,[109] I sought to increase solubility at the original DNA attachment site of the molecule, as well as exploring a truncation of the original 661-0 molecule.

To characterize the molecular inhibitory capacities, a fluorescence polarization (FP) assay would need to be developed for ALKBH5. FP is ideal for small-molecule testing with enzymes because it is a widely used, rapid, and provides quantitative analysis of molecular interactions.[110] First described by Perrin in 1926, FP eventually became adopted in HTS methods to facilitate drug discovery.[110,111] In FP, a fluorophore is excited by light; the fluorophore's emission is read by both a perpendicular and parallel polarizer, and the intensities of both signals are processed, producing fluorescence polarization data, measured in milliPolarization (mP) units (**Figure *3-5***). Low affinity molecules experience greater free rotation and will have similar levels of perpendicular and

parallel emissions. High affinity molecules will experience much more limited free rotation, and will emit perpendicular or parallel light preferentially over the other, producing a rise in FP signal.[110,112] For my purposes, a fluorescent probe, known to bind to ALKBH5 will be used; the small molecules will be titrated into the experiment at increasing concentrations, displacing the probe and giving the attached fluorophore greater molecular rotation, and decreasing the FP signal at increasing concentrations of the inhibitor.

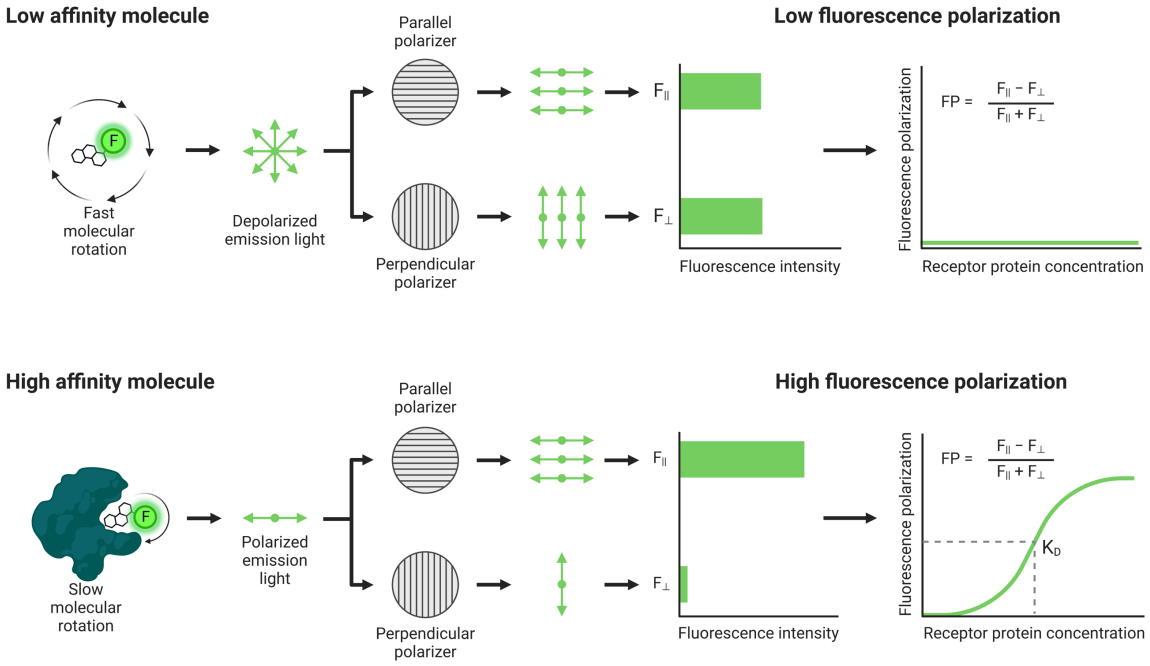

Figure 3-5: Visual representation of the mechanics of FP to produce a signal (created in Biorender)

3.2 Results and Discussion

The goal of this project was to synthesize compounds **13** and **14**, develop an FP assay for molecular examination against ALKBH5, and evaluate the compounds that FP assay. I hoped to significantly improved IC_{50} data, undertake a structure-activity relationship (SAR) campaign to further develop the molecule, and create a novel, selective inhibitor of ALKBH5.

As suggested in the meta-analysis for the optimization of hit compounds, using N,N-dimethylethylenediamine in the original DNA attachment site has been reported to increase

compound solubility, and potentially assist in molecular binding to its target. Additionally, since truncation products are also a common strategy when optimizing hits, the first deletion building block compound would also be examined (**Figure *3-6***).[109]

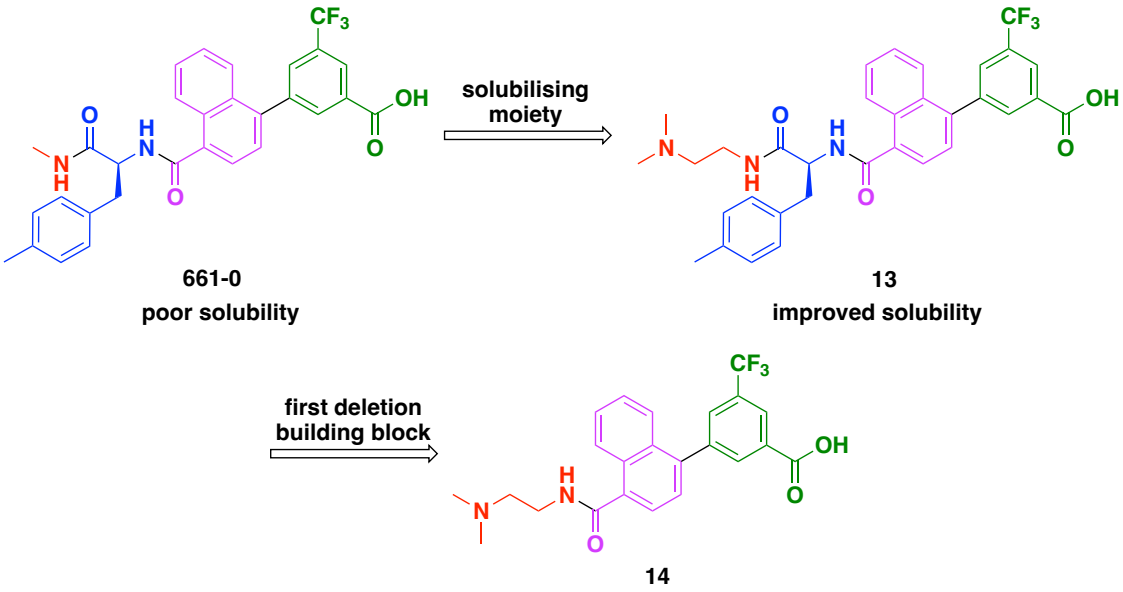

Figure 3-6: Synthetic strategy for hit optimization of 661-0

3.2.1 Synthesis of truncation compound 14

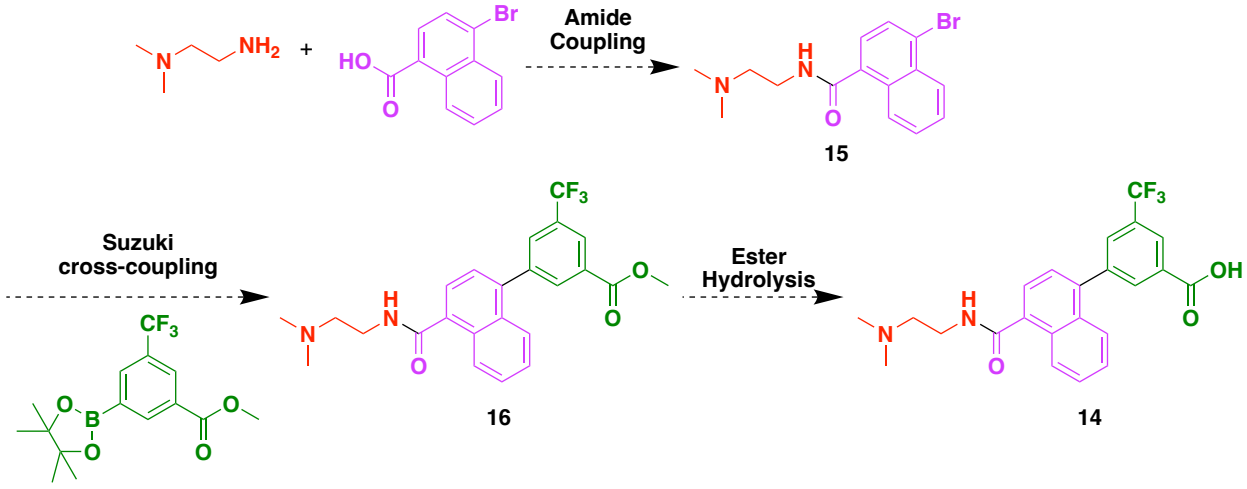

Scheme 3-1: Schematic pathway to 14

To begin the synthesis of compound **14**, the first step was amide bond formation between 4-bromo-1-naphthoic acid and N,N-dimethylethylenediamine (**Scheme *3-1***). My first attempt followed an adapted protocol using classic amide bond-forming reagent EDC (1-ethyl-3-(3-dimethylaminopropyl)carbodiimide), as well as hydroxybenzotriazole and *N*-methylmorpholine.[113] While the crude NMR appeared to indicate successful synthesis, many impurities remained in the mixture. I purified the compound with column chromatography, employing a 0-10% MeOH/DCM gradient as the eluent. The ^{1}H NMR of the purified compound contained some desired peaks, however several peaks could not be accounted for in the desired product **15**. Further spectroscopic analysis by ^{13}C NMR and mass spectrometry indicated the purified product was unfortunately the EDC adduct of the carboxylic acid, without final conversion to the desired amide. I decided to seek a new protocol for the transformation.

I found and adapted a two-step procedure using oxalyl-chloride and catalytic DMF to form the amide bond via an acid chloride intermediate.[114] After column purification of the crude mixture, the ^{1}H NMR indicated a successful synthesis of **15**. ^{13}C NMR and mass spectral analysis (Expected: 320.0524, Found: 321.0590 (M+1)) further confirmed the product synthesis, in an 88% yield.

The final coupling step in the synthesis of **14** was a Suzuki cross-coupling between the 4-brominated naphthoic diamine and the pinacol ester of 3-(methoxycarbonyl)-5-triflouromethylphenylboronic acid. Prior to committing any compound **15** to a protocol, I wanted to test a couple cross-coupling reaction conditions using napthyl substrates. 1-bromonaphthalene and phenylboronic acid, pinacol ester, were chosen as the substituents to test the protocol, with a workup adapted from Dong *et. al.* (**Scheme *3-2i***).[115,116]

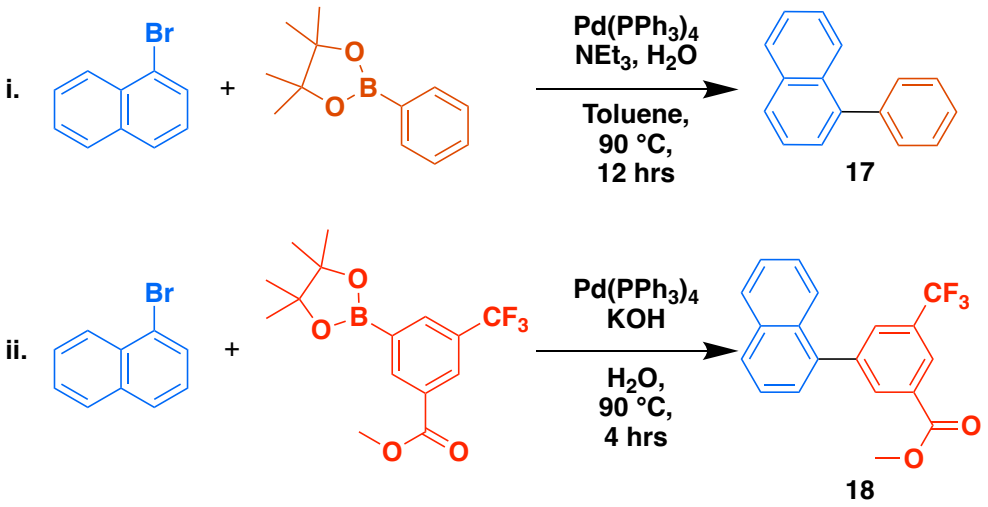

Scheme 3-2: Suzuki cross-coupling conditions

A TLC of the reaction mixture upon workup of the overnight reaction indicated complete conversion of the starting material under the conditions, and my ^{1}H NMR analysis revealed the synthesis of **17** was successful, and the product was formed cleanly.

The second cross-coupling protocol I wanted to try was adapted from a report by Dong *et. al.*, and which I had taken the workup from already (**Scheme *3-2ii***).[116] I wanted to try this protocol because of the greener conditions: water was used as a solvent and a shorter reported reaction time. Additionally, to offer a clearer handle of the product by ^{1}H NMR, I used 3-(methoxycarbonyl)-5-triflouromethyl boronic acid, pinacol ester in this example; the methyl ester handle would provide a clear singlet in the NMR spectrum outside of the aromatic region. This boronic acid would also be the coupling partner I would be using for the synthesis of **13** and **14**. Unfortunately, I encountered poor solubility when attempting the reaction, and the formation of **18** was unsuccessful. I chose the first protocol to move forward with for compound synthesis.

I then attempted the Suzuki cross-coupling reaction between **15** and the pinacol ester of 3-(methoxycarbonyl)-5-trifluoromethyl boronic acid. The crude product was purified by column chromatography with 0-10% methanol/DCM solvent system. Unfortunately, low yields were also encountered with these conditions, resulting in 5% for this coupling step, and 4.20 mg of product being isolated. However, **16** was successfully synthesized, as confirmed by ^{1}H NMR, ^{13}C NMR, and mass spec data. Despite the low yield, enough material existed to attempt a hydrolysis of the ester, forming the desired compound **14**.

I found a simple ester hydrolysis protocol using 2 N NaOH on a substrate with two methyl esters, so I adapted this to a 1 N NaOH for my compound with a single methyl ester.[117] Upon completion of the reaction, 1.55 mg were recovered, and unfortunately the ^{1}H NMR did not contain the hydroxide proton, instead the methyl singlet remained.

I then performed the Suzuki cross-coupling again on a larger scale to furnish additional **16** for further ester hydrolysis experimentation. However, upon purification, isolation, and analysis of the 'product', I found that the reaction did not proceed at all this time, and I recovered essentially 100% of the starting material. I decided to pursue an alternative cross-coupling strategy.

Luckily, our lab had already found success with a protocol reported by Ma *et. al.* in 2008, this time employing sodium carbonate as base, in a 3:1 dioxane:water solvent mixture.[118] The crude ^{1}H NMR appeared to show successful cross-coupling, although the spectrum ultimately required purification of the compound to yield the final methyl ester **16**. After testing several solvent systems for resolution of the product via TLC, I decided to move forward with column purification of the product using 0-20% Methanol/Dichloromethane + 1% Triethylamine (TEA). I then analyzed the purified compounds' ^{1}H and ^{13}C NMR spectra, and mass spectrum.

The mass spectrometry analysis was initially confusing (Expected: 444.1661, Found: 431.1572) though I became much more excited when I realized the expected mass of hydrolyzed methyl ester, i.e. compound **14**, (Expected 430.1504). The MS analysis revealed that the compound was not the methyl ester, but the desired carboxylic acid **14**. The NMR spectra further confirmed these results, though a significant amount of TEA remained as well. After trying couple modified solvent systems to remove TEA by column chromatography, I decided the easiest way to remove TEA at this stage was to take up the compound in dichloromethane, wash once with an aqueous 10% hydrochloric acid mixture, dry, and concentrate. After 'cleaning up' the material, the NMR spectra showed the expected peaks, free of lingering TEA, with a final yield of 19%. Compound **14** was complete.

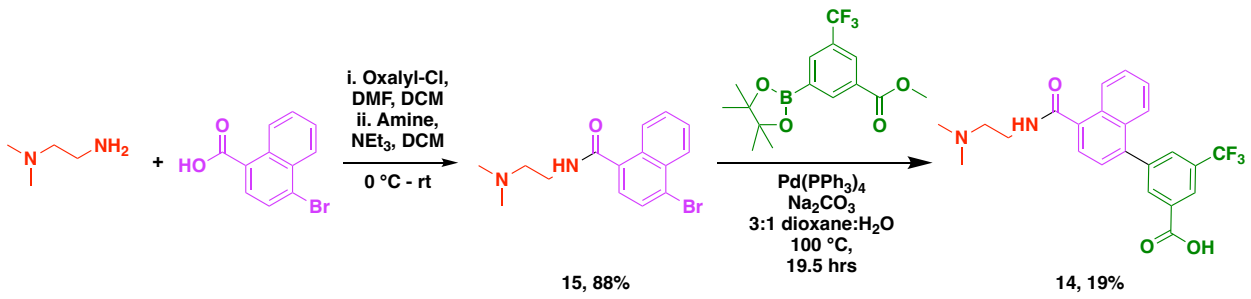

Scheme 3-3: Synthesis of 14

3.2.2 Synthesis of full-length compound 13

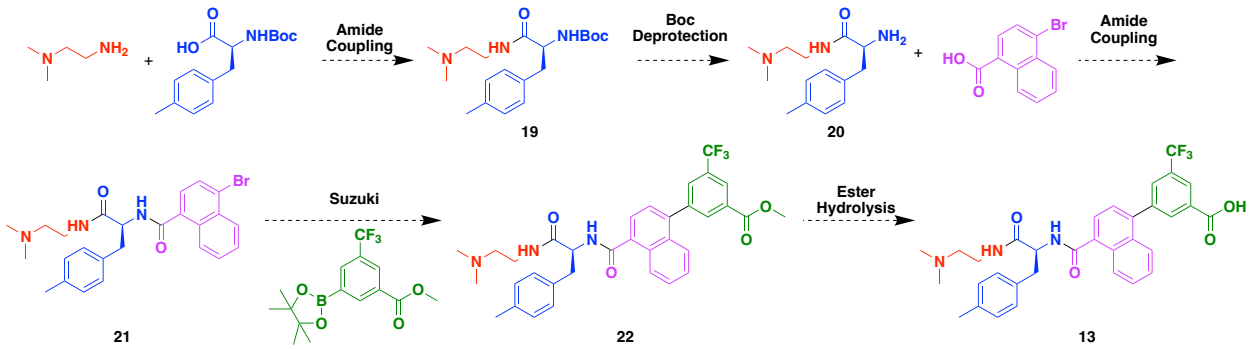

Scheme 3-4: Schematic pathway to 13

While more steps are involved relative to the synthesis of **14**, theoretically the synthesis of **13** (**Scheme *3-4***) is almost identical; there are just additional amide bond coupling and deprotection steps.

Given the success of the oxalyl-chloride amide bond protocol, the same conditions were applied to *N*,*N*-dimethyl-ethylenediamine and boc-protected (4-methyl)-*L*-phenylalanine. After purification and spectroscopic analysis, I found product **19** was successfully synthesized at a 62% yield.

My next step was Boc-deprotection this product using a conventional triflouroacetic acid protocol.[119] Unfortunately, while the ^{1}H NMR seemed to indicate a successful deprotection, the mass was not found for the desired compound.

I re-did the oxalyl-chloride amide bond protocol, and after purification, ^{1}H NMR, ^{13}C NMR, and mass spec data were obtained. The proton spectrum did not contain the boc group, which was initially quite worrisome. However, upon further inspection of that spectrum, as well

as comparison with the carbon NMR, the boc-deprotected free amine compound **20** was observed. This was further corroborated by mass spec data (expected: 249.1841, found: 250.1899 (M+1)). Interestingly, no presence of the boc-containing group was displayed in the MS data, indicating a total deprotection of the boc-group *in situ*. My hypothesis was that the HCl generated during the second step of the amide synthesis was responsible for the deprotection (**Scheme *3-5***). A recent report on the use of oxalyl-chloride for mild N-boc deprotection also suggested HCl generated during the reaction was the cause.[120]

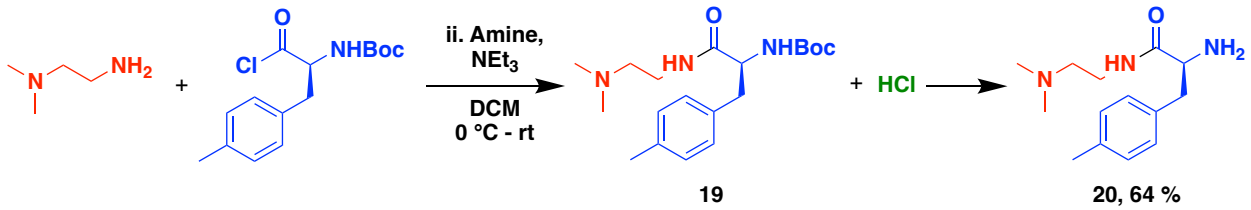

Scheme 3-5: In situ deprotection of the boc group from acid chloride intermediate

Having successfully and efficiently generated **20**, another amide bond needed to be formed with the 4-bromo-naphthoic acid. The oxalyl-chloride reaction was performed, generating **21** in a 73% yield after purification. Verification of the product was confirmed with ^{1}H and ^{13}C NMR, and mass spec data (expected: 481.1365, found: 482.1424 (M+1)).

The next step was to proceed with the Suzuki cross-coupling, using the same protocol from **14**. I was also hoping to see the same hydrolysis of the methyl ester upon review of the synthesized product. I set up the cross-coupling reaction with the same pinacol ester of the boronic acid. This reaction proceeded much more slowly than with **14**, as monitored by TLC; in the end the reaction time was essentially doubled. This time, upon concentration and 1H NMR analysis of the crude product, it was much less clear whether the product was synthesized, due to the presence of impurities and a more crowded spectrum in general. I moved forward with column chromatography purification, using the same 0-20% methanol/dichloromethane + 1% TEA system. The desired fractions were collected, concentrated, and examined by NMR.

By proton and carbon NMR, the desired product **13** had been synthesized in a 20% yield. As with **14** there was TEA remaining in these spectra. I subjected the 'purified' compound to the same aqueous 10% HCl wash, which successfully removed the impurity. The found mass (592.2407, M+1) was as expected for **13** (591.2345). Compound **13** was complete (**Scheme *3-6***).

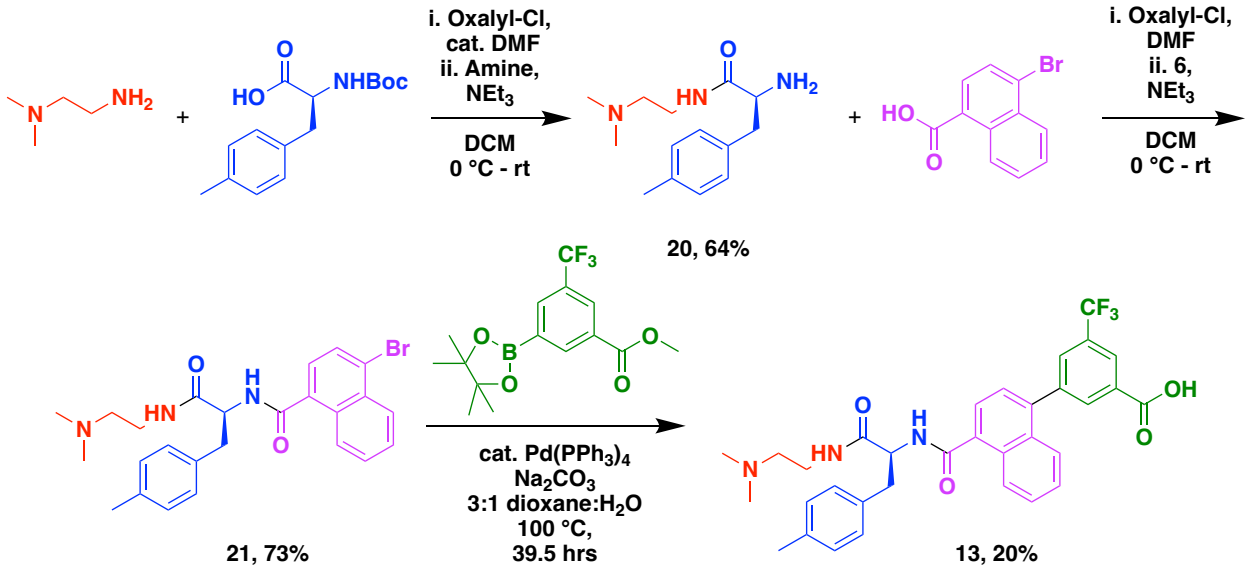

Scheme 3-6: Synthetic pathway of 13

3.2.3 Development of the ALKBH5 Fluorescence Polarization assay

Having synthesized my compounds to test against ALKBH5, my next step was to develop and confirm efficacy of the FP assay I would be using, followed by using it to evaluate both compounds' inhibitory affinities. A general protocol was used as a guide for assay development.[121] The first step in this process was to titrate ALKBH5 from low to high concentrations against a fixed concentration of a fluorescent probe. The fluorescent probe was a 20 nucleotide RNA sequence with a fluorescein molecule at the 5' end, and a single m^6A in the middle. The goal of this step was to produce the binding curve of the fluorescent probe with an increasing concentration of ALKBH5 such that maximal fluorescence emission is achieved within the system. The desired protein concentration is where 50-80% of the max fluorescence polarization is found on the curve.

As directed in the protocol, I used the ALKBH5 storage buffer (25 mM HEPES, 300 mM NaCl, 0.5 mM TCEP, 10% glycerol, 0.04% Triton X-100, pH 7.5) and attempted the titration. The first few experiments were hampered by issues with the FP reader. The instrument was fixed and began to generate coherent results. All experiments were run in duplicate. With this initial buffer, several attempts were made at ALKBH5 titration, using in-well concentrations of ALKBH5 of 659, 329.5, 164.8, 82.4, 41.2, 20.6, 10.3, 5.5, and 2.6 nM, and eventually including 1977 and 988.5

nM concentrations as well to bolster the concentration high end and promote a plateau region. However, after repeated, inconsistent results, I decided to examine the buffers themselves with the fluorescent probe; I compared the storage buffer with a simple 50 mM HEPES buffer, pH 7.5 previously used in an alternate ALKBH5 FP assay.[122] I found that the storage buffer produced a higher polarization values without protein present, which indicated the buffer was partially restricting free movement of the probe. I opted to switch to the simpler buffer moving forward.

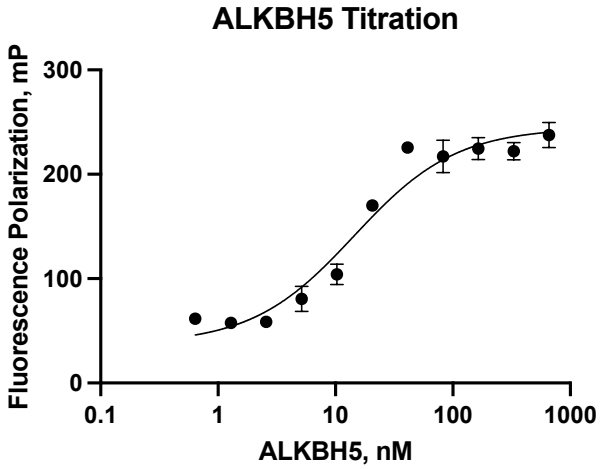

Figure 3-7: ALKBH5 titration curve

Finally, I was able to produce a respectable binding curve for the ALKBH5 titration. To really draw out the plateau at the top of the curve, I repeated the assay with additional high concentrations (329 and 659 nM in-assay concentrations), which very clearly displayed the sought after sigmoidal curve (**Figure *3-7***). From this graph, an ALKBH5 concentration of 20 nM produced an ~65% signal, and would be taken forward as the working protein concentration for the assay. My next step for assay development was to determine the concentration of the positive control probe, again through titration.

The positive control probe was the same RNA sequence as the fluorescent probe, but without the fluorescein molecule. The initial concentrations I used for the positive control probe were achieved by a two-fold dilution series, from 250, down to 0.98 nM. The results of this first experiment displayed a 'half-curve', showing an initial plateau and the beginning of a drop and ending there. This showed me I needed higher concentrations of the positive control probe to displace the fluorescent probe and produce a the low mP plateau region. This time, I used in-well

concentrations starting at 500 nM and following two-fold dilution series down to 2.4 nM. Unfortunately, sufficient results were still not found. Next, I tried in-well concentrations starting with 2000 nM and diluting down to 1.95 nM. The resulting curve was respectable (**Figure *3-8***). The error on the lower concentrations was higher than I would have liked, but there were two main objectives for this experiment: i) to show that with this assay an inhibition curve could be produced, and ii) to find a concentration where the positive control probe obliterates the fluorescent probe binding (1000 nM). Both were achieved here. The last step I wanted to try for assay development was to find a positive control molecule to validate that this assay produces the same result, though this step was not strictly required for the assay.

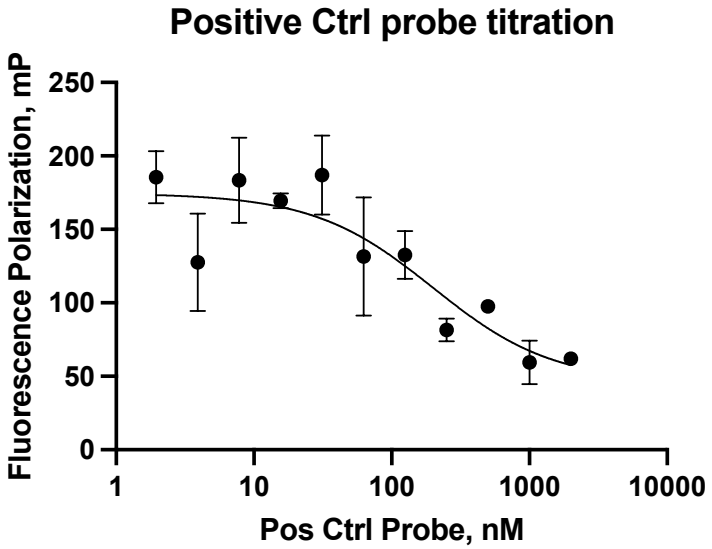

Figure 3-8: Inhibition curve with the positive control probe

From the literature, succinic acid produces reduced activity in ALKBH5, and a IC_{50} value of 30 μM.[11] Since the molecule was easily available, I decided to try it in this assay. I started with in-assay concentrations of 300 μM down to 2.34 μM through seven sequential two-fold dilutions, and the result data showed results I was not entirely surprised to find (**Figure *3-9***): given the obvious structural similarities between succinic acid and 2-OG, adding in any concentration of this molecule will not affect the fluorescence of the probe. 2-OG binds in conjunction with m^6A-containing species, and thus is likely how succinic acid interacts with ALKBH5. Since the FP assay produces signal only when the fluorescent probe is displaced, succinic acid is not displacing

the probe in the catalytic domain, and no signal is produced. I decided to move ahead and examine the molecules I had synthesized.

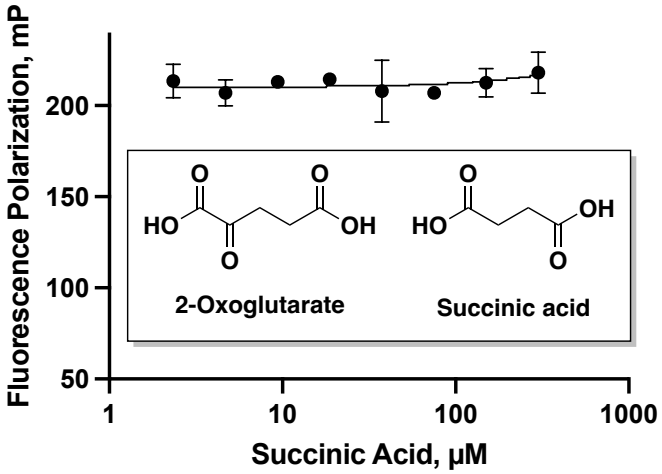

Figure 3-9: FP data from succinic acid (Inset: 2OG and Succinic Acid structures)

An established method in our lab of performing a quick FP assay is using examining a molecule with a high concentration and a low concentration, to parse whether the molecule exhibits any activity towards the protein. Given my low stock of both molecules, I decided to try this type of assay first. For **13**, I used 376 µM and 0.376 µM; for **14**, I used 984 µM and 0.984 µM. Unfortunately, the results of this assay were not clear (**Table *3-1***). For compound **13**, the lower concentration provided a slightly lower FP average than the ten-fold higher concentration, but both concentrations produced an FP signal within the range of fluorescent probe bound to ALKBH5. This meant the compound appeared to produce no change in signal within the context of this high-low assay experiment. For compound **14**, the lower concentration produced a higher average FP signal than the high concentration. This counterintuitive result points to this experiment not providing concrete results about either molecules ability to inhibit ALKBH5 or not. Ultimately though, the FP signal for both concentrations was still within the range of the fluorescent probe bound to ALKBH5. Nothing can truly be gleaned from these results regarding the molecules, and further examination of both should be undertaken.

Table 3-1: Fluorescence Polarization data from a high-low concentration assay of compounds 13 and 14

Inhibitor	Inhibitor Concentration, μM	Fluorescence Polarization, mP		
		Run 1	Run 2	Average
13	0.376	202	203	202.5
	376	234	189	211.5
14	0.984	209	213	211
	984	217	184	200.5

3.3 Conclusions and Next Steps

Over the course of this project, I successfully and efficiently synthesized two molecules which were hoped to exhibit inhibitory capacity towards ALKBH5. I developed a fluorescence polarization assay, using a fluorescein-labeled m^6A-containing RNA probe as the fluorophore. I then performed a high-concentration-low-concentration experiment using the synthesized molecules, to inconclusive results.

The next steps for this project would be to produce a slightly larger stock of the synthesized molecules, then run a proper screening assay of both molecules to observe inhibitory activity. Pending the results of that assay, a structure-activity relationship (SAR) campaign should be undertaken, which would create a greater understanding of how these inhibitors interact with ALKBH5, and to see whether these hit molecules could be modified further to produce higher affinity molecules. A screening of selectivity towards ALKBH5 would need to be subsequently performed, to examine the selectivity of the 'best binding' molecules towards the other proteins in the ALKBH family. Finally, if a selective ALKBH5 molecule had been produced through this campaign, the molecule would be given Dr. Hanson He's cancer research lab at Princess Margaret Hospital in Toronto for further testing of the ALKBH5 pathways as they relate to cancer pathologies.

3.4 Experimental details and supporting data

3.4.1 General information

^{1}H NMR spectra were recorded at 400 MHz on a Bruker spectrometer. Processing of the spectra was performed with MestReNova software. Analytical thin-layer chromatography (TLC) was performed on aluminum plates pre-coated with silica gel 60F_{254} as the adsorbent. The developed plates were air-dried and exposed to UV light. Column chromatography was performed using Silicycle SiliaFlash® F60 silica, 40-63 µm (230-400 mesh). Unless otherwise noted, water was purified with the Direct-Q® 3 UV Water Purification System. ALKBH5 was purchased from Active Motif (Cat. No. 31589). All ALKBH5 FP assays were analyzed using a Biotek Synergy H4 plate reader, in polarization mode. The detection method was set to 'Fluorescence', read type 'End Point', read speed 'Normal', lamp 'Xenon Flash', with 'Use Filter Wheel' and 'Fluorescence Polarization' options chosen. Excitation was set to '485/20', while emission was '528/20'. Optics were set to 'top', Gain at '110', and Vertical Offset set to 7.0 mm. 1X buffer used was 50 mM HEPES buffer, pH 7.5.

3.4.2 Synthetic procedures and supporting data

4-bromo-*N*-(2-(dimethylamino)ethyl)-1-naphthamide, 15

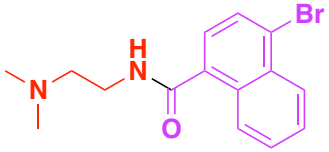

i. 4-bromo-1-naphthoic acid (0.797 mmol, 200 mg, 1 equiv.) was dissolved in DCM (2.4 mL). 2 drops of DMF were added to the solution while stirring. The solution was cooled to 0°C, and oxalyl-chloride (1.593 mmol, 135 µL, 2 equiv.) was added dropwise. The solution was warmed to room temperature while stirring, and reaction progress was monitored by TLC (10% MeOH/DCM). After 3.5 hours, the starting material had been consumed, and the reaction mixture was concentrated.

ii. N,N-dimethylethylenediamine (0.956 mmol, 104.6 µL, 1.2 equiv.) and triethylamine (1.196 mmol, 166.8 µL, 1.5 equiv.) were dissolved in DCM (1.2 mL). This mixture

was cooled to 0°C, the acid chloride from i was dissolved in DCM (1 mL) and added dropwise to stirred solution. Stirring was continued as the solution warmed to room temperature. After 6.75 hours, TLC revealed consumption of the acid chloride. The solution was washed with brine (10 mL), dried over Na_2SO_4, and concentrated.

The crude mixture was purified by column chromatography using a 0-10% MeOH/DCM gradient, affording **15**. ^{1}H NMR (400 MHz, $CDCl_3$) δ 8.29 (qd, J = 1.8 Hz, 8.0 Hz, 2H), 7.72 (d, J = 7.6 Hz, 1H), 7.58 (m, 2H), 7.40 (d, J = 7.6 Hz, 1H), 6.80 (br s, 1H), 3.57 (q, J = 5.8 Hz, 2H), 2.54 (t, J = 6 Hz, 2H), 2.25 (s, 6H). ^{13}C NMR (101 MHz, $CDCl_3$) δ 169.0, 134.7, 132.2, 131.6, 129.0, 127.9, 127.6, 126.1, 125.5, 125.3, 57.7, 45.1, 37.5, 37.3, 29.8. HRMS calcd for $C_{15}H_{17}BrN_2O$ $[MH]^+$: 321.0524 Found: 321.0590

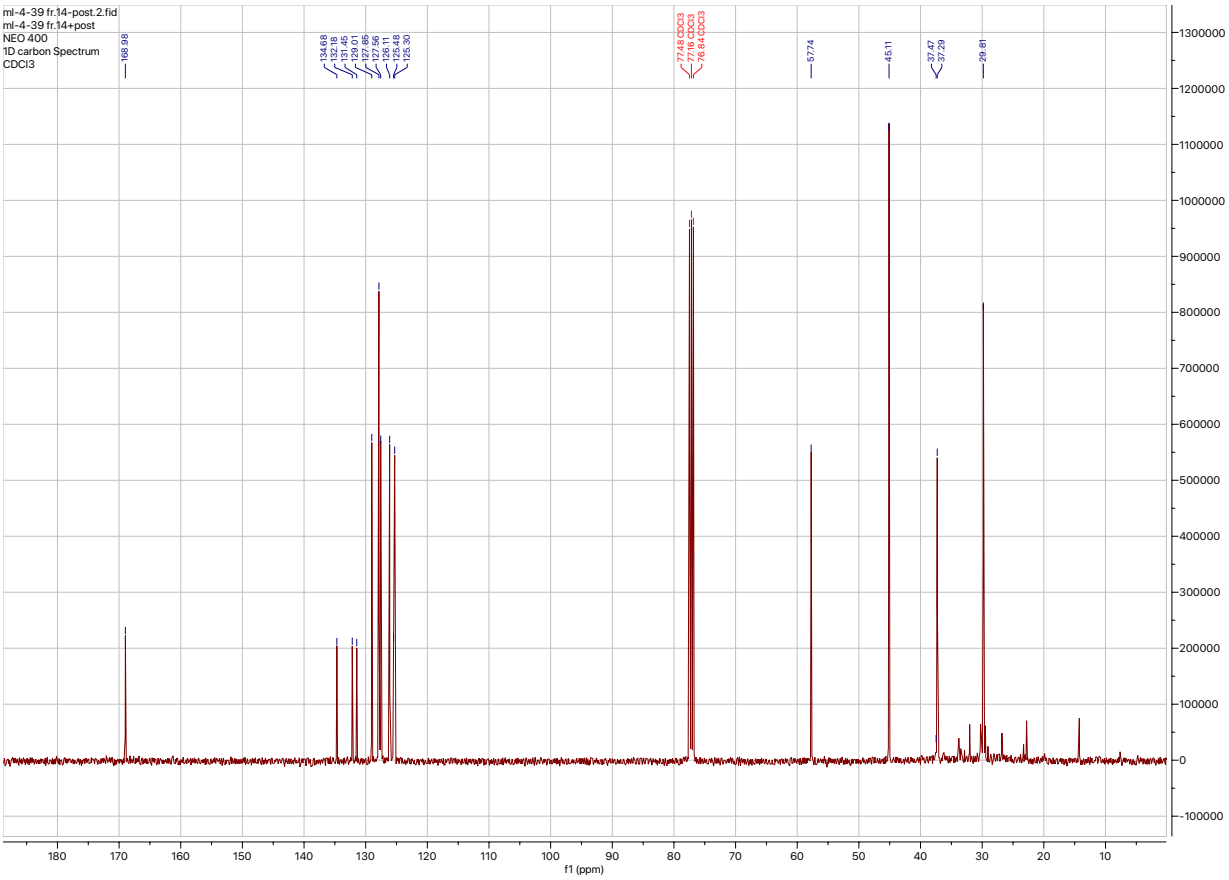

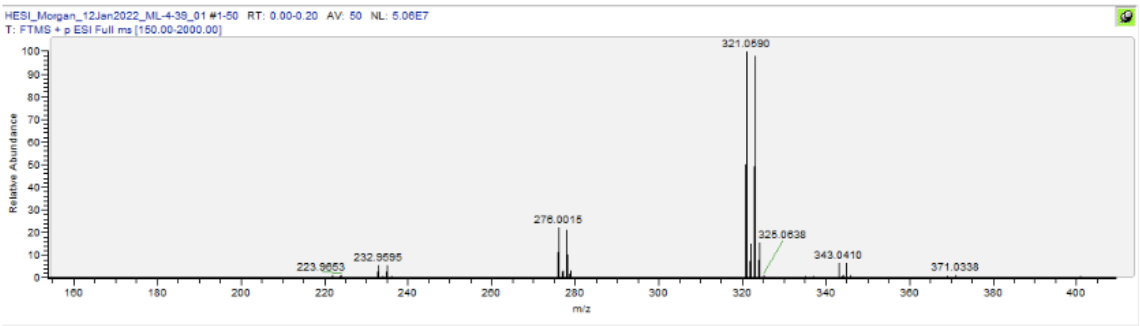

1-phenylnaphthalene, 17

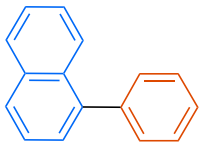

In a 1-dram vial, Palladium tetrakis(triphenylphosphine) ($Pd(PPh_3)_4$) (0.0018 mmol, 11.57 mg, 0.03 equiv.) was dissolved in toluene (1.6 mL) and stirred for 30 min at room temperature. 1-Bromonapthalene (0.327 mmol, 45.6 µL, 1 equiv.) was added to the vial, followed by

phenylboronic acid, pinacol ester (0.490 mmol, 99.78 mg, 1.5 equiv,), triethylamine (0.653 mmol, 91 µL, 2 equiv.), and water (0.653 mmol, 11.8 µL, 2 equiv). The reaction was heated to 90°C and stirred overnight (12 hours). After consumption of starting material, the reaction was dilute with 5 mL of water. The mixture was extracted with DCM (3 x 5 mL), and the combined organics were dried over Na_2SO_4. The organic layer was then concentrated. A crude NMR was taken.

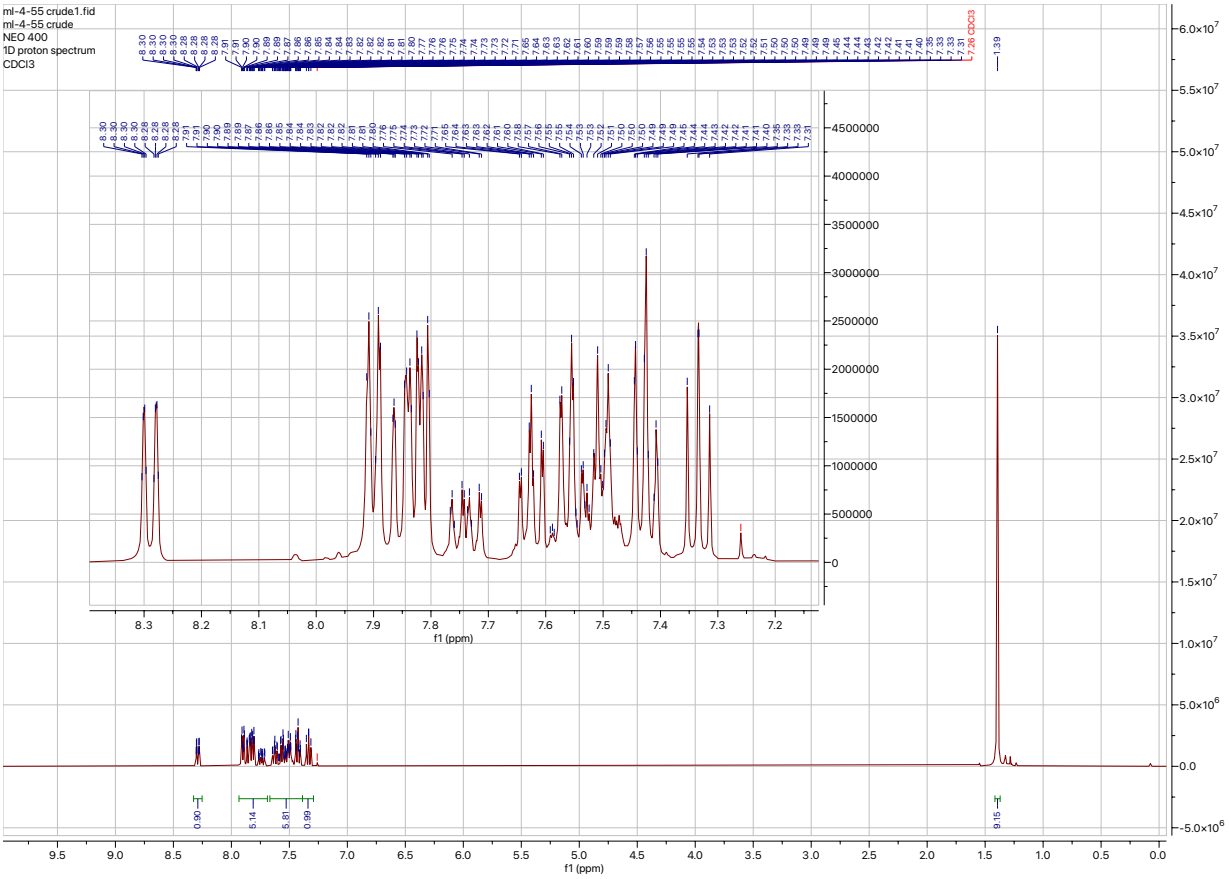

Methyl 3-(naphthalen-1-yl)-5-(trifluoromethyl)benzoate, 18

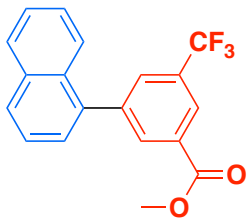

1-Bromonaphthalene (0.101 mmol, 14.14 µL, 1 equiv.), 3-(methoxycarbonyl)-5-triflouromethylphenylboronic acid, pinacol ester (0.121 mmol, 39.80 mg, 1.2 equiv.), KOH (0.151 mmol, 9.44 µL, of 16.01 M solution, 1.5 equiv), and $Pd(PPh_3)_4$ (0.005 mmol, 6 mg, 0.05 equiv.)

were added to a 1-dram vial. Water (606 µL) was added to the vial, and the reaction was heated to 90°C while stirring. After 4 hours, starting material was consumed by TLC. The mixture was dilute with 4 mL dH_2O, and the aqueous mixture was extracted with DCM (3 x 5 mL). The combined organics were dried over Na_2SO_4, filtered, and concentrated. A crude ^1H NMR was taken.

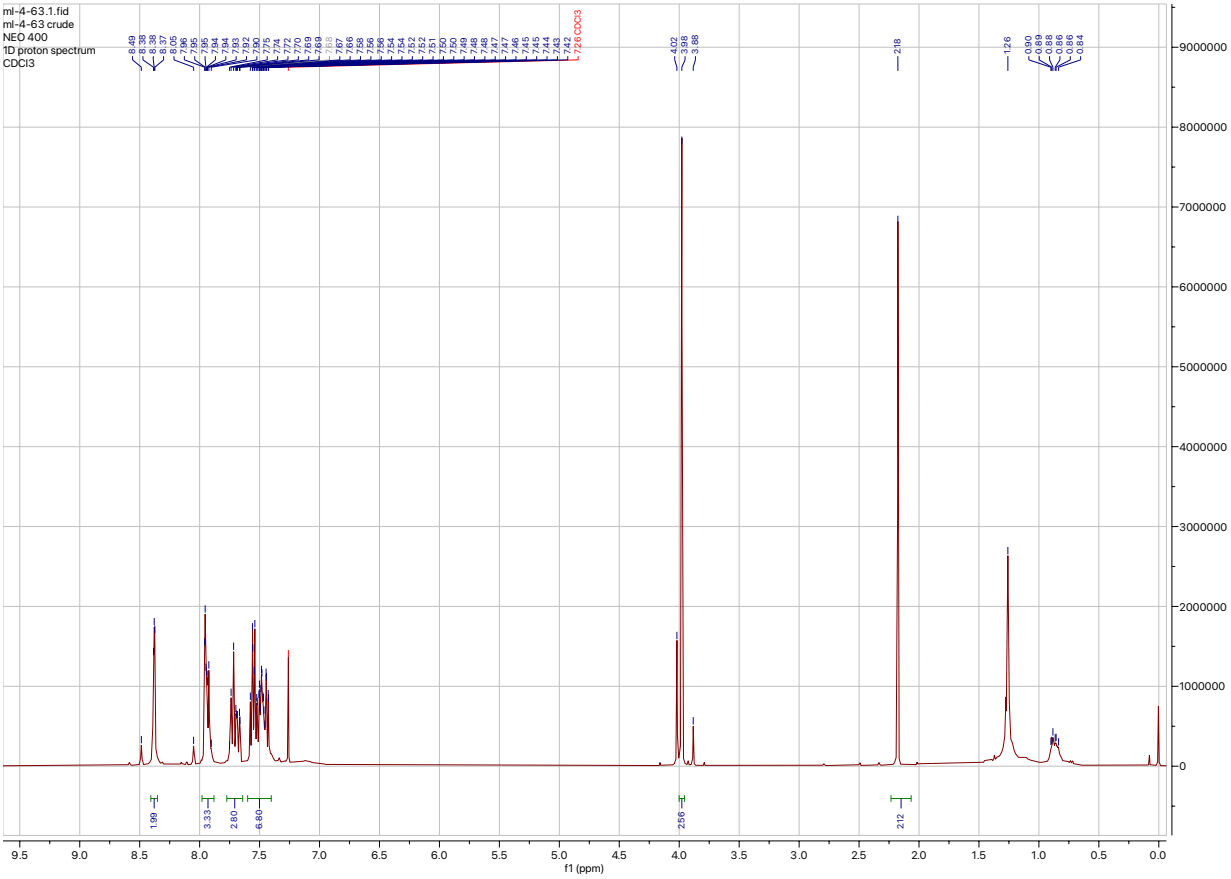

3-(4-((2-(dimethylamino)ethyl)carbamoyl)naphthalen-1-yl)-5-(trifluoromethyl)benzoic acid, 14

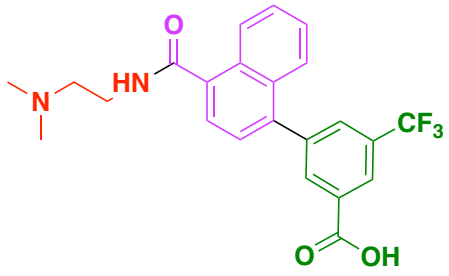

15 (0.156 mmol, 51 mg, 1 equiv.), 3-(methoxycarbonyl)-5-triflouromethylenebenzene boronic acid, pinacol ester (0.187 mmol, 61.8 mg, 1.2 equiv.), $Pd(PPh_3)_4$ (0.007 mmol, 9.1 mg, 0.05 equiv.)

and sodium carbonate (51.5 mg, 0.467 mmol, 3 equiv.) were dissolved in 3.1 mL 3:1 dioxane:water. The reaction was heated to 100°C and stirred overnight. TLC indicated starting material consumption after 20 hours. The reaction was cooled to room temperature, and the solution was added to 15 mL of 10% sodium carbonate solution and extracted with EtOAc (4 x 10 mL). The combined organics were washed with brine (30 mL), dried over Na_2SO_4, filtered, and concentrated. The crude material was purified by column chromatography using 0-10% MeOH/DCM + 1% TEA. ^{1}H NMR (400 MHz, $CDCl_3$) δ 11.93 (s), 8.97 (s, 1H), 8.53 (d, J = 8.6 Hz, 1H), 7.87 (d, J = 7.2 Hz, 1H), 7.73 (s, 1H), 7.64 (s, 1H), 7.60 (s, 1H), 7.45 (t, J = 7.4 Hz, 1H), 7.28 (m, 4H), 4.10 (br s, 2H), 3.63 (br s, 2H), 3.0821 (s, 6H). ^{13}C NMR (101 MHz, $CDCl_3$) δ 171.6, 170.0, 140.4, 140.3, 137.1, 133.8, 133.5, 131.2, 130.5, 130.2, 129.9, 128.2, 126.7, 126.5, 125.9, 125.8, 125.4, 124.9, 122.6, 63.3, 58.0, 57.0, 52.9, 43.0, 35.2, 29.6, 22.6, 21.7, 8.0. HRMS calcd for $C_{23}H_{21}F_3N_2O_3$ $[MH]^+$: 431.1504 Found: 431.1572

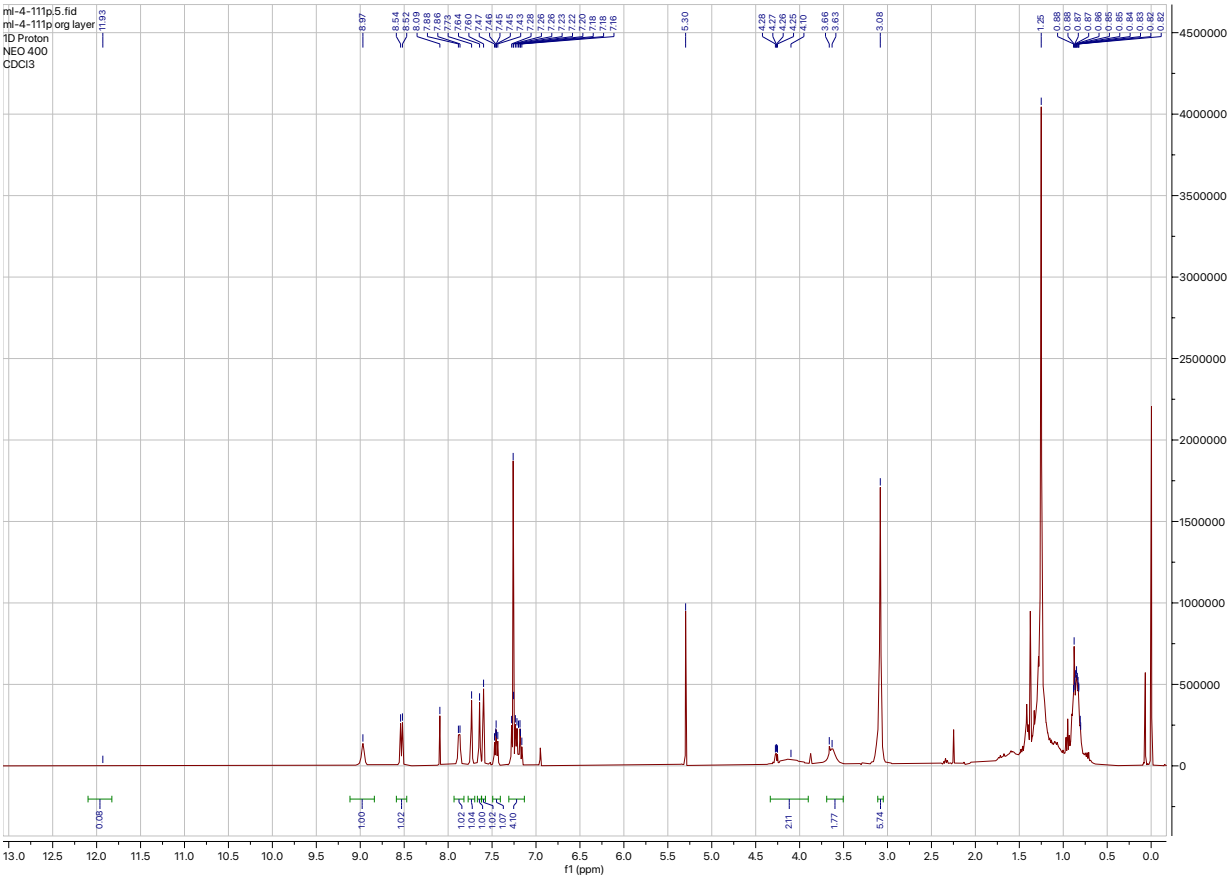

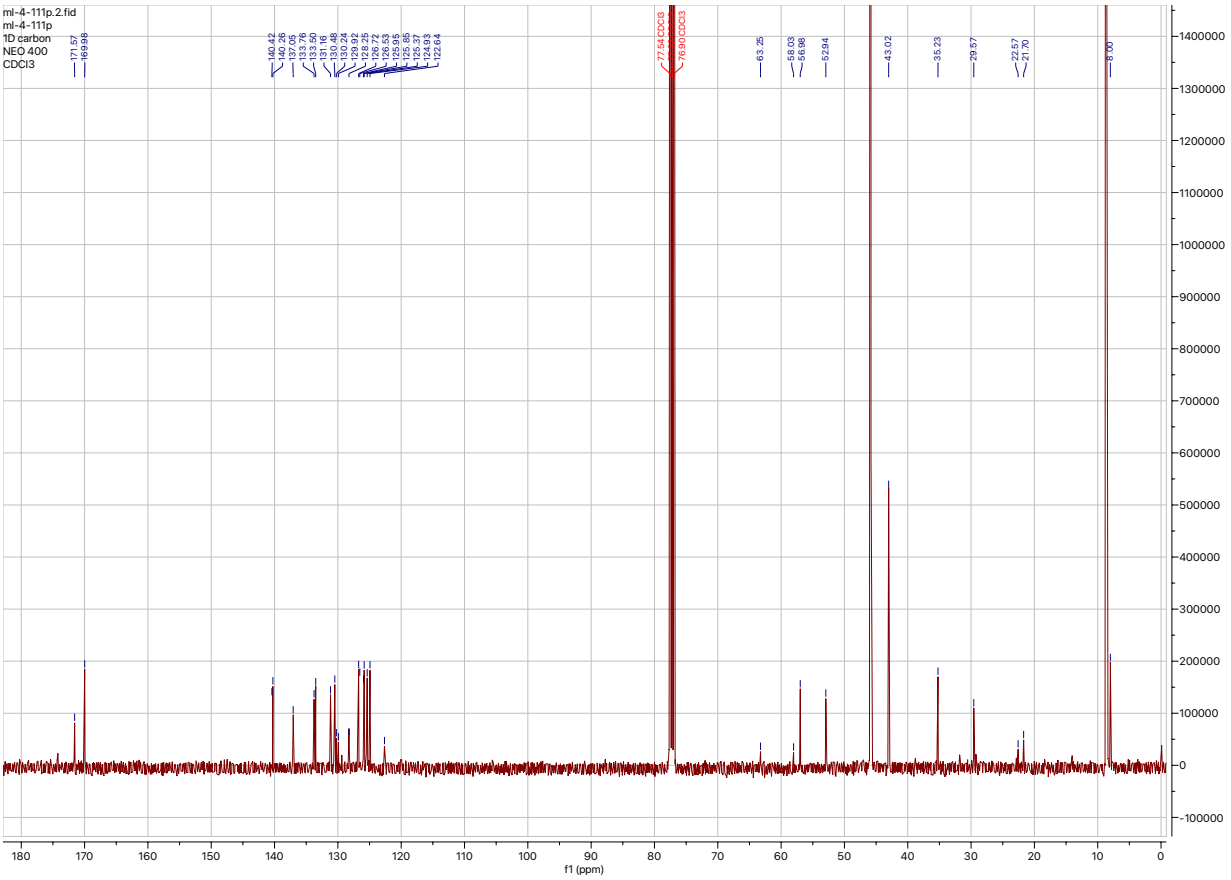
ml-4-111p.2.fid
ml-4-111p
1D carbon
NEO 400
CDCl3
171.57
169.98
140.42
140.26
137.05
133.76
133.50
131.16
130.48
130.24
129.92
128.25
126.72
126.63
125.93
125.85
125.37
123.43
122.64
77.54 CDCl3
76.90 CDCl3
63.25
58.03
56.98
52.94
43.02
35.23
29.57
22.57
21.70
8.00
f1 (ppm)

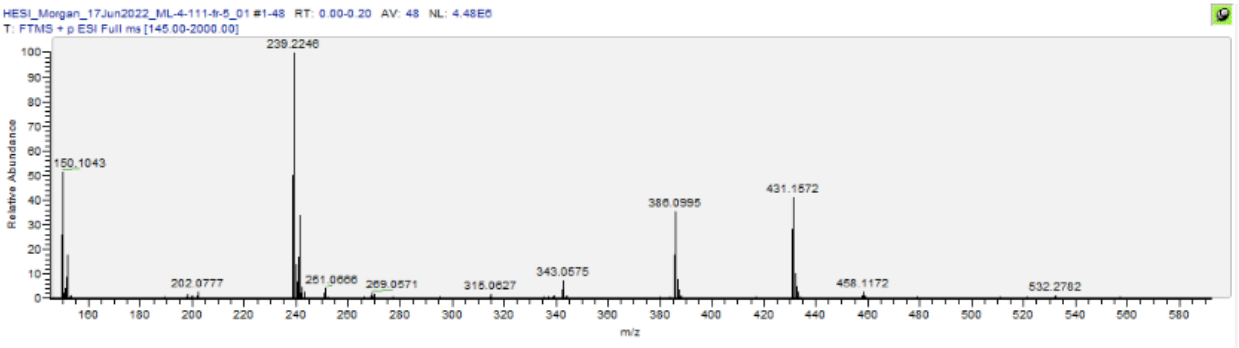
HESI_Morgan_17Jun2022_ML-4-111-fr-5_01 #1-48 RT: 0.00-0.20 AV: 48 NL: 4.48E6
T: FTMS + p ESI Full ms [145.00-2000.00]
239.2246
150.1043
386.0995
431.1572
202.0777
261.0666
269.0571
315.0627
343.0575
458.1172
532.2782
Relative Abundance
m/z

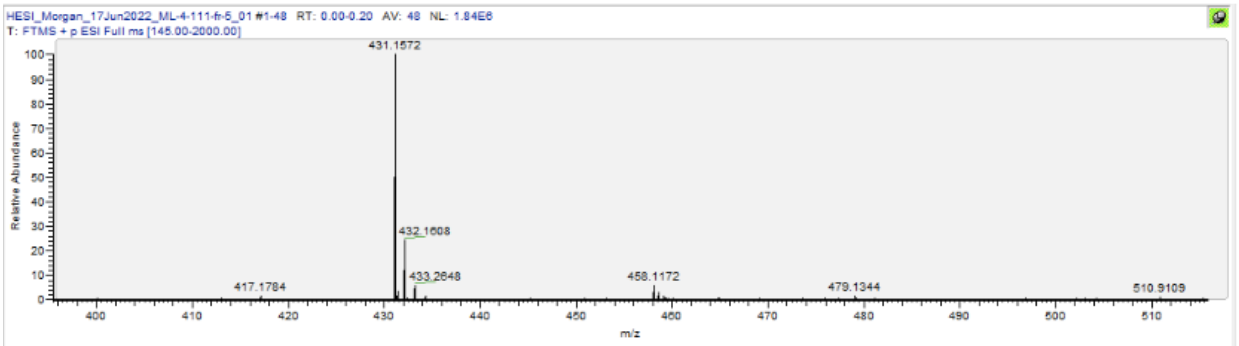
HESI_Morgan_17Jun2022_ML-4-111-fr-5_01 #1-48 RT: 0.00-0.20 AV: 48 NL: 1.84E6
T: FTMS + p ESI Full ms [145.00-2000.00]
431.1572
432.1608
433.2648
417.1784
458.1172
479.1344
510.9109
Relative Abundance
m/z

(*S*)-2-amino-*N*-(2-(dimethylamino)ethyl)-3-(*p*-tolyl)propenamide, 20

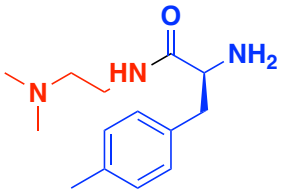

Compound **20** was synthesized using the same protocol listed for compound **15**.

^{1}H NMR (400 MHz, $CDCl_3$) δ 8.27 (qd, J = 7.9, 1.8 Hz, 2H), 7.71 (d, J = 7.6 Hz, 1H), 7.58 (m, 2H), 7.39 (d, J = 7.6 Hz, 1H), 6.80 (br s, 1H), 3.56 (q, J = 5.6 Hz, 2H), 2.54 (t, J = 6.0 Hz, 2H), 2.25 (s, 6H) ppm. ^{13}C NMR (101 MHz, $CDCl_3$) δ 174.4, 136.2, 134.8, 129.2, 129.1, 58.0, 56.6, 45.0, 40.7, 36.5, 21.0 ppm. HRMS calcd for $C_{14}H_{23}N_3O$ $[MH]^+$: 250.1841 Found: 250.1896

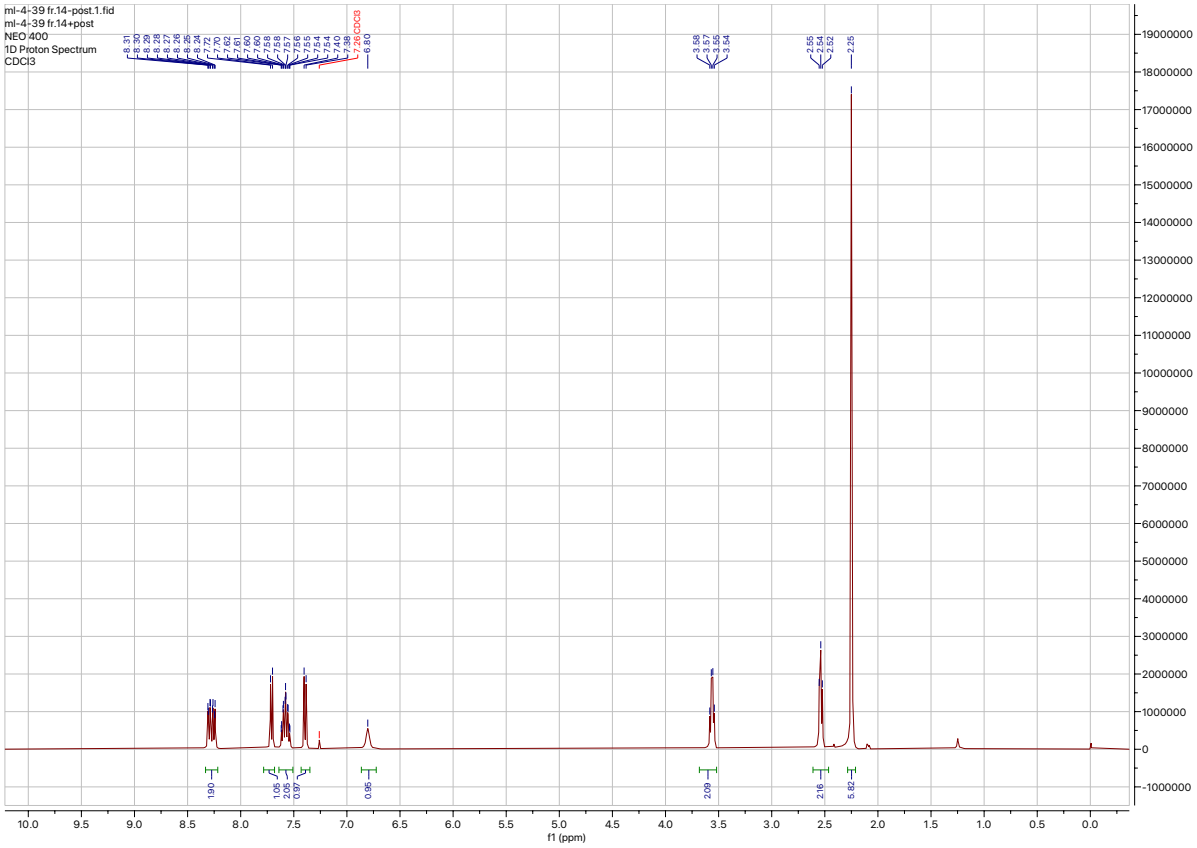

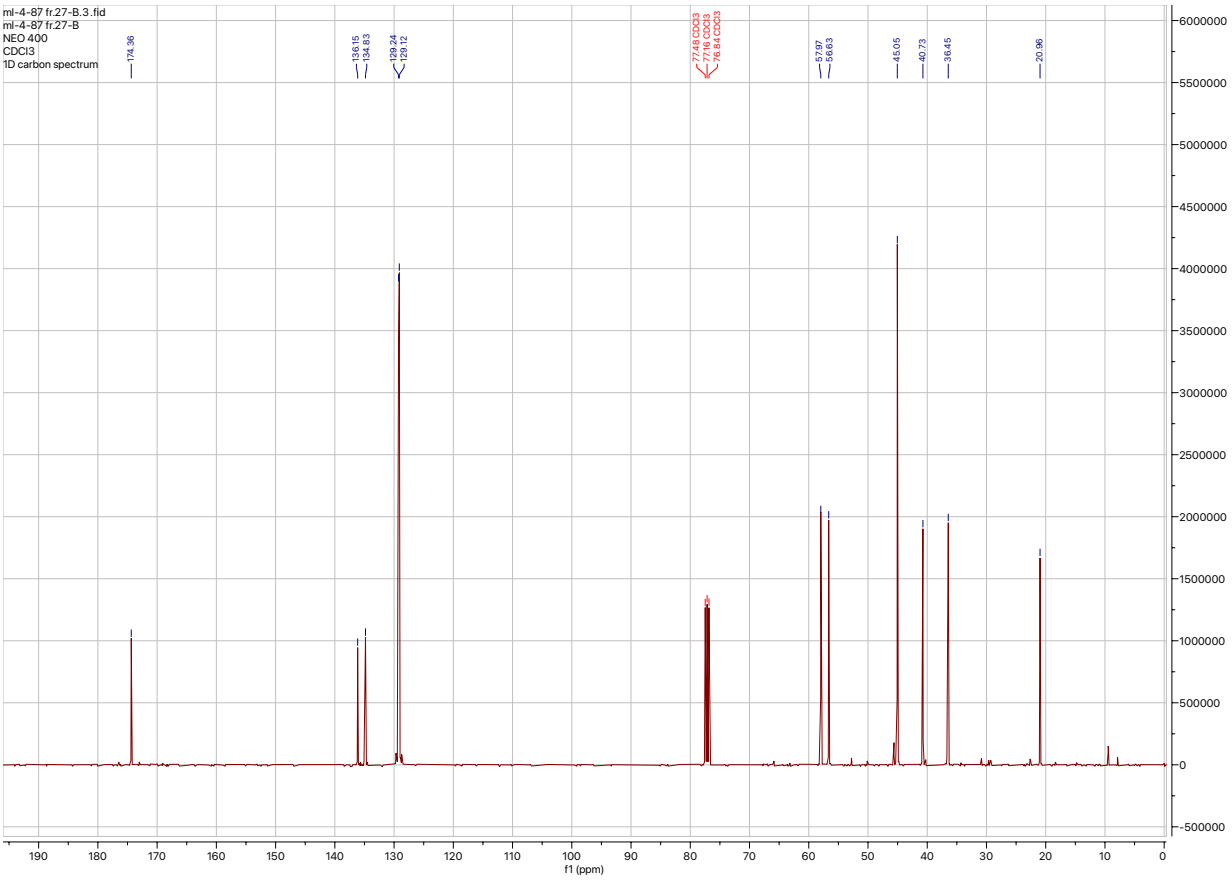

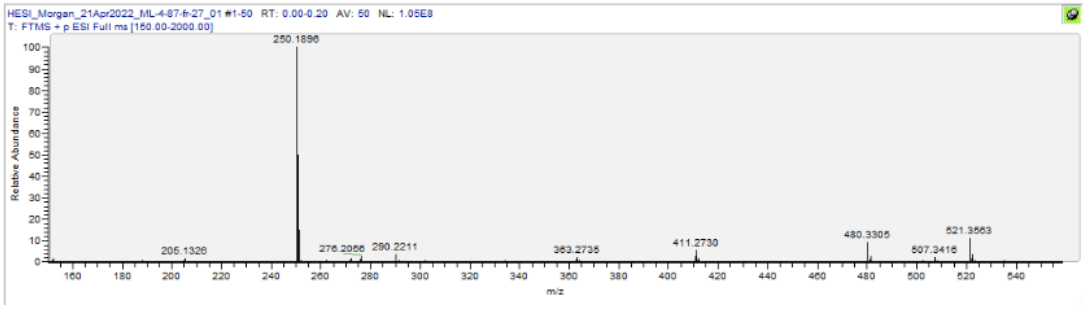

(*S*)-4-bromo-*N*-(1-((2-(dimethylamino)ethyl)amino)-1-oxo-3-(*p*-tolyl)propan-2-yl)-1-naphthamide, 21

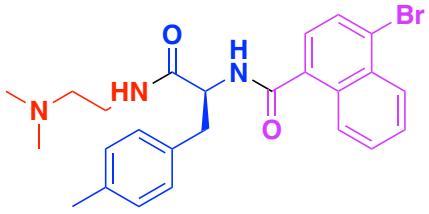

Compound **21** was synthesized following the same protocol listed for compound **15**.

1H NMR (400 MHz, CDCl3) δ 8.24 (d, *J* = 8.4 Hz, 1H), 8.03 (d, *J* = 8.2 Hz, 1H), 7.73 (d, *J* = 7.6 Hz, 1H), 7.59 (td, *J* = 8.4, 6.8, 1.3 Hz, 1H), 7.48 (td, *J* = 8.4, 6.9, 1.4 Hz, 1H), 7.43 (d, *J* = 7.7 Hz, 1H), 7.18 (d, *J* = 8.1 Hz, 3H), 7.09 (d, *J* = 7.6 Hz, 4H), 5.58 (s, 1H), 4.98 (q, *J* = 7.8 Hz, 1H), 3.54 (q, *J* = 7.3 Hz, 4H), 3.39 (m, 4H), 3.07 (q, *J* = 7.3 Hz, 9H), 2.62 (m, 3H), 2.39 (s, 6H), 2.30 (d, *J* = 6.6 Hz, 5H) ppm. ^{13}C NMR (75 MHz, $CDCl_3$) δ 171.2, 168.5, 136.5, 133.9, 133.8, 132.1, 131.4, 129.4, 129.0, 127.8, 127.8, 127.5, 126.1, 125.8, 125.7, 63.4, 57.3, 55.3, 53.0, 45.9, 44.5, 38.5, 36.1, 21.2, 8.8, 8.1 ppm. HRMS for $C_{25}H_{28}BrN_3O_2$ $[MH]^+$: 482.1365 Found: 482.1424

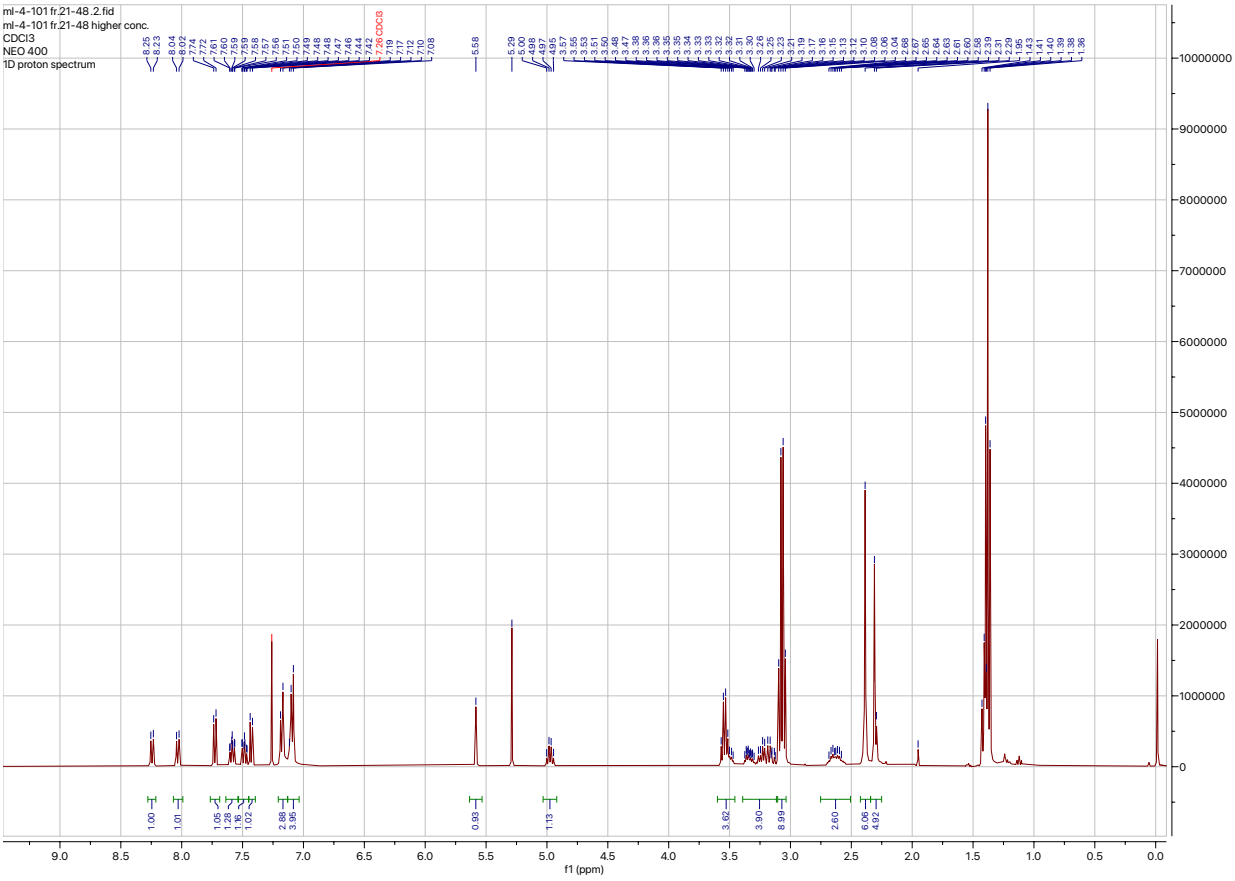

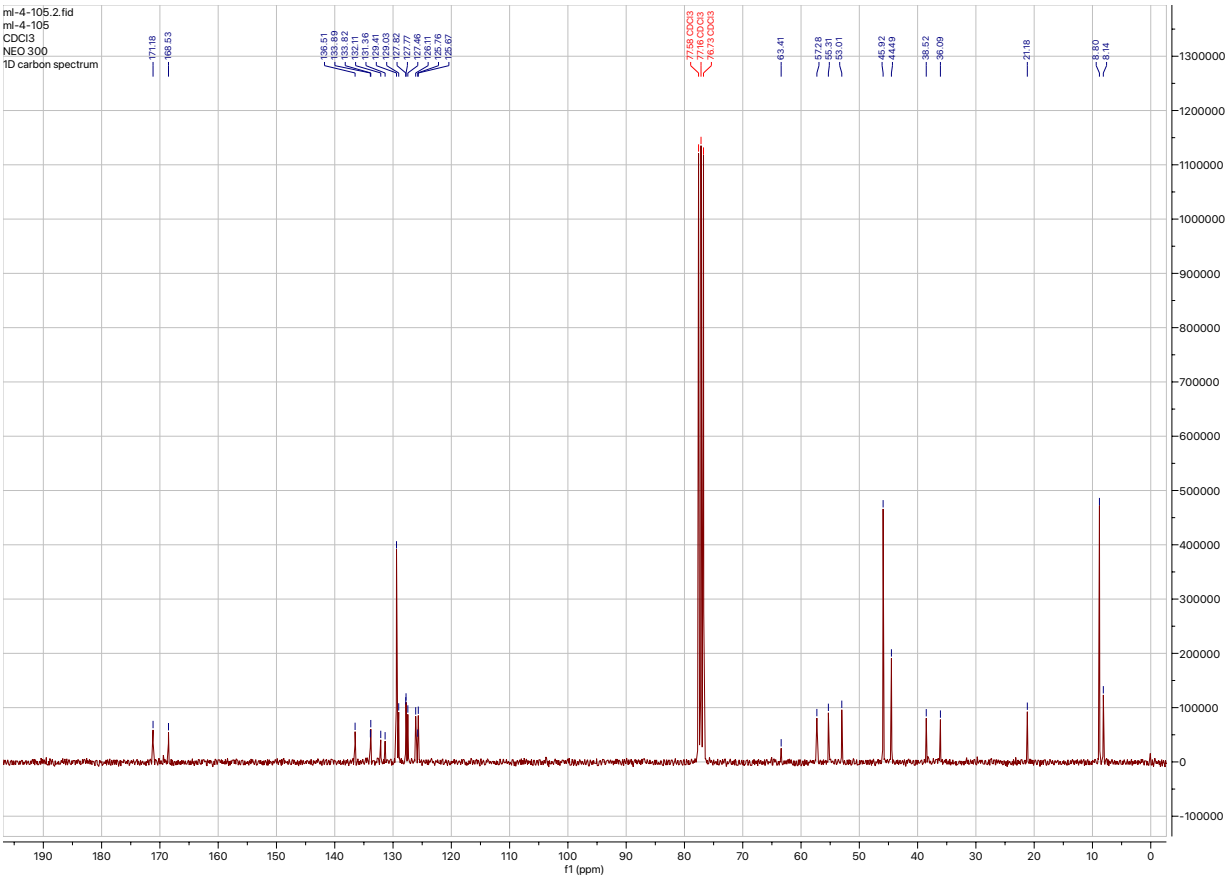

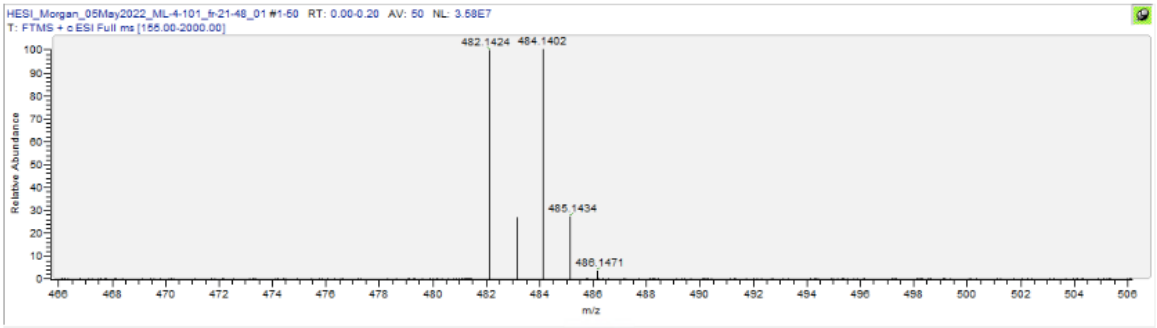

(*S*)-3-(4-((1-((2-(dimethylamino)ethyl)amino)-1-oxo-3-(*p*-tolyl)propan-2-yl)carbamoyl)naphthalen-1-yl)-5-(trifluoromethyl)benzoic acid, 13

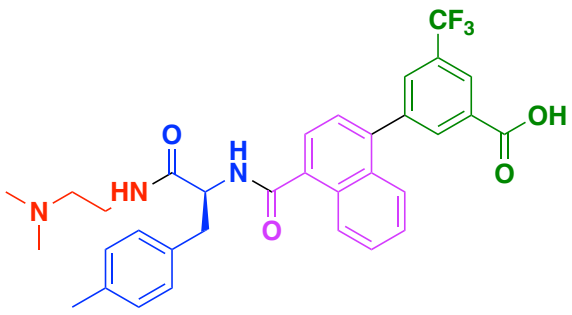

Compound **13** was synthesized following the same protocol listed for compound **14**.

^{1}H NMR (400 MHz, $CDCl_3$) δ 11.03 (s, 1H), 8.51 (s, 1H), 8.33 (s, 1H), 8.07 (s, 1H), 7.85 (d, *J* = 8.2 Hz, 1H), 7.61 (s, 1H), 7.53 (d, *J* = 8.2 Hz, 2H), 7.45 (m, 1H), 7.20 (s, 1H), 7.12 (m, 5H), 5.09 (hex, *J* = 5.2 Hz, 1H), 3.77 (s, 1H), 3.50 (m, 1H), 3.35 (dd, *J* = 14.1, 5.2 Hz, 1H), 3.06 (q, *J* = 7.3 Hz, 8H), 3.00 (m, 3H), 2.63 (s, 4H), 2.26 (s, 3H), 1.30 (t, *J* = 7.4 Hz, 10H) ppm. ^{13}C NMR (101 MHz, $CDCl_3$) δ 176.4, 172.3, 171.4, 169.2, 140.8, 140.6, 137.6, 136.3, 133.9, 133.8, 131.4, 130.4, 130.1, 129.3, 129.1, 128.7, 126.7, 126.6, 125.9, 125.7, 125.5, 125.4, 124.6, 122.7, 57.1, 55.3, 45.5, 43.6, 38.2, 35.3, 29.7, 22.4, 21.1, 8.6 ppm. HRMS calcd for $C_{33}H_{32}F_3N_3O$ $[MH]^+$: 592.2345 Found 592.2407

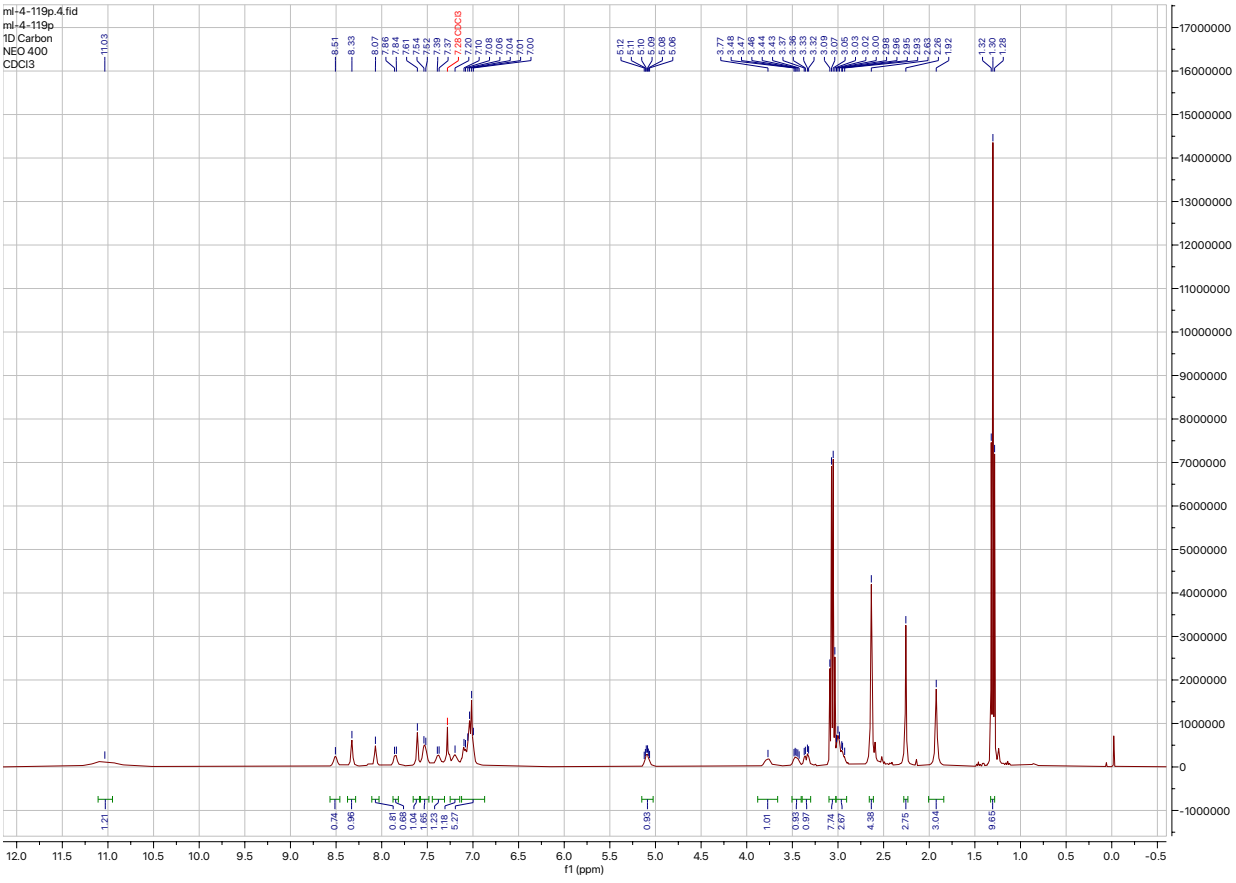

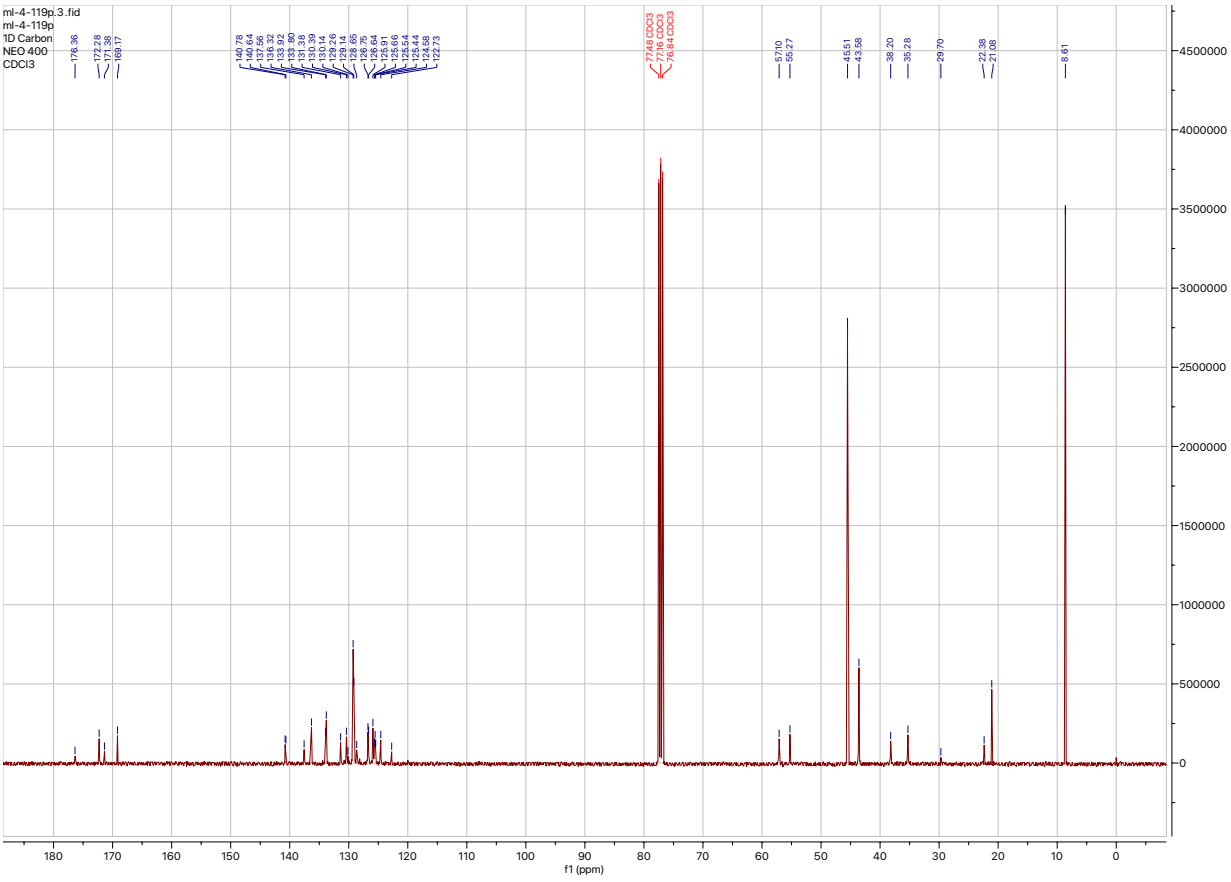

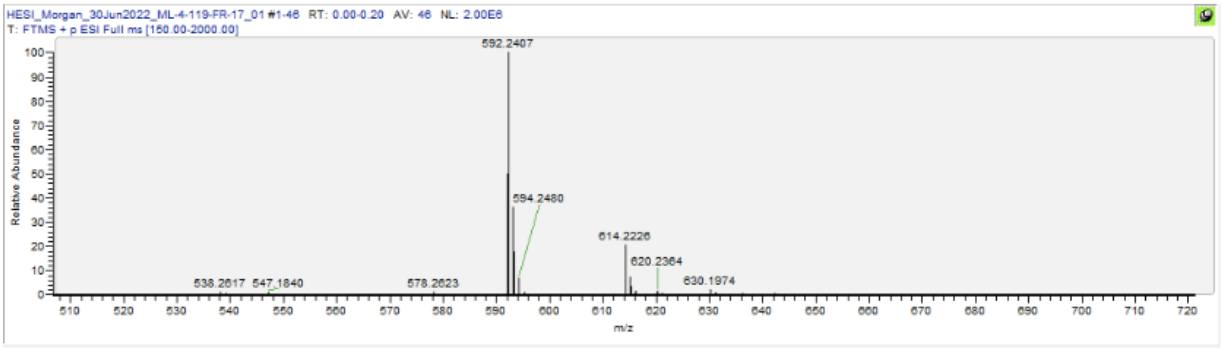

FP assay, ALKBH5 titration

Each well contained 2.5 µL nuclease-free water, 4.5 µL 2x buffer, 1 µL 30% DMSO in Ambion nuclease-free water, 1 µL of ALKBH5 stock concentrations (diluted in 1x buffer) of 6590, 3295, 1648, 824, 412, 206, 103, 51.5, and 26 nM (1 per well) and 1 µL 50 nM fluorescein-labeled RNA probe (fl-CUCGAUACGm^{6}AUCCGGUCAAA). Each well was mixed by pipet 15x, and the plate was incubated in the dark at room temperature for 20 minutes before imaging.

FP assay, positive control titration

Positive control titrations were conducted in similar fashion as above. Each well contained 4.5 µL 2x buffer, 1 µL 30% DMSO in nuclease-free water, 1 µL unlabeled RNA positive control probe (CUCGAUACGm^{6}AUCCGGUCAAA) from 8, 4, 2, 1, 0.5, 0.25, 0.125, 0.063, 0.031, 0.016, 0.008 µM stock solutions dilute with MilliQ purified water, 1 µL ALKBH5 (200 nM stock in 1x buffer), 1 µL 50 nM fluorescent probe (as above). The experiment was conducted as described above.

FP assay, small molecule assessments

Small molecule assessments were conducted in similar fashion to the positive control titration, above. Each well contained 4.5 µL 2x buffer, 1 µL 30% DMSO in nuclease-free water, 1 µL of stock solutions of small molecules at concentrations described for each analysis, dilute with MilliQ purified water, 1 µL ALKBH5 (200 nM stock in 1x buffer), 1 µL 50 nM fluorescent probe (as above). The experiment was conducted as described above.

REFERENCES

(1) Minchin, S.; Lodge, J. Understanding Biochemistry: Structure and Function of Nucleic Acids. *Essays Biochem.* **2019**, *63* (4), 433–456. https://doi.org/10.1042/EBC20180038.

(2) Dahm, R. Discovering DNA: Friedrich Miescher and the Early Years of Nucleic Acid Research. *Hum. Genet.* **2008**, *122* (6), 565–581. https://doi.org/10.1007/s00439-007-0433-0.

(3) WATSON, J. D.; CRICK, F. H. C. Molecular Structure of Nucleic Acids: A Structure for Deoxyribose Nucleic Acid. *Nature* **1953**, *171* (4356), 737–738. https://doi.org/10.1038/171737a0.

(4) FRANKLIN, R. E.; GOSLING, R. G. Molecular Configuration in Sodium Thymonucleate. *Nature* **1953**, *171* (4356), 740–741. https://doi.org/10.1038/171740a0.

(5) Moore, P. B.; Steitz, T. A. The Roles of RNA in the Synthesis of Protein. *Cold Spring Harb. Perspect. Biol.* **2011**, *3* (11), a003780–a003780. https://doi.org/10.1101/cshperspect.a003780.

(6) Greenberg, M. V. C.; Bourc'his, D. The Diverse Roles of DNA Methylation in Mammalian Development and Disease. *Nat. Rev. Mol. Cell Biol.* **2019**, *20* (10), 590–607. https://doi.org/10.1038/s41580-019-0159-6.

(7) Boccaletto, P.; Machnicka, M. A.; Purta, E.; Piątkowski, P.; Bagiński, B.; Wirecki, T. K.; de Crécy-Lagard, V.; Ross, R.; Limbach, P. A.; Kotter, A.; Helm, M.; Bujnicki, J. M. MODOMICS: A Database of RNA Modification Pathways. 2017 Update. *Nucleic Acids Res.* **2018**, *46* (D1), D303–D307. https://doi.org/10.1093/nar/gkx1030.

(8) Dumelin, C. E.; Chen, Y.; Leconte, A. M.; Chen, Y. G.; Liu, D. R. Discovery and Biological Characterization of Geranylated RNA in Bacteria. *Nat. Chem. Biol.* **2012**, *8* (11), 913–919. https://doi.org/10.1038/nchembio.1070.

(9) Sakai, Y.; Miyauchi, K.; Kimura, S.; Suzuki, T. Biogenesis and Growth Phase-Dependent Alteration of 5-Methoxycarbonylmethoxyuridine in tRNA Anticodons. *Nucleic Acids Res.* **2016**, *44* (2), 509–523. https://doi.org/10.1093/nar/gkv1470.

(10) Nechay, M.; Kleiner, R. E. High-Throughput Approaches to Profile RNA-Protein Interactions. *Curr. Opin. Chem. Biol.* **2020**, *54*, 37–44. https://doi.org/10.1016/j.cbpa.2019.11.002.

(11) Perry, G. S.; Das, M.; Woon, E. C. Y. Inhibition of AlkB Nucleic Acid Demethylases: Promising New Epigenetic Targets. *J. Med. Chem.* **2021**, *64* (23), 16974–17003. https://doi.org/10.1021/acs.jmedchem.1c01694.

(12) *DNA and RNA Modification Enzymes: Structure, Mechanism, Function and Evolution*; Grosjean, H., Ed.; Molecular biology intelligence unit; Landes Bioscience: Austin, Tex, 2009.

(13) Desrosiers, R.; Friderici, K.; Rottman, F. Identification of Methylated Nucleosides in Messenger RNA from Novikoff Hepatoma Cells. *Proc. Natl. Acad. Sci.* **1974**, *71* (10), 3971–3975. https://doi.org/10.1073/pnas.71.10.3971.

(14) Perry, R. P.; Kelley, D. E. Existence of Methylated Messenger RNA in Mouse L Cells. *Cell* **1974**, *1* (1), 37–42. https://doi.org/10.1016/0092-8674(74)90153-6.

(15) Wang, X.; Zhao, B. S.; Roundtree, I. A.; Lu, Z.; Han, D.; Ma, H.; Weng, X.; Chen, K.; Shi, H.; He, C. N6-Methyladenosine Modulates Messenger RNA Translation Efficiency. *Cell* **2015**, *161* (6), 1388–1399. https://doi.org/10.1016/j.cell.2015.05.014.

(16) Zhou, J.; Wan, J.; Gao, X.; Zhang, X.; Jaffrey, S. R.; Qian, S.-B. Dynamic m6A mRNA Methylation Directs Translational Control of Heat Shock Response. *Nature* **2015**, *526* (7574), 591–594. https://doi.org/10.1038/nature15377.

(17) Kierzek, E. The Thermodynamic Stability of RNA Duplexes and Hairpins Containing N6-Alkyladenosines and 2-Methylthio-N6-Alkyladenosines. *Nucleic Acids Res.* **2003**, *31* (15), 4472–4480. https://doi.org/10.1093/nar/gkg633.

(18) Xiao, W.; Adhikari, S.; Dahal, U.; Chen, Y.-S.; Hao, Y.-J.; Sun, B.-F.; Sun, H.-Y.; Li, A.; Ping, X.-L.; Lai, W.-Y.; Wang, X.; Ma, H.-L.; Huang, C.-M.; Yang, Y.; Huang, N.; Jiang, G.-B.; Wang, H.-L.; Zhou, Q.; Wang, X.-J.; Zhao, Y.-L.; Yang, Y.-G. Nuclear m 6 A Reader YTHDC1 Regulates mRNA Splicing. *Mol. Cell* **2016**, *61* (4), 507–519. https://doi.org/10.1016/j.molcel.2016.01.012.

(19) Roost, C.; Lynch, S. R.; Batista, P. J.; Qu, K.; Chang, H. Y.; Kool, E. T. Structure and Thermodynamics of N ^{6} -Methyladenosine in RNA: A Spring-Loaded Base Modification. *J. Am. Chem. Soc.* **2015**, *137* (5), 2107–2115. https://doi.org/10.1021/ja513080v.

(20) Jacob, R.; Zander, S.; Gutschner, T. The Dark Side of the Epitranscriptome: Chemical Modifications in Long Non-Coding RNAs. *Int. J. Mol. Sci.* **2017**, *18* (11), 2387. https://doi.org/10.3390/ijms18112387.

(21) Dominissini, D.; Moshitch-Moshkovitz, S.; Schwartz, S.; Salmon-Divon, M.; Ungar, L.; Osenberg, S.; Cesarkas, K.; Jacob-Hirsch, J.; Amariglio, N.; Kupiec, M.; Sorek, R.; Rechavi, G. Topology of the Human and Mouse m6A RNA Methylomes Revealed by m6A-Seq. *Nature* **2012**, *485* (7397), 201–206. https://doi.org/10.1038/nature11112.

(22) Meyer, K. D.; Saletore, Y.; Zumbo, P.; Elemento, O.; Mason, C. E.; Jaffrey, S. R. Comprehensive Analysis of mRNA Methylation Reveals Enrichment in 3′ UTRs and near Stop Codons. *Cell* **2012**, *149* (7), 1635–1646. https://doi.org/10.1016/j.cell.2012.05.003.

(23) Fang, Z.; Mei, W.; Qu, C.; Lu, J.; Shang, L.; Cao, F.; Li, F. Role of m6A Writers, Erasers and Readers in Cancer. *Exp. Hematol. Oncol.* **2022**, *11* (1), 45. https://doi.org/10.1186/s40164-022-00298-7.

(24) Zhang, C.; Fu, J.; Zhou, Y. A Review in Research Progress Concerning m6A Methylation and Immunoregulation. *Front. Immunol.* **2019**, *10*, 922. https://doi.org/10.3389/fimmu.2019.00922.

(25) Roundtree, I. A.; Evans, M. E.; Pan, T.; He, C. Dynamic RNA Modifications in Gene Expression Regulation. *Cell* **2017**, *169* (7), 1187–1200. https://doi.org/10.1016/j.cell.2017.05.045.

(26) Jiang, X.; Liu, B.; Nie, Z.; Duan, L.; Xiong, Q.; Jin, Z.; Yang, C.; Chen, Y. The Role of m6A Modification in the Biological Functions and Diseases. *Signal Transduct. Target. Ther.* **2021**, *6* (1), 74. https://doi.org/10.1038/s41392-020-00450-x.

(27) Wei, W.; Ji, X.; Guo, X.; Ji, S. Regulatory Role of N ^{6} -Methyladenosine (m ^{6} A) Methylation in RNA Processing and Human Diseases: R EGULATORY R OLE O F m ^{6} A. *J. Cell. Biochem.* **2017**, *118* (9), 2534–2543. https://doi.org/10.1002/jcb.25967.

(28) Deng, L.-J.; Deng, W.-Q.; Fan, S.-R.; Chen, M.-F.; Qi, M.; Lyu, W.-Y.; Qi, Q.; Tiwari, A. K.; Chen, J.-X.; Zhang, D.-M.; Chen, Z.-S. m6A Modification: Recent Advances, Anticancer Targeted Drug Discovery and Beyond. *Mol. Cancer* **2022**, *21* (1), 52. https://doi.org/10.1186/s12943-022-01510-2.

(29) Gu, C.; Shi, X.; Dai, C.; Shen, F.; Rocco, G.; Chen, J.; Huang, Z.; Chen, C.; He, C.; Huang, T.; Chen, C. RNA m6A Modification in Cancers: Molecular Mechanisms and Potential Clinical Applications. *The Innovation* **2020**, *1* (3), 100066. https://doi.org/10.1016/j.xinn.2020.100066.

(30) Huang, H.; Weng, H.; Chen, J. m6A Modification in Coding and Non-Coding RNAs: Roles and Therapeutic Implications in Cancer. *Cancer Cell* **2020**, *37* (3), 270–288. https://doi.org/10.1016/j.ccell.2020.02.004.

(31) Aravind, L.; Koonin, E. V. The DNA-Repair Protein AlkB, EGL-9, and Leprecan Define New Families of 2-Oxoglutarate- and Iron-Dependent Dioxygenases. *Genome Biol.* **2001**, *2* (3), research0007.1-0007.8.

(32) Zheng, G.; Dahl, J. A.; Niu, Y.; Fedorcsak, P.; Huang, C.-M.; Li, C. J.; Vågbø, C. B.; Shi, Y.; Wang, W.-L.; Song, S.-H.; Lu, Z.; Bosmans, R. P. G.; Dai, Q.; Hao, Y.-J.; Yang, X.; Zhao, W.-M.; Tong, W.-M.; Wang, X.-J.; Bogdan, F.; Furu, K.; Fu, Y.; Jia, G.; Zhao, X.; Liu, J.; Krokan, H. E.; Klungland, A.; Yang, Y.-G.; He, C. ALKBH5 Is a Mammalian RNA Demethylase That Impacts RNA Metabolism and Mouse Fertility. *Mol. Cell* **2013**, *49* (1), 18–29. https://doi.org/10.1016/j.molcel.2012.10.015.

(33) Zou, S.; Toh, J. D. W.; Wong, K. H. Q.; Gao, Y.-G.; Hong, W.; Woon, E. C. Y. N6-Methyladenosine: A Conformational Marker That Regulates the Substrate Specificity of Human Demethylases FTO and ALKBH5. *Sci. Rep.* **2016**, *6* (1), 25677. https://doi.org/10.1038/srep25677.

(34) Tang, B.; Yang, Y.; Kang, M.; Wang, Y.; Wang, Y.; Bi, Y.; He, S.; Shimamoto, F. m6A Demethylase ALKBH5 Inhibits Pancreatic Cancer Tumorigenesis by Decreasing WIF-1 RNA Methylation and Mediating Wnt Signaling. *Mol. Cancer* **2020**, *19* (1), 3. https://doi.org/10.1186/s12943-019-1128-6.

(35) Yang, P.; Wang, Q.; Liu, A.; Zhu, J.; Feng, J. ALKBH5 Holds Prognostic Values and Inhibits the Metastasis of Colon Cancer. *Pathol. Oncol. Res.* **2020**, *26* (3), 1615–1623. https://doi.org/10.1007/s12253-019-00737-7.

(36) Zhang, C.; Zhi, W. I.; Lu, H.; Samanta, D.; Chen, I.; Gabrielson, E.; Semenza, G. L. Hypoxia-Inducible Factors Regulate Pluripotency Factor Expression by ZNF217- and ALKBH5-Mediated Modulation of RNA Methylation in Breast Cancer Cells. *Oncotarget* **2016**, *7* (40), 64527–64542. https://doi.org/10.18632/oncotarget.11743.

(37) Tsuchiya, K.; Yoshimura, K.; Iwashita, Y.; Inoue, Y.; Ohta, T.; Watanabe, H.; Yamada, H.; Kawase, A.; Tanahashi, M.; Ogawa, H.; Funai, K.; Shinmura, K.; Suda, T.; Sugimura, H. m6A Demethylase ALKBH5 Promotes Tumor Cell Proliferation by Destabilizing IGF2BPs Target Genes and Worsens the Prognosis of Patients with Non-Small-Cell Lung Cancer. *Cancer Gene Ther.* **2022**. https://doi.org/10.1038/s41417-022-00451-8.

(38) Zhu, H.; Gan, X.; Jiang, X.; Diao, S.; Wu, H.; Hu, J. ALKBH5 Inhibited Autophagy of Epithelial Ovarian Cancer through miR-7 and BCL-2. *J. Exp. Clin. Cancer Res.* **2019**, *38* (1), 163. https://doi.org/10.1186/s13046-019-1159-2.

(39) Malacrida, A.; Rivara, M.; Di Domizio, A.; Cislaghi, G.; Miloso, M.; Zuliani, V.; Nicolini, G. 3D Proteome-Wide Scale Screening and Activity Evaluation of a New ALKBH5 Inhibitor in U87 Glioblastoma Cell Line. *Bioorg. Med. Chem.* **2020**, *28* (4), 115300. https://doi.org/10.1016/j.bmc.2019.115300.

(40) Tang, C.; Klukovich, R.; Peng, H.; Wang, Z.; Yu, T.; Zhang, Y.; Zheng, H.; Klungland, A.; Yan, W. ALKBH5-Dependent m6A Demethylation Controls Splicing and Stability of Long 3′-UTR mRNAs in Male Germ Cells. *Proc. Natl. Acad. Sci.* **2018**, *115* (2). https://doi.org/10.1073/pnas.1717794115.

(41) Aik, W.; McDonough, M. A.; Thalhammer, A.; Chowdhury, R.; Schofield, C. J. Role of the Jelly-Roll Fold in Substrate Binding by 2-Oxoglutarate Oxygenases. *Curr. Opin. Struct. Biol.* **2012**, *22* (6), 691–700. https://doi.org/10.1016/j.sbi.2012.10.001.

(42) Doudna, J. A.; Cech, T. R. The Chemical Repertoire of Natural Ribozymes. *Nature* **2002**, *418* (6894), 222–228. https://doi.org/10.1038/418222a.

(43) Zovoilis, A.; Cifuentes-Rojas, C.; Chu, H.-P.; Hernandez, A. J.; Lee, J. T. Destabilization of B2 RNA by EZH2 Activates the Stress Response. *Cell* **2016**, *167* (7), 1788-1802.e13. https://doi.org/10.1016/j.cell.2016.11.041.

(44) Moore, P. B.; Steitz, T. A. The Involvement of RNA in Ribosome Function. *Nature* **2002**, *418* (6894), 229–235. https://doi.org/10.1038/418229a.

(45) Sonenberg, N.; Hinnebusch, A. G. Regulation of Translation Initiation in Eukaryotes: Mechanisms and Biological Targets. *Cell* **2009**, *136* (4), 731–745. https://doi.org/10.1016/j.cell.2009.01.042.

(46) Serganov, A.; Patel, D. J. Ribozymes, Riboswitches and beyond: Regulation of Gene Expression without Proteins. *Nat. Rev. Genet.* **2007**, *8* (10), 776–790. https://doi.org/10.1038/nrg2172.

(47) Caruthers, M. H. Gene Synthesis Machines: DNA Chemistry and Its Uses. *Science* **1985**, *230* (4723), 281–285. https://doi.org/10.1126/science.3863253.

(48) Saik, Randall K; Gelfand, D. H.; Stoffel, S.; Scharf, S. J.; Higuchi, R.; Horn, G. T.; Mullis, K. B.; Erlich, H. A. Primer-Directed Enzymatic Amplification of DNA with a Thermostable DNA Polymerase. *Science* **1988**, *239* (4839), 487–491.

(49) Ellington, A. D.; Szostak, J. W. In Vitro Selection of RNA Molecules That Bind Specific Ligands. *Nature* **1990**, *346* (6287), 818–822. https://doi.org/10.1038/346818a0.

(50) Robertson, D. L.; Joyce, G. F. Selection in Vitro of an RNA Enzyme That Specifically Cleaves Single-Stranded DNA. *Nature* **1990**, *344* (6265), 467–468. https://doi.org/10.1038/344467a0.

(51) Tuerk, C.; Gold, L. Systematic Evolution of Ligands by Exponential Enrichment: RNA Ligands to Bacteriophage T4 DNA Polymerase. *Science* **1990**, *249* (4968), 505–510. https://doi.org/10.1126/science.2200121.

(52) Mehta, J.; Van Dorst, B.; Rouah-Martin, E.; Herrebout, W.; Scippo, M.-L.; Blust, R.; Robbens, J. In Vitro Selection and Characterization of DNA Aptamers Recognizing Chloramphenicol. *J. Biotechnol.* **2011**, *155* (4), 361–369. https://doi.org/10.1016/j.jbiotec.2011.06.043.

(53) Khvorova, A.; Watts, J. K. The Chemical Evolution of Oligonucleotide Therapies of Clinical Utility. *Nat. Biotechnol.* **2017**, *35* (3), 238–248. https://doi.org/10.1038/nbt.3765.

(54) Wang, T.; Chen, C.; Larcher, L. M.; Barrero, R. A.; Veedu, R. N. Three Decades of Nucleic Acid Aptamer Technologies: Lessons Learned, Progress and Opportunities on Aptamer Development. *Biotechnol. Adv.* **2019**, *37* (1), 28–50. https://doi.org/10.1016/j.biotechadv.2018.11.001.

(55) Obexer, R.; Nassir, M.; Moody, E. R.; Baran, P. S.; Lovelock, S. L. Modern Approaches to Therapeutic Oligonucleotide Manufacturing. *Science* **2024**, *384* (6692).

(56) Wilson, D. S.; Szostak, J. W. In Vitro Selection of Functional Nucleic Acids. *Annu. Rev. Biochem.* **1999**, *68* (1), 611–647. https://doi.org/10.1146/annurev.biochem.68.1.611.

(57) Keefe, A. D.; Pai, S.; Ellington, A. Aptamers as Therapeutics. *Nat. Rev. Drug Discov.* **2010**, *9* (7), 537–550. https://doi.org/10.1038/nrd3141.

(58) Shigdar, S.; Macdonald, J.; O'Connor, M.; Wang, T.; Xiang, D.; Al.Shamaileh, H.; Qiao, L.; Wei, M.; Zhou, S.-F.; Zhu, Y.; Kong, L.; Bhattacharya, S.; Li, C.; Duan, W. Aptamers as Theranostic Agents: Modifications, Serum Stability and Functionalisation. *Sensors* **2013**, *13* (10), 13624–13637. https://doi.org/10.3390/s131013624.

(59) Khan, N.; Maddaus, A.; Song, E. A Low-Cost Inkjet-Printed Aptamer-Based Electrochemical Biosensor for the Selective Detection of Lysozyme. *Biosensors* **2018**, *8* (1), 7. https://doi.org/10.3390/bios8010007.

(60) Tapsin, S.; Sun, M.; Shen, Y.; Zhang, H.; Lim, X. N.; Susanto, T. T.; Yang, S. L.; Zeng, G. S.; Lee, J.; Lezhava, A.; Ang, E. L.; Zhang, L. H.; Wang, Y.; Zhao, H.; Nagarajan, N.; Wan, Y. Genome-Wide Identification of Natural RNA Aptamers in Prokaryotes and Eukaryotes. *Nat. Commun.* **2018**, *9* (1), 1289. https://doi.org/10.1038/s41467-018-03675-1.

(61) Dunn, M. R.; Jimenez, R. M.; Chaput, J. C. Analysis of Aptamer Discovery and Technology. *Nat. Rev. Chem.* **2017**, *1* (10), 0076. https://doi.org/10.1038/s41570-017-0076.

(62) McKenzie, L. K.; El-Khoury, R.; Thorpe, J. D.; Damha, M. J.; Hollenstein, M. Recent Progress in Non-Native Nucleic Acid Modifications. *Chem. Soc. Rev.* **2021**, *50* (8), 5126–5164. https://doi.org/10.1039/D0CS01430C.

(63) Catani, M.; Luca, C. D.; Alcântara, J. M. G.; Manfredini, N.; Perrone, D.; Marchesi, E.; Weldon, R.; Müller-Späth, T.; Cavazzini, A.; Morbidelli, M.; Sponchioni, M. Oligonucleotides: Current Trends and Innovative Applications in the Synthesis, Characterization, and Purification. *Biotechnol J* **2020**.

(64) Brown, A.; Brill, J.; Amini, R.; Nurmi, C.; Li, Y. Development of Better Aptamers: Structured Library Approaches, Selection Methods, and Chemical Modifications. *Angew. Chem. Int. Ed.* **2024**, *63* (16), e202318665. https://doi.org/10.1002/anie.202318665.

(65) Vaught, J. D.; Bock, C.; Carter, J.; Fitzwater, T.; Otis, M.; Schneider, D.; Rolando, J.; Waugh, S.; Wilcox, S. K.; Eaton, B. E. Expanding the Chemistry of DNA for in Vitro Selection. *J. Am. Chem. Soc.* **2010**, *132* (12), 4141–4151. https://doi.org/10.1021/ja908035g.

(66) Eulberg, D.; Klussmann, S. Spiegelmers: Biostable Aptamers. *ChemBioChem* **2003**, *4* (10), 979–983. https://doi.org/10.1002/cbic.200300663.

(67) Kong, D.; Lei, Y.; Yeung, W.; Hili, R. Enzymatic Synthesis of Sequence-Defined Synthetic Nucleic Acid Polymers with Diverse Functional Groups. *Angew. Chem. Int. Ed.* **2016**, *55* (42), 13164–13168.

(68) Kong, D.; Yeung, W.; Hili, R. In Vitro Selection of Diversely Functionalized Aptamers. *J. Am. Chem. Soc.* **2017**, *139* (40), 13977–13980. https://doi.org/10.1021/jacs.7b07241.

(69) Davies, D. R.; Gelinas, A. D.; Zhang, C.; Rohloff, J. C.; Carter, J. D.; O'Connell, D.; Waugh, S. M.; Wolk, S. K.; Mayfield, W. S.; Burgin, A. B.; Edwards, T. E.; Stewart, L. J.; Gold, L.; Janjic, N.; Jarvis, T. C. Unique Motifs and Hydrophobic Interactions Shape the Binding of Modified DNA Ligands to Protein Targets. *Proc. Natl. Acad. Sci.* **2012**, *109* (49), 19971–19976. https://doi.org/10.1073/pnas.1213933109.

(70) Pfeiffer, F.; Rosenthal, M.; Siegl, J.; Ewers, J.; Mayer, G. Customised Nucleic Acid Libraries for Enhanced Aptamer Selection and Performance. *Curr. Opin. Biotechnol.* **2017**, *48*, 111–118. https://doi.org/10.1016/j.copbio.2017.03.026.

(71) Gawande, B. N.; Rohloff, J. C.; Carter, J. D.; von Carlowitz, I.; Zhang, C.; Schneider, D. J.; Janjic, N. Selection of DNA Aptamers with Two Modified Bases. *Proc. Natl. Acad. Sci.* **2017**, *114* (11), 2898–2903. https://doi.org/10.1073/pnas.1615475114.

(72) Lei, Y.; Kong, D.; Hili, R. A High-Fidelity Codon Set for the T4 DNA Ligase-Catalyzed Polymerization of Modified Oligonucleotides. *ACS Comb. Sci.* **2015**, *17* (12), 716–721. https://doi.org/10.1021/acscombsci.5b00119.

(73) Kong, D.; Yeung, W.; Hili, R. Generation of Synthetic Copolymer Libraries by Combinatorial Assembly on Nucleic Acid Templates. *ACS Comb. Sci.* **2016**, *18* (7), 355–370. https://doi.org/10.1021/acscombsci.6b00059.

(74) Matteucci, M. D.; Caruthers, M. H. Synthesis of Deoxyoligonucleotides on a Polymer Support. *J. Am. Chem. Soc.* **1981**, *103* (11), 3185–3191. https://doi.org/10.1021/ja00401a041.

(75) Reddy, M. P.; Hanna, N. B.; Farooqui, F. Ultrafast Cleavage and Deprotection of Oligonucleotides Synthesis and Use of C ^{Ac} Derivatives. *Nucleosides Nucleotides* **1997**, *16* (7–9), 1589–1598. https://doi.org/10.1080/07328319708006236.

(76) Bhushan, K. R. Light-Directed Maskless Synthesis of Peptide Arrays Using Photolabile Amino Acid Monomers. *Org. Biomol. Chem.* **2006**, *4* (10), 1857. https://doi.org/10.1039/b601390b.

(77) Guibé, F. Allylic Protecting Groups and Their Use in a Complex Environment Part I : Allylic Protection of Alcohols. *Tetrahedron* **1997**, *53* (40), 13509–13556.

(78) Guibé, F. Allylic Protecting Groups and Their Use in a Complex Environment Part II: Allylic Protecting Groups and Their Removal through Catalytic Palladium ‘TC-AllyM1ethodology. *Tetrahedron* **1998**, *54*, 2967–3042.

(79) Khadtare, N.; Stephani, R.; Korlipara, V. Design, Synthesis and Evaluation of 1,3,6-Trisubstituted-4-Oxo-1,4-Dihydroquinoline-2-Carboxylic Acid Derivatives as ETAreceptor Selective Antagonists Using FRET Assay. *Bioorg. Med. Chem. Lett.* **2017**, *27* (11), 2281–2285. https://doi.org/10.1016/j.bmcl.2017.04.049.

(80) Khadem, S.; Joseph, R.; Rastegar, M.; Leek, D. M.; Oudatchin, K. A.; Arya, P. A Solution- and Solid-Phase Approach to Tetrahydroquinoline-Derived Polycyclics Having a 10-Membered Ring. *J. Comb. Chem.* **2004**, *6* (5), 724–734. https://doi.org/10.1021/cc049941o.

(81) Specht, A.; Thomann, J. S.; Alarcon, K.; Wittayanan, W.; Ogden, D.; Furuta, T.; Kurakawa, Y.; Goeldner, M. New Photoremovable Protecting Groups for Carboxylic Acids with High Photolytic Efficiencies at Near-UV Irradiation. Application to the Photocontrolled Release of L-Glutamate. *ChemBioChem* **2006**, *7* (11), 1690–1695. https://doi.org/10.1002/cbic.200600111.

(82) Ho, Y. T. C.; Leng, D. J.; Ghiringhelli, F.; Wilkening, I.; Bushell, D. P.; Kostner, O.; Riva, E.; Havemann, J.; Passarella, D.; Tosin, M. Novel Chemical Probes for the Investigation of Nonribosomal Peptide Assembly. *Chem. Commun.* **2017**, *53* (92), 12481–12481. https://doi.org/10.1039/C7CC90432K.

(83) Hurevich, M.; Tal-Gan, Y.; Klein, S.; Barda, Y.; Levitzki, A.; Gilon, C. Novel Method for the Synthesis of Urea Backbone Cyclic Peptides Using New Alloc-Protected Glycine Building Units. *J. Pept. Sci.* **2010**, *16* (4), 178–185. https://doi.org/10.1002/psc.1218.

(84) Hurevich, M.; Tal-Gan, Y.; Klein, S.; Barda, Y.; Levitzki, A.; Gilon, C. Novel Method for the Synthesis of Urea Backbone Cyclic Peptides Using New Alloc-Protected Glycine Building Units. *J. Pept. Sci.* **2010**, *16* (4), 178–185. https://doi.org/10.1002/psc.1218.

(85) Wang, X.; Peng, L.; Liu, R.; Gill, S. S.; Lam, K. S. Partial Alloc-Deprotection Approach for Ladder Synthesis of “One-Bead One-Compound” Combinatorial Libraries. *J. Comb. Chem.* **2005**, *7*, 197–209.

(86) Thieriet, N.; Alsina, J.; Giralt, E.; Guibé, F.; Albericio, F. Use of Alloc-Amino Acids in Solid-Phase Peptide Synthesis. Tandem Deprotection-Coupling Reactions Using Neutral Conditions. *Tetrahedron Lett.* **1997**, *38* (41), 7275–7278.

(87) Grieco, P.; Gitu, P. M.; Hruby, V. J. Preparation of ‘Side-chain-to-side-chain’ Cyclic Peptides by Allyl and Alloc Strategy: Potential for Library Synthesis. *J. Pept. Res.* **2001**, *57*, 250–256.

(88) Guo, C.; Mahdavi-Amiri, Y.; Hili, R. Influence of Linker Length on Ligase-Catalyzed Oligonucleotide Polymerization. *ChemBioChem* **2019**, *20* (6), 793–799. https://doi.org/10.1002/cbic.201800616.

(89) Eason, R. G.; Burkhardt, D. M.; Phillips, S. J.; Smith, D. P.; David, S. S. Synthesis and Characterization of 8-Methoxy-2'-Deoxyadenosine-Containing Oligonucleotides to Probe the Syn Glycosidic Conformation of 2'-Deoxyadenosine Within DNA. *Nucleic Acids Res.* **1996**, *24* (5), 890–897. https://doi.org/10.1093/nar/24.5.890.

(90) De Paulis, T.; Kumar, Y.; Johansson, L.; Raemsby, S.; Hall, H.; Saellemark, M.; Aengeby-Moeller, K.; Oegren, S. O. Potential Neuroleptic Agents. 4. Chemistry, Behavioral Pharmacology, and Inhibition of [3H]Spiperone Binding of 3,5-Disubstituted N-[(1-Ethyl-2-Pyrrolidinyl)Methyl]-6-Methoxysalicylamides. *J. Med. Chem.* **1986**, *29* (1), 61–69. https://doi.org/10.1021/jm00151a010.

(91) Khadem, S.; Joseph, R.; Rastegar, M.; Leek, D. M.; Oudatchin, K. A.; Arya, P. A Solution- and Solid-Phase Approach to Tetrahydroquinoline-Derived Polycyclics Having a 10-Membered Ring. *J. Comb. Chem.* **2004**, *6* (5), 724–734. https://doi.org/10.1021/cc049941o.

(92) Specht, A.; Thomann, J.-S.; Alarcon, K.; Wittayanan, W.; Ogden, D.; Furuta, T.; Kurakawa, Y.; Goeldner, M. New Photoremovable Protecting Groups for Carboxylic Acids with High Photolytic Efficiencies at Near-UV Irradiation. Application to the Photocontrolled Release of L-Glutamate. *ChemBioChem* **2006**, *7* (11), 1690–1695. https://doi.org/10.1002/cbic.200600111.

(93) Ho, Y. T. C.; Leng, D. J.; Ghiringhelli, F.; Wilkening, I.; Bushell, D. P.; Köstner, O.; Riva, E.; Havemann, J.; Passarella, D.; Tosin, M. Novel Chemical Probes for the Investigation of Nonribosomal Peptide Assembly. *Chem. Commun.* **2017**, *53* (52), 7088–7091. https://doi.org/10.1039/C7CC02427D.

(94) Tierney, M. T.; Grinstaff, M. W. Synthesis and Stability of Oligodeoxynucleotides Containing C8-Labeled 2'-Deoxyadenosine: Novel Redox Nucleobase Probes for DNA-Mediated Charge-Transfer Studies. *Org. Lett.* **2000**, *2* (22), 3413–3416. https://doi.org/10.1021/ol006303f.

(95) Singh, D.; Kumar, V.; Ganesh, K. N. Oligonucleotides, Part 5+: Synthesis and Fluorescence Studies of DNA Oligomers d(AT)5 Containing Adenines Covalently Linked at 0-8 with Dansyl Fluorophore. *Nucleic Acids Res.* **1990**, *18* (11), 3339–3345.

(96) Wei, C.-M.; Gershowitz, A.; Moss, B. Methylated Nucleotides Block 5′ Terminus of HeLa Cell Messenger RNA. *Cell* **1975**, *4* (4), 379–386. https://doi.org/10.1016/0092-8674(75)90158-0.

(97) Jia, G.; Fu, Y.; Zhao, X.; Dai, Q.; Zheng, G.; Yang, Y.; Yi, C.; Lindahl, T.; Pan, T.; Yang, Y.-G.; He, C. N6-Methyladenosine in Nuclear RNA Is a Major Substrate of the Obesity-

Associated FTO. *Nat. Chem. Biol.* **2011**, *7* (12), 885–887. https://doi.org/10.1038/nchembio.687.

(98) Brenner, S.; Lerner, R. A. Encoded Combinatorial Chemistry. *Proc. Natl. Acad. Sci.* **1992**, *89* (12), 5381–5383. https://doi.org/10.1073/pnas.89.12.5381.

(99) de Pedro Beato, E.; Priego, J.; Gironda-Martínez, A.; González, F.; Benavides, J.; Blas, J.; Martín-Ortega, M. D.; Toledo, M. Á.; Ezquerra, J.; Torrado, A. Mild and Efficient Palladium-Mediated C–N Cross-Coupling Reaction between DNA-Conjugated Aryl Bromides and Aromatic Amines. *ACS Comb. Sci.* **2019**, *21* (2), 69–74. https://doi.org/10.1021/acscombsci.8b00142.

(100) Stress, C. J.; Sauter, B.; Schneider, L. A.; Sharpe, T.; Gillingham, D. A DNA-Encoded Chemical Library Incorporating Elements of Natural Macrocycles. *Angew. Chem. Int. Ed.* **2019**, *58* (28), 9570–9574. https://doi.org/10.1002/anie.201902513.

(101) Neri, D.; Lerner, R. A. DNA-Encoded Chemical Libraries: A Selection System Based on Endowing Organic Compounds with Amplifiable Information. *Annu. Rev. Biochem.* **2018**, *87* (1), 479–502. https://doi.org/10.1146/annurev-biochem-062917-012550.

(102) Fitzgerald, P. R.; Paegel, B. M. DNA-Encoded Chemistry: Drug Discovery from a Few Good Reactions. *Chem. Rev.* **2021**, *121* (12), 7155–7177. https://doi.org/10.1021/acs.chemrev.0c00789.

(103) Ottl, J.; Leder, L.; Schaefer, J. V.; Dumelin, C. E. Encoded Library Technologies as Integrated Lead Finding Platforms for Drug Discovery. *Molecules* **2019**, *24* (8), 1629. https://doi.org/10.3390/molecules24081629.

(104) Clark, M. A.; Acharya, R. A.; Arico-Muendel, C. C.; Belyanskaya, S. L.; Benjamin, D. R.; Carlson, N. R.; Centrella, P. A.; Chiu, C. H.; Creaser, S. P.; Cuozzo, J. W.; Davie, C. P.; Ding, Y.; Franklin, G. J.; Franzen, K. D.; Gefter, M. L.; Hale, S. P.; Hansen, N. J. V.; Israel, D. I.; Jiang, J.; Kavarana, M. J.; Kelley, M. S.; Kollmann, C. S.; Li, F.; Lind, K.; Mataruse, S.; Medeiros, P. F.; Messer, J. A.; Myers, P.; O'Keefe, H.; Oliff, M. C.; Rise, C. E.; Satz, A. L.; Skinner, S. R.; Svendsen, J. L.; Tang, L.; van Vloten, K.; Wagner, R. W.; Yao, G.; Zhao, B.; Morgan, B. A. Design, Synthesis and Selection of DNA-Encoded Small-Molecule Libraries. *Nat. Chem. Biol.* **2009**, *5* (9), 647–654. https://doi.org/10.1038/nchembio.211.

(105) Franzini, R. M.; Ekblad, T.; Zhong, N.; Wichert, M.; Decurtins, W.; Nauer, A.; Zimmermann, M.; Samain, F.; Scheuermann, J.; Brown, P. J.; Hall, J.; Gräslund, S.; Schüler, H.; Neri, D. Identification of Structure-Activity Relationships from Screening a Structurally Compact DNA-Encoded Chemical Library. *Angew. Chem. Int. Ed.* **2015**, *54* (13), 3927–3931. https://doi.org/10.1002/anie.201410736.

(106) Yuen, L. H.; Dana, S.; Liu, Y.; Bloom, S. I.; Thorsell, A.-G.; Neri, D.; Donato, A. J.; Kireev, D.; Schüler, H.; Franzini, R. M. A Focused DNA-Encoded Chemical Library for

the Discovery of Inhibitors of NAD $^{+}$ -Dependent Enzymes. *J. Am. Chem. Soc.* **2019**, *141* (13), 5169–5181. https://doi.org/10.1021/jacs.8b08039.

(107) Zimmermann, G.; Li, Y.; Rieder, U.; Mattarella, M.; Neri, D.; Scheuermann, J. Hit-Validation Methodologies for Ligands Isolated from DNA-Encoded Chemical Libraries. *ChemBioChem* **2017**, *18* (9), 853–857. https://doi.org/10.1002/cbic.201600637.

(108) Johnson, B. M.; Shu, Y.-Z.; Zhuo, X.; Meanwell, N. A. Metabolic and Pharmaceutical Aspects of Fluorinated Compounds. *J. Med. Chem.* **2020**, *63* (12), 6315–6386. https://doi.org/10.1021/acs.jmedchem.9b01877.

(109) Reiher, C. A.; Schuman, D. P.; Simmons, N.; Wolkenberg, S. E. Trends in Hit-to-Lead Optimization Following DNA-Encoded Library Screens. *ACS Med. Chem. Lett.* **2021**, *12* (3), 343–350. https://doi.org/10.1021/acsmedchemlett.0c00615.

(110) Lea, W. A.; Simeonov, A. Fluorescence Polarization Assays in Small Molecule Screening. *Expert Opin. Drug Discov.* **2011**, *6* (1), 17–32. https://doi.org/10.1517/17460441.2011.537322.

(111) Perrin, F. Polarisation de la lumière de fluorescence. Vie moyenne des molécules dans l'etat excité. *J. Phys. Radium* **1926**, *7* (12), 390–401. https://doi.org/10.1051/jphysrad:01926007012039000.

(112) Presolski, S. I.; Hong, V. P.; Finn, M. G. Copper-Catalyzed Azide–Alkyne Click Chemistry for Bioconjugation. *Curr. Protoc. Chem. Biol.* **2011**, *3* (4), 153–162. https://doi.org/10.1002/9780470559277.ch110148.

(113) Bréthous, L.; Garcia-Delgado, N.; Schwartz, J.; Bertrand, S.; Bertrand, D.; Reymond, J.-L. Synthesis and Nicotinic Receptor Activity of Chemical Space Analogues of *N* -(3 *R*)-1-Azabicyclo[2.2.2]Oct-3-Yl-4-Chlorobenzamide (PNU-282,987) and 1,4-Diazabicyclo[3.2.2]Nonane-4-Carboxylic Acid 4-Bromophenyl Ester (SSR180711). *J. Med. Chem.* **2012**, *55* (10), 4605–4618. https://doi.org/10.1021/jm300030r.

(114) Zhang, G.; Zhu, J.; Tong, C.; Ding, C. Pharmaceutical-Oriented Methoxylation of Aryl C(Sp2)–H Bonds Using Copper Catalysts. *Synlett* **2018**, *29* (11), 1451–1554. https://doi.org/10.1055/s-0037-1610132.

(115) Cartagenova, D.; Bachmann, S.; Püntener, K.; Scalone, M.; Newton, M. A.; Peixoto Esteves, F. A.; Rohrbach, T.; Zimmermann, P. P.; van Bokhoven, J. A.; Ranocchiari, M. Highly Selective Suzuki Reaction Catalysed by a Molecular Pd–P-MOF Catalyst under Mild Conditions: Role of Ligands and Palladium Speciation. *Catal. Sci. Technol.* **2022**, 10.1039.D1CY01351C. https://doi.org/10.1039/D1CY01351C.

(116) Dong, C.; Zhang, L.; Xue, X.; Li, H.; Yu, Z.; Tang, W.; Xu, L. Pd-Catalyzed Ligand-Free Suzuki Reaction of β-Substituted Allylic Halides with Arylboronic Acids in Water. *RSC Adv* **2014**, *4* (22), 11152–11158. https://doi.org/10.1039/C3RA47813K.

(117) Fa, S.; Zhao, Y. General Method for Peptide Recognition in Water through Bioinspired Complementarity. *Chem. Mater.* **2019**, *31* (13), 4889–4896. https://doi.org/10.1021/acs.chemmater.9b01613.

(118) Ma, M.; Li, C.; Li, X.; Wen, K.; Liu, Y. A. Efficient Synthesis of 6-Aryl-2-Chloronicotinic Acids via Pd Catalyzed Regioselective Suzuki Coupling of 2,6-Dichloronicotinic Acid. *J. Heterocycl. Chem.* **2008**, *45* (6), 1847–1849. https://doi.org/10.1002/jhet.5570450646.

(119) Shendage, D. M.; Fröhlich, R.; Haufe, G. Highly Efficient Stereoconservative Amidation and Deamidation of α-Amino Acids. *Org. Lett.* **2004**, *6* (21), 3675–3678. https://doi.org/10.1021/ol0487711.

(120) George, N.; Ofori, S.; Parkin, S.; Awuah, S. G. Mild Deprotection of the *N*-*Tert* -Butyloxycarbonyl (*N* -Boc) Group Using Oxalyl Chloride. *RSC Adv.* **2020**, *10* (40), 24017–24026. https://doi.org/10.1039/D0RA04110F.

(121) Moerke, N. J. Fluorescence Polarization (FP) Assays for Monitoring Peptide-Protein or Nucleic Acid-Protein Binding. *Curr. Protoc. Chem. Biol.* **2009**, *1* (1), 1–15. https://doi.org/10.1002/9780470559277.ch090102.

(122) Fang, Z.; Mu, B.; Liu, Y.; Guo, N.; Xiong, L.; Guo, Y.; Xia, A.; Zhang, R.; Zhang, H.; Yao, R.; Fan, Y.; Li, L.; Yang, S.; Xiang, R. Discovery of a Potent, Selective and Cell Active Inhibitor of m6A Demethylase ALKBH5. *Eur. J. Med. Chem.* **2022**, *238*, 114446. https://doi.org/10.1016/j.ejmech.2022.114446.